Title

Spatial Patterns in the Response of California's Kelp Forests to Climate Variability and Extremes

Author

Cavanaugh, Katherine

Publication Date

2024

Peer reviewed|Thesis/dissertation

UNIVERSITY OF CALIFORNIA

Los Angeles

Spatial Patterns in the Response of California's Kelp Forests to Climate Variability and Extremes

A dissertation submitted in partial satisfaction of the requirements for the degree Doctor of Philosophy in Geography

by

Katherine C. Cavanaugh

2024

ABSTRACT OF THE DISSERTATION

Spatial Patterns in the Response

of California's Kelp Forests to Climate Variability and Extremes

by

Katherine C. Cavanaugh

Doctor of Philosophy in Geography

University of California, Los Angeles, 2024

Professor Kyle C. Cavanaugh, Chair

Kelp forests, like many marine ecosystems, are being exposed to more frequent and intense disturbances. Marine heatwaves are major drivers of widespread and sustained kelp forest losses, as temperature directly affects the distribution and persistence of populations. Heatwave effects have been examined on large scales using satellite-derived data, but there is also variability in kelp responses on local to regional scales, driven by marine microclimates such as localized upwelling. Field and drone-based monitoring efforts have been employed along the California coastline to capture local dynamics, but these surveys only cover samples from selected kelp beds. Consequently, field and drone-based datasets represent one end of the spatial spectrum for observing kelp canopy response and recovery after disturbance events,

while satellite observations represent the other end. Neither method alone can fully resolve both local and regional to global-scale dynamics.

The development of CubeSat constellations has enabled a workaround for these trade-offs, with global imagery available near-daily at meter-scale. In my first chapter, I develop methods to create spatially continuous time series of California kelp population dynamics from high-resolution CubeSat data. In my second chapter, I employ these time series to highlight local-scale variability in California kelp populations that have been impacted by marine heatwave events, helping to better identify areas of concern and understand the drivers of heatwave-mediated loss and stability. In my third chapter, I scale these methods to effectively map kelp canopy across the state of California. I develop deep learning models for estimating kelp canopy presence and apply these models to a time series of CubeSat data.

My findings contribute new perspectives for addressing and understanding kelp forest disturbance regimes. Mapping kelp populations with CubeSat constellation data allowed for the identification of areas of vulnerability, providing utility in prioritizing areas for strategic protection and restoration. Classifying sections of coastline that supported kelp forests amidst marine heatwave events showed the presence of refugia, where subpopulations have been able to persist in habitats that are buffered from disturbance. Further, mapping these populations across California will allow for the development of new indicators of ecosystem functioning and health.

The dissertation of Katherine C. Cavanaugh is approved.

Michelle Gierach

Thomas Welch Gillespie

Gregory Stewart Okin

Elsa Marianne Ordway

Laura Rogers-Bennett

Kyle C. Cavanaugh, Committee Chair

University of California, Los Angeles

2024

Table of Contents

List of Figures

ACKNOWLEDGEMENTS

UCLA provided an exceptional environment for conducting this research. A special acknowledgment is owed to the dedicated undergraduates, research technicians, graduate students, and mentors who generously contributed their time and expertise to support this work.

I would like to extend my heartfelt gratitude to my advisor, Dr. Kyle Cavanaugh. His unwavering support and guidance have shaped both my scientific journey and personal growth. His belief in my abilities has been a cornerstone of my confidence, especially as a woman in STEM. He has been there during challenging times, offering solutions and opening new doors of opportunity. His advocacy for my research and dedication to my career development have been invaluable. From helping me secure funding for fieldwork to guiding me through grant proposals and encouraging my participation in conferences, Dr. Cavanaugh has always prioritized my growth and success. His calm and understanding nature, especially during difficult moments, has been a source of reassurance and strength. His support has made an immeasurable impact on my life, and I will always be grateful for his guidance.

Arriving at UCLA, I had little knowledge about kelp forests, let alone kelp mapping. However, under the mentorship of Dr. Tom Bell, who revolutionized kelp forest mapping with Landsat, I found invaluable support and guidance. Dr. Bell generously sat with me, collaborated on code, and shared his expertise, allowing me to contribute to the advancement of the field. His mentorship has been instrumental in my journey, and I look forward to continuing our collaboration throughout my career.

I appreciate the rest of my dissertation committee for their advice and encouragement during my graduate career at UCLA. Dr. Michelle Gierach encouraged me to pursue my PhD, and for that, I am grateful. She is full of ideas on pushing the bounds of remote sensing-based

ecology, and I feel fortunate to have her on my team. Dr. Tom Gillespie, on both my Masters and Dissertation committee, brought deep knowledge of the field and intense optimism that reminded me to enjoy the little things in science. Dr. Greg Okin was instrumental in helping push the bounds of kelp forest mapping with new technologies; I always looked up to his scientific expertise and confidence. Dr. Elsa Ordway, a late addition to my committee, deeply cares for her students, and I appreciate her academic advice and encouragement. Her lab and research focus embody my aspirations for the future. Dr. Laura Rogers-Bennett, as a field ecologist, reminded me why my science is important. With Dr. Rogers-Bennett, I saw kelp forests from beneath the surface for the first time, changing my perspective indefinitely.

The camaraderie within Cavanaugh Lab at UCLA, shared among my dear colleagues Daniel Jensen, Cheryl Doughty, Emelly Villa, Lori Berberian, Max Callahan, Kyle Emery, Billie Beckley, and Henry Houskeeper, played a crucial role in sustaining my happiness. Each of you holds a special place in my heart, and I owe much of my success to your scientific support and friendship. I am deeply grateful for the friends and family who formed my support system, guiding me to the finish line. To my mom and dad, Meg and Mike Cavanaugh, who were never shy in reminding me that there is a balance between work and life, and who offered support in every category imaginable. To my sister and brother, Courtney and Chris Cavanaugh, whose understanding surpasses words. To Keri McGlone and Victoria Ferrante, whose unwavering confidence in me often exceeded my own. And to Joe Maltese, whose presence has changed my life for the better.

Katherine C. Cavanaugh
Department of Geography, University of California, Los Angeles 90095

Education

University of California – Los Angeles, Los Angeles, CA
M.A., Geography 2020
Gettysburg College, Gettysburg, PA
B.S., Environmental Studies
2016 Minors, Physics and Latin

Research and Professional Experience

2023 *Ocean Remote Sensing Graduate Mentor*
NASA Student Airborne Research Program
2018-2024 *Research and Teaching Assistant*
University of California – Los Angeles, Los Angeles,
CA 2017-2018 *Geoinformatics Fellow*, NASA DEVELOP Program
NASA Jet Propulsion Lab, Pasadena, CA
2016-2017 *Remote Sensing Analyst*, NASA DEVELOP
Program NASA Jet Propulsion Lab, Pasadena, CA
2015-2016 *Water Quality Analyst*
Star Island Corporation, Star Island, Isles of Shoals, NH

Publications

Cavanaugh, K.C., Cavanaugh, K.C., Pawlak, C.C., Bell, T.W., Saccomanno, V.R. (2023). CubeSats show persistence of bull kelp refugia amidst a regional collapse in California. *Remote Sensing of Environment.*

Saccomanno, V.R., Bell, T., Pawlak, C., Stanley, C.K., **Cavanaugh, K.C**., Hohman, R., Klausmeyer, K.R., Cavanaugh, K., Nickels, A., Hewerdine, W., Garza, C., Fleener, G. and Gleason, M. (2022), Using unoccupied aerial vehicles to map and monitor changes in emergent kelp canopy after an ecological regime shift. *Remote Sensing in Ecology and Conservation.*

Bell, T.W., Cavanaugh, K.C., Saccomanno, V.R., **Cavanaugh, K.C.**, Houskeeper, H.F., Eddy, N., Schuetzenmeister, F., Rindlaub, N., Gleason, M., (2022). Kelpwatch: A new visualization and analysis tool to explore kelp canopy dynamics reveals variable resistance and resilience to marine heat waves. *bioRxiv*.

Houskeeper, H.F., Rosenthal, I.S., **Cavanaugh, K.C.**, Pawlak, C., Trouille, L., Byrnes, J.E.K., Bell, T.W., Cavanaugh, K.C., (2022). Automated satellite remote sensing of giant kelp at the Falkland Islands (Islas Malvinas). *PLoS One*.

Elsmore, K., Nickols, K.J., Ford, T., **Cavanaugh, K.C.**, Cavanaugh, K.C., Gaylord, B., (2022). Macrocystis pyrifera forest development shapes the physical environment through current velocity reduction. *Marine Ecology Progress Series*.

Arafeh-Dalmau, N., Cavanaugh, K.C., Possingham, H.P., Munguia-Vega, A., Montaño-Moctezuma, G., Bell, T.W., **Cavanaugh, K.C.**, Micheli, F., (2021). Southward decrease in the protection of persistent giant kelp forests in the northeast Pacific. *Communications Earth & Environment*.

Cavanaugh, K.C., Bell, T., Costa, M., Eddy, N.E., ..., **Cavanaugh, K.C.**, ..., Schroeder, S.B.

(2021). A review of the opportunities and challenges for using remote sensing for management of surface-canopy forming kelps. *Frontiers in Marine Science*.

Cavanaugh, K.C., Cavanaugh, K.C., Bell, T.W., Hockridge, E.G. (2021). An automated method for mapping giant kelp canopy dynamics from UAV. *Frontiers in Environmental Scienc*e.

Bell, T.W., Nidzieko, N.J., Siegel, D.A., Miller, R.J., Cavanaugh, K.C, Nelson, N., Reed, D., Federov, D., **Cavanaugh, KC.**, Moran, C., Snyder, J., Griffith, M. (2020). The utility of satellites and autonomous remote sensing platforms for monitoring offshore aquaculture farms: a case study for canopy forming kelps. *Frontiers in Marine Science*.

Rodriguez-Alvarez, N., Holt, B., Jaruwatanadilok, S., Podest, E., **Cavanaugh, K.C.** (2019). An Arctic sea ice multi-step classification based on GNSS-R data from the TDS-1 mission. *Remote Sensing of Environment.*

Selected Presentations

International Temperate Reef Symposium (ITRS) 2023, Hobart, Tasmania, Australia
The role of refugia in the persistence and recovery of northern California bull kelp forests
***Third place in student presentation competition**

Western Society of Naturalists (WSN) 2022, Oxnard, CA
Quantifying the spatial distribution of kelp canopy traits with imaging spectroscopy
***Best student talk in observational ecology**

Invited Talks

2023 Guest Lecture, West Coast Ocean Alliance Workshop, Costa Mesa, CA
2023 Guest Lecture, UCLA Marine Science Center Spring Meeting, Los Angeles, CA
2023 Guest Lecture, UCLA Department of Atmospheric and Oceanic Sciences, Los Angeles, CA *2023 Counterforce Lab Salon Series*, UCLA Design Media Arts Department, Los Angeles, CA 2*022 NASA SHIFT Science Team Meeting,* Santa Barbara, California
2022 University of California Drone Camp Lecture Series, Virtual Attendance
2018 Annual Earth Science Applications Showcase, NASA Headquarters, Washington, D.C.
2017 ECOSTRESS Science Team Meeting, Davis, CA

Scholarships, Fellowships, and Awards

UCLA Best Graduate Student Publication in Physical Geography, 2023
UCLA Graduate Travel Fellowship, 2022 ($6500)
Strategic University Research Partnerships Graduate Fellowship, 2021-2024 ($60,000/year)
UCLA Graduate Research Mentorship Program, 2019-2020 ($20,000)
United States Geospatial Intelligence Foundation Graduate Scholarship, 2018-2019 ($5,000)

UCLA Geography Department Service

Colloquium Representative, 2019-2023
Grad to Grad Mentor, 2020-2024
Graduate Student Liaison for Faculty Hires, 2022-2023

Chapter 1. Introduction

Kelp forests support highly diverse ecosystems along temperate global coastlines (Krumhansl et al., 2016). Species distributions are spatially and temporally variable (Blanfuné et al., 2019), but the productivity and structure of forests enhance the abundance and diversity of the dependent community. Anchored to the rocky reef with a holdfast, individuals are buoyed towards the ocean surface with gas-filled pneumatocysts, introducing a three-dimensional habitat to the local system (Graham et al., 2007b). High rates of net primary production (NPP) contribute to a significant source of nutrition for herbivores (Elliott Smith and Fox, 2022) and detritus-based food webs as beach wrack (Duggins et al., 1989). There is also evidence that kelp forests play a significant role in marine carbon cycles, with the potential to sequester 173 TgC via deep ocean export (Krause-Jensen and Duarte, 2016).

Changing temperature regimes, associated with both climate trends and extreme events, have become a threat to global biodiversity (Díaz et al., 2019). Consequently, temperature-related impacts to kelp forests are of particular concern, as changes in the stability and performance of these organisms impact the community and ecosystem as a whole (Staehr and Wernberg, 2009). Over the last century, the intensification of marine heatwaves has resulted in record-breaking events across ocean basins (Oliver et al., 2018). These events, characterized by positive sea surface temperature anomalies that persist from days to months, result in rapid and extreme changes to upwelling and nutrient dynamics (Sanford et al., 2019).

Marine heatwaves have emerged as a primary driver of kelp forest loss, precipitating population declines in many global regions (Krumhansl et al., 2016), including certain sections of coastal California (Bell et al., 2023; Cavanaugh et al., 2019; Michaud et al., 2022; Rogers-Bennett and Catton, 2019). Here, in the winter of 2013 to 2014, a large warm-water anomaly

formed in the North Pacific that persisted through 2016. This multiyear heatwave was concurrent with reduced upwelling and limited nutrient availability, which had negative consequences for many ecosystems (Benthuysen et al., 2020; Oliver et al., 2018). Primary production decreased along the affected range, and many species of fish, mammals, and birds constricted their geographical ranges northward (Cavole et al., 2016). However, impacts to two canopy-forming kelps, giant kelp (*Macrocystis pyrifera*) and bull kelp (*Nereocystis luetkeana*), were highly variable. In some regions (e.g., Santa Barbara), kelp canopy recovered soon after the end of the heatwave (Cavanaugh et al., 2019), while in others (e.g., northern California), the effects of the heatwave were still apparent several years after the heatwave ended (McPherson et al., 2021).

California kelp populations are strongly influenced by temperature and nutrient conditions (Bell et al., 2015a), making them particularly vulnerable to the extreme nature of heatwave events. Therefore, variability in temperature and nutrient conditions during and after the heatwave may explain the geographic inconsistencies in observed recovery (Hollarsmith et al., 2020). California kelp population dynamics have been examined on large scales using satellite-derived data products (Bell et al., 2023, 2020), but there is almost certainly also large variability in the response of kelp canopy on local to regional scales, which may be driven by marine microclimates, such as localized upwelling (Mora-Soto et al., 2024; Starko et al., 2022; Verdura et al., 2021). Field and drone-based monitoring efforts have been employed along the coastline to capture these fine-scale changes in local kelp canopy dynamics (Saccomanno et al., 2023a), but restrictions with cost, time, and data collection inhibit their utility for conducting routine kelp mapping efforts across large-scale, continuous landscapes (Gray et al., 2022).

Mapping kelp canopy coverage within and across coastal ecosystems would allow for the identification of areas of vulnerability, providing utility in prioritizing areas for strategic

protection and restoration (Hamilton et al., 2022). For example, classifying sections of coastline that have supported kelp populations amidst the extreme environmental stressors associated with the heatwave may indicate the presence of refugia, where subpopulations have been able to persist in habitat that is decoupled from regional climate variability (i.e., deeper, cooler waters) (Assis et al., 2016; Davis et al., 2021; Graham et al., 2007a). Kelp in refugia are likely the primary source of spores necessary for recolonization, making them important hotspots for management. Additionally, information on the underlying drivers of kelp survival can inform predictions of kelp forest changes under various climate scenarios, which has been implemented in other ecosystems, such as coral reefs (Asner et al., 2017).

The central goal of this work is to map kelp abundance along the California coastline using methods that can adequately spatially capture highly disturbed and fragmented kelp forests. Specifically, I developed time series of canopy abundance at fine spatial scales to better identify the extent of kelp forest extinction and recolonization after the 2014 to 2016 marine heatwave. I employed these time series to characterize kelp populations that were able to persist through the disturbance. Finally, I investigated the role of spatial heterogeneity across northern California in providing kelp individuals with refuges, such as habitat features that facilitate the transport of deeper, cooler water during and after marine heatwave events.

1.1 References

Asner, G.P., Vaughn, N.R., Heckler, J., Knapp, D.E., Balzotti, C., Shafron, E., Martin, R.E., Neilson, B.J., Gove, J.M., Russell Brainard, by E., Burns, J., 2017. Large-scale mapping of live corals to guide reef conservation. PNAS 117, 33711–33718. https://doi.org/10.1073/pnas.2017628117/-/DCSupplemental

Assis, J., Coelho, N.C., Lamy, T., Valero, M., Alberto, F., Serrão, E.Á., 2016. Deep reefs are climatic refugia for genetic diversity of marine forests. J Biogeogr 43, 833–844. https://doi.org/https://doi.org/10.1111/jbi.12677

Bell, T.W., Allen, J.G., Cavanaugh, K.C., Siegel, D.A., 2020. Three decades of variability in California's giant kelp forests from the Landsat satellites. Remote Sens Environ 238, 110811.

Bell, T.W., Cavanaugh, K.C., Reed, D.C., Siegel, D.A., 2015. Geographical variability in the controls of giant kelp biomass dynamics. J Biogeogr 42, 2010–2021.

Bell, T.W., Cavanaugh, Kyle C, Saccomanno, V.R., Cavanaugh, Katherine C, Houskeeper, H.F., Eddy, N., Schuetzenmeister, F., Rindlaub, N., Gleason, M., 2023. Kelpwatch: A new visualization and analysis tool to explore kelp canopy dynamics reveals variable response to and recovery from marine heatwaves. PLoS One 18, e0271477-.

Benthuysen, J.A., Oliver, E.C.J., Chen, K., Wernberg, T., 2020. Advances in understanding marine heatwaves and their impacts. Front Mar Sci 7, 147.

Blanfuné, A., Boudouresque, C.F., Verlaque, M., Thibaut, T., 2019. The ups and downs of a canopy-forming seaweed over a span of more than one century. Sci Rep 9, 5250. https://doi.org/10.1038/s41598-019-41676-2

Cavanaugh, K.C., Reed, D.C., Bell, T.W., Castorani, M.C.N., Beas-Luna, R., 2019. Spatial Variability in the Resistance and Resilience of Giant Kelp in Southern and Baja California to a Multiyear Heatwave. Front Mar Sci 6.

Cavole, L.M., Demko, A.M., Diner, R.E., Giddings, A., Koester, I., Pagniello, C.M.L.S., Paulsen, M.-L., Ramirez-Valdez, A., Schwenck, S.M., Yen, N.K., 2016. Biological impacts of the

2013–2015 warm-water anomaly in the Northeast Pacific: winners, losers, and the future. Oceanography 29, 273–285.

Davis, T.R., Champion, C., Coleman, M.A., 2021. Climate refugia for kelp within an ocean warming hotspot revealed by stacked species distribution modelling. Mar Environ Res 166, 105267. https://doi.org/https://doi.org/10.1016/j.marenvres.2021.105267

Díaz, S., Settele, J., Brondízio, E.S., Ngo, H.T., Agard, J., Arneth, A., Balvanera, P., Brauman, K.A., Butchart, S.H.M., Chan, K.M.A., 2019. Pervasive human-driven decline of life on Earth points to the need for transformative change. Science (1979) 366, eaax3100.

Duggins, D.O., Simenstad, C.A., Estes, J.A., 1989. Magnification of secondary production by kelp detritus in coastal marine ecosystems. Science (1979) 245, 170–173.

Elliott Smith, E.A., Fox, M.D., 2022. Characterizing energy flow in kelp forest food webs: a geochemical review and call for additional research. Ecography 2022, e05566. https://doi.org/https://doi.org/10.1111/ecog.05566

Graham, M.H., Kinlan, B.P., Druehl, L.D., Garske, L.E., Banks, S., 2007a. Deep-water kelp refugia as potential hotspots of tropical marine diversity and productivity. Proceedings of the National Academy of Sciences 104, 16576–16580. https://doi.org/10.1073/pnas.0704778104

Graham, M.H., Vasquez, J.A., Buschmann, A.H., 2007b. Global ecology of the giant kelp Macrocystis: from ecotypes to ecosystems. Oceanography and marine biology 45, 39.

Gray, P.C., Larsen, G.D., Johnston, D.W., 2022. Drones address an observational blind spot for biological oceanography. Front Ecol Environ 20, 413–421. https://doi.org/https://doi.org/10.1002/fee.2472

Hamilton, S.L., Gleason, M.G., Godoy, N., Eddy, N., Grorud-Colvert, K., 2022. Ecosystem-based management for kelp forest ecosystems. Mar Policy 136, 104919. https://doi.org/https://doi.org/10.1016/j.marpol.2021.104919

Hollarsmith, J.A., Buschmann, A.H., Camus, C., Grosholz, E.D., 2020. Varying reproductive success under ocean warming and acidification across giant kelp (Macrocystis pyrifera) populations. J Exp Mar Biol Ecol 522, 151247.

Krause-Jensen, D., Duarte, C.M., 2016. Substantial role of macroalgae in marine carbon sequestration. Nat Geosci 9, 737–742.

Krumhansl, K.A., Okamoto, D.K., Rassweiler, A., Novak, M., Bolton, J.J., Cavanaugh, K.C., Connell, S.D., Johnson, C.R., Konar, B., Ling, S.D., Micheli, F., Norderhaug, K.M., Pérez-Matus, A., Sousa-Pinto, I., Reed, D.C., Salomon, A.K., Shears, N.T., Wernberg, T., Anderson, R.J., Barrett, N.S., Buschmann, A.H., Carr, M.H., Caselle, J.E., Derrien-Courtel, S., Edgar, G.J., Edwards, M., Estes, J.A., Goodwin, C., Kenner, M.C., Kushner, D.J., Moy, F.E., Nunn, J., Steneck, R.S., Vásquez, J., Watson, J., Witman, J.D., Byrnes, J.E.K., 2016. Global patterns of kelp forest change over the past half-century. Proceedings of the National Academy of Sciences 113, 13785–13790. https://doi.org/10.1073/pnas.1606102113

McPherson, M.L., Finger, D.J.I., Houskeeper, H.F., Bell, T.W., Carr, M.H., Rogers-Bennett, L., Kudela, R.M., 2021. Large-scale shift in the structure of a kelp forest ecosystem co-occurs with an epizootic and marine heatwave. Commun Biol 4, 298. https://doi.org/10.1038/s42003-021-01827-6

Michaud, K.M., Reed, D.C., Miller, R.J., 2022. The Blob marine heatwave transforms California kelp forest ecosystems. Commun Biol 5, 1143. https://doi.org/10.1038/s42003-022-04107-z

Mora-Soto, A., Schroeder, S., Gendall, L., Wachmann, A., Narayan, G.R., Read, S., Pearsall, I., Rubidge, E., Lessard, J., Martell, K., Wills, P., Costa, M., 2024. Kelp dynamics and environmental drivers in the southern Salish Sea, British Columbia, Canada. Front Mar Sci 11. https://doi.org/10.3389/fmars.2024.1323448

Oliver, E.C.J., Donat, M.G., Burrows, M.T., Moore, P.J., Smale, D.A., Alexander, L. V, Benthuysen, J.A., Feng, M., Sen Gupta, A., Hobday, A.J., Holbrook, N.J., Perkins-Kirkpatrick, S.E., Scannell, H.A., Straub, S.C., Wernberg, T., 2018. Longer and more frequent marine heatwaves over the past century. Nat Commun 9, 1324. https://doi.org/10.1038/s41467-018-03732-9

Rogers-Bennett, L., Catton, C.A., 2019. Marine heat wave and multiple stressors tip bull kelp forest to sea urchin barrens. Sci Rep 9, 15050. https://doi.org/10.1038/s41598-019-51114-y

Saccomanno, V.R., Bell, T., Pawlak, C., Stanley, C.K., Cavanaugh, K.C., Hohman, R., Klausmeyer, K.R., Cavanaugh, K., Nickels, A., Hewerdine, W., Garza, C., Fleener, G., Gleason, M., 2023. Using unoccupied aerial vehicles to map and monitor changes in emergent kelp canopy after an ecological regime shift. Remote Sens Ecol Conserv 9, 62–75. https://doi.org/https://doi.org/10.1002/rse2.295

Sanford, E., Sones, J.L., García-Reyes, M., Goddard, J.H.R., Largier, J.L., 2019. Widespread shifts in the coastal biota of northern California during the 2014–2016 marine heatwaves. Sci Rep 9, 4216.

Staehr, P.A., Wernberg, T., 2009. Physiological responses of Ecklonia radiata (laminariales) to a latitudinal gradient IN ocean temperature 1. J Phycol 45, 91–99.

Starko, S., Neufeld, C.J., Gendall, L., Timmer, B., Campbell, L., Yakimishyn, J., Druehl, L., Baum, J.K., 2022. Microclimate predicts kelp forest extinction in the face of direct and indirect marine heatwave effects. Ecological Applications 32, e2673. https://doi.org/https://doi.org/10.1002/eap.2673

Verdura, J., Santamaría, J., Ballesteros, E., Smale, D.A., Cefalì, M.E., Golo, R., de Caralt, S., Vergés, A., Cebrian, E., 2021. Local-scale climatic refugia offer sanctuary for a habitat-forming species during a marine heatwave. Journal of Ecology 109, 1758–1773. https://doi.org/https://doi.org/10.1111/1365-2745.13599

Chapter 2. CubeSats show persistence of bull kelp refugia amidst a regional collapse in California

This chapter has been accepted in its current form to *Remote Sensing of Environment* as Cavanaugh, K. C., K. C. Cavanaugh, C. C. Pawlak, T. W. Bell, and V. R. Saccomanno. 2023. CubeSats show persistence of bull kelp refugia amidst a regional collapse in California. Remote Sensing of Environment 290:113521.

Abstract: Bull kelp populations in northern California declined drastically in response to the 2014-2016 marine heatwave, sea star wasting disease, and subsequently large increases in herbivorous purple urchin populations. Despite the regional kelp forest collapse, there were small, remnant populations where bull kelp was able to survive. Moderate resolution satellites (i.e., Landsat) have been important for creating long-term, large-scale time series of bull kelp forests, however, these have been shown to underestimate or entirely exclude refugia due to their low densities and proximity to the coastline. While measurements from Unoccupied Aerial Vehicles (UAV) are spatially detailed, they are temporally limited and difficult to collect over regional scales. The development of CubeSat constellations has enabled a workaround for these tradeoffs, with global imagery available near-daily at meter-scale.

We developed a method for mapping bull kelp canopy across the different sensor cohorts in the PlanetScope constellation. This required correcting surface reflectance measurements to account for differences in the spectral response functions among the sensors and leveraging the temporal frequency of PlanetScope data to increase the automation of classifying kelp canopy in imagery with increased noise. Using the PlanetScope derived kelp canopy extents, we identified

locations where bull kelp refugia have persisted in northern California. We found that bull kelp refugia occupied about 2% of the total available habitat in the region and about 9.4% of the average canopy area observed prior to 2014. These areas may be critical to the success of kelp forest re-establishment in northern California, which increases their importance for ongoing monitoring, conservation, and restoration efforts.

2.1. Introduction

Climate change is reshaping global biodiversity by altering abiotic conditions and biological interactions (Rosenzweig et al., 2008). The cumulative effects of contemporary climatic trends and local disturbances are exceeding the adaptive capacity and environmental tolerance of many organisms (Blowes et al., 2019), and species distributional shifts have been widely observed (Chen et al., 2011). There is also evidence that species can retreat to or persist in refuge areas that provide protection against environmental stressors, particularly when the landscape is heterogeneous (Cacciapaglia and van Woesik, 2015; Verdura et al., 2021). Here, subpopulations are likely to experience microclimates that are decoupled from regional climate variability or ecological disturbance (Andrew and Warrener, 2017; Dobrowski, 2011). However, detecting the existence of these refugia remains challenging, as it requires observations that are sufficiently fine-scaled for target species (i.e., less than 1 km; Ashcroft, 2010; Kavousi and Keppel, 2018; Keppel et al., 2012).

Northern California bull kelp (*Nereocystis luetkeana*) forests constitute an example of an ecosystem that is increasingly vulnerable to climate variability. A large marine heatwave persisted along the Pacific coast of North America from 2014 to 2016, resulting in widespread temperature anomalies of up to 2.5°C (Bond et al., 2015; Oliver et al., 2018). The heatwave coincided with mass mortality of sea star species (Harvell et al., 2019), which greatly reduced urchin predation by the sunflower sea star (*Pycnopodia helianthoides*). The combined effects of the heatwave and increased grazing pressure precipitated a regional ecosystem shift from bull kelp forests to urchin barrens, resulting in deforested clearings ranging from small, meter-scale gaps to the complete denudation of entire forests across hundreds of kilometers (Rogers-Bennett and Catton, 2019). Despite the presence of expansive urchin barrens, certain sections of coastline

have continued to support bull kelp populations throughout northern California (Saccomanno et al., 2022).

Bull kelp is a canopy-forming species, and the floating biomass on the water surface has been successfully quantified using aerial and satellite imagery (Finger et al., 2021; Hamilton et al., 2020; McPherson et al., 2021; Rogers-Bennett and Catton, 2019; Saccomanno et al., 2022; Schroeder et al., 2020). However, the quantification of refugia has been difficult to achieve, as the remnant populations in northern California occur in small and isolated patches that vary in density depending on the number and proximity of individuals (i.e., a single individual to a continuous forest spanning over a kilometer; Saccomanno et al., 2022). Previous work has shown that scale is important for accurately describing the existence and location of refugia, and that existing methods manifest tradeoffs between spatial, temporal, and spectral resolutions (Finger et al., 2020; Saccomanno et al., 2022).

For example, the California Department of Fish and Wildlife (CDFW) has produced annual, high resolution (2 m) statewide maps of kelp canopy from aerial surveys that date back to 1989 (Veisze et al., 1999). These maps were used to reveal the scale (> 300 km of coastline), magnitude (> 90%), and timing (within one year) of the northern California bull kelp declines, and they provided evidence that some populations were able to persist throughout the multiyear heatwave event (Rogers-Bennett and Catton, 2019). However, the last successful surveys were completed in 2016, and so they cannot be used to monitor trends in refugia or recovery following the heatwave. More recent work (e.g., Saccomanno et al., 2022) partially filled this gap with UAV equipped with RGB sensors, which were used to survey 36 non-contiguous priority sites dispersed across 90 km of affected coastline in 2019 and 2020. At 3 cm resolution, these data successfully elucidated the location of relict kelp populations within surveyed areas. However,

regional UAV data collection was not cost or time effective, and classification of emergent canopy from RGB-based UAV imagery required extensive manual input. Current methods rely on thresholding vegetation indices to distinguish kelp from water (Cavanaugh et al., 2021), and high levels of spectral variability necessitated manual threshold selection and additional editing (Saccomanno et al., 2022).

Moderate resolution satellite sensors, such as the Landsat Enhanced Thematic Mapper Plus (ETM+), Operational Land Imager (OLI), and Operational Land Imager 2 (OLI-2), provide a continuous and spatially comprehensive time series of bull kelp refugia habitat in northern California. Progress in the automation of kelp canopy detection from these data (e.g., Bell et al., 2020) includes using a binary decision tree to classify Landsat pixels that contain canopy and subsequently modeling the pixels as a combination of kelp canopy and seawater using Multiple Endmember Spectral Mixture Analysis (MESMA) to estimate fractional kelp canopy cover at a 30 m pixel scale. This method has been successfully applied to capture the abrupt ecosystem shift in northern California (McPherson et al., 2021), but the moderate resolution (30 m) was not sufficient for identifying the presence or amount of refugia that were able to persist during and after the 2014 to 2016 marine heatwave (Finger et al., 2021). These data often failed to capture microclimatic habitats that were smaller than the coverage of a single Landsat pixel (900 m^2), which could potentially provide important refugia (Asner et al., 2022).

The development of CubeSat constellations has enabled a workaround for these tradeoffs, as the integration of data from multiple satellites collectively achieves higher frequency data sampling, with the ability to acquire global coverage at high spatial resolution. Planet is one of the most recognized CubeSat constellation operators, and their PlanetScope constellation contains nearly 130 active satellites. The PlanetScope CubeSats provide daily observations at 3

m resolution for many global areas (Roy et al., 2021), and so they show great potential for monitoring fine-scale ecological dynamics (e.g., flowering events) across multiple years, at large spatial scales, and in heterogeneous landscapes (Dixon et al., 2021; Zeng et al., 2020). However, considerable geolocation inaccuracy and radiometric inconsistency between satellites and sensors remain as major challenges to the general applicability of the PlanetScope constellation for measuring environmental dynamics (Frazier and Hemingway, 2021; Leach et al., 2019). While PlanetScope data have been successfully used to detect other species of floating macroalgae (*Macrocystis pyrifera*), these methods were not automated and required manual delineation of over 75 images (Elsmore et al., 2022).

In this study, we develop and validate a model for deriving bull kelp canopy from a time series of PlanetScope CubeSat data. The PlanetScope constellation offers the high spatial (3 m) and temporal (near daily) means for mapping bull kelp refugia, and the first image collections coincide with the last statewide aerial survey conducted by CDFW in 2016. The model uses spectral features to predict bull kelp presence, and we apply it to derive annual maps of canopy coverage in northern California from 2016 to 2021.

2.2 Methods

2.2.1 Study Region

Bull kelp is distributed in the northeast Pacific from San Luis Obispo County in California to Unimak Island in the eastern Aleutians (Abbott et al., 1992; Miller and Estes, 1989). Our study area included the Sonoma and Mendocino County coastlines in northern California, extending approximately 215 km from north to south (Fig. 1). This region was

historically productive and supported abundant bull kelp forests prior to the collapse that started in 2014 (Rogers-Bennett and Catton, 2019).

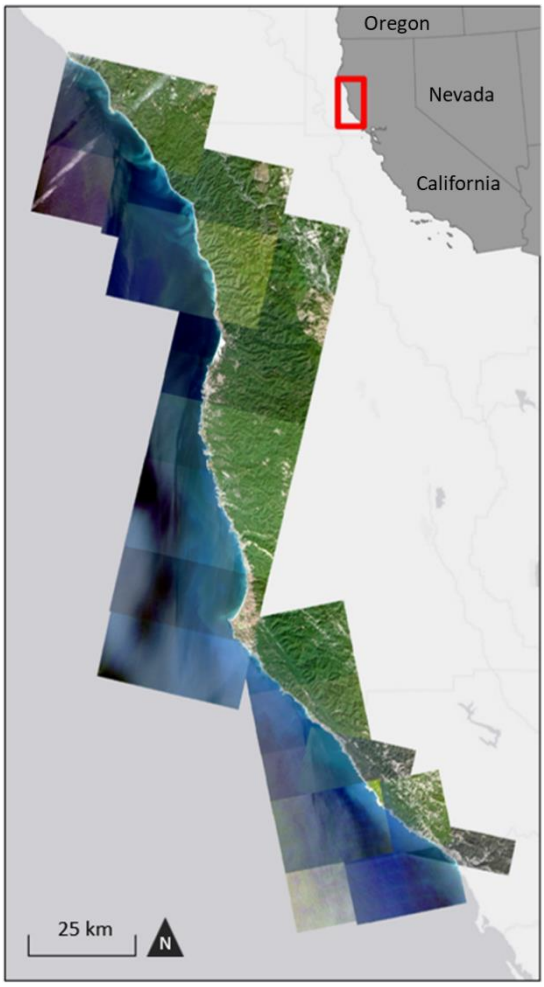

Fig. 2.1. Sonoma and Mendocino County regions of northern California overlaid with images from multiple PlanetScope satellites.

2.2.2 Image Acquisition

PlanetScope 4-band Surface Reflectance data were acquired from Planet Explorer. PlanetScope images are generated from the PlanetScope satellite constellation, which contains

over 130 operational 3U CubeSats (10 x 10 x 30 cm) and provides imagery at near-daily resolution. Each sensor has an approximate ground resolution of 3 m (Planet, 2021). We acquired each pixel in the study area at ~ weekly resolution (about 5 images per month) during September and October from 2016 to 2021, resulting in a total of 2,070 images. Bull kelp is an annual species and will typically undergo a full lifecycle within one calendar year. Individuals appear in the early spring, grow to canopy height by mid-summer, and reach maximum photosynthesis and canopy area in the fall before senescing in winter (Nicholson, 1970; Vadas, 1972). Imagery from September and October capture the period of peak abundance, making these months ideal for estimating refugia occupancy during and after each heatwave year. We manually digitized the coastline using PlanetScope imagery taken at low tide and masked pixels found within the coastline boundary. We masked pixels within 10 m of the identified coastline to reduce potential misclassification from intertidal algae and terrestrial vegetation. We also masked pixels greater than 3 km from the coastline to improve data processing times, as kelp has not historically been identified this far offshore (CDFW, 2021).

2.2.3 Image Processing

Merging data from the PlanetScope constellation to derive consistent kelp canopy maps through time presents various challenges, as PlanetScope sensors are not uniform across each satellite. All sensors provide four spectral bands (blue, green, red, NIR) and the same approximate ground resolution, but Planet has introduced sensor cohorts with varying relative spectral responses and levels of noise (Planet, 2021). These cohorts are distinguished using unique 2-character satellite identification (ID) codes, which currently include 0c, 0d, 0e, 0f, 10, 11, and 20 (Planet, 2021). A number of studies have proposed methods for normalizing

radiometric inconsistencies among PlanetScope data, but these often rely on image spectra from reference datasets such as Landsat 8 (Leach et al., 2019) and Sentinel-2 (Latte and Lejeune, 2020). Co-registering PlanetScope data with a reference dataset is difficult over coastal areas, as even minute differences in temporal capture may introduce significant error between pixel matchups (i.e., tides and currents). Furthermore, geolocation accuracy has been highlighted as a challenge by a number of studies that have applied these data for coastal analyses (Leach et al., 2019; Traganos et al., 2017; Wicaksono and Lazuardi, 2018).

We applied a log-residual correction (Green and Craig, 1985) to all surface reflectance images to standardize spectral reflectance values taken by different sensors in the PlanetScope constellation using the function *logResiduals* in Matlab 2020a. The log residual correction divides the spectrum of each pixel by the spectral geometric mean (mean of all bands for each pixel) and the spatial geometric mean (mean of all pixels for each band), before finally multiplying the output by the mean of all pixels in all bands (Eq. 1). This has been shown to help remove the effects of solar irradiance, atmospheric transmittance, instrument gain, and topographic effects from image data (Ganesh et al., 2013; Green and Craig, 1985). All calculations are performed using logarithms of the data values.

$$L = |e^{input\ data - spectral\ mean - spatial\ mean + entire\ mean}| \qquad \text{(Eq. 1)}$$

We applied the Usable Data Mask asset supplied in the PlanetScope image bundle to mask any pixels identified as unusable by Planet (i.e., sensor error, image artifacts, etc.). The Usable Data Mask 2 (UDM2) product was not used, as it was introduced by Planet in August 2018 (Planet, 2021) and was not consistently available for our imagery. We additionally masked

pixels altered by sun glint and crashing waves using gray-level co-occurrence matrices (GLCM).

2.2.4 Kelp Canopy Classification

Bull kelp can be visually distinguished from water with high resolution satellite imagery (Fig. 2). Similar to terrestrial vegetation, emergent kelp canopy prominently reflects the NIR wavelength range (700 to 1000 nm). Due to the high absorbance of water in the NIR, this region of the electromagnetic spectrum is advantageous for distinguishing floating canopy from the surrounding seawater (Fig. 2; Cavanaugh et al., 2021; Timmer et al., 2022). We manually classified a total of 93 images (~3 images per month from 2017 to 2019) covering a bull kelp bed off the coast of Ella Beach in British Columbia (48.363°, -123.757°) into two classes, 'kelp' and ‘water' to capture data covered by different PlanetScope satellites, acquisition times, and view angles.

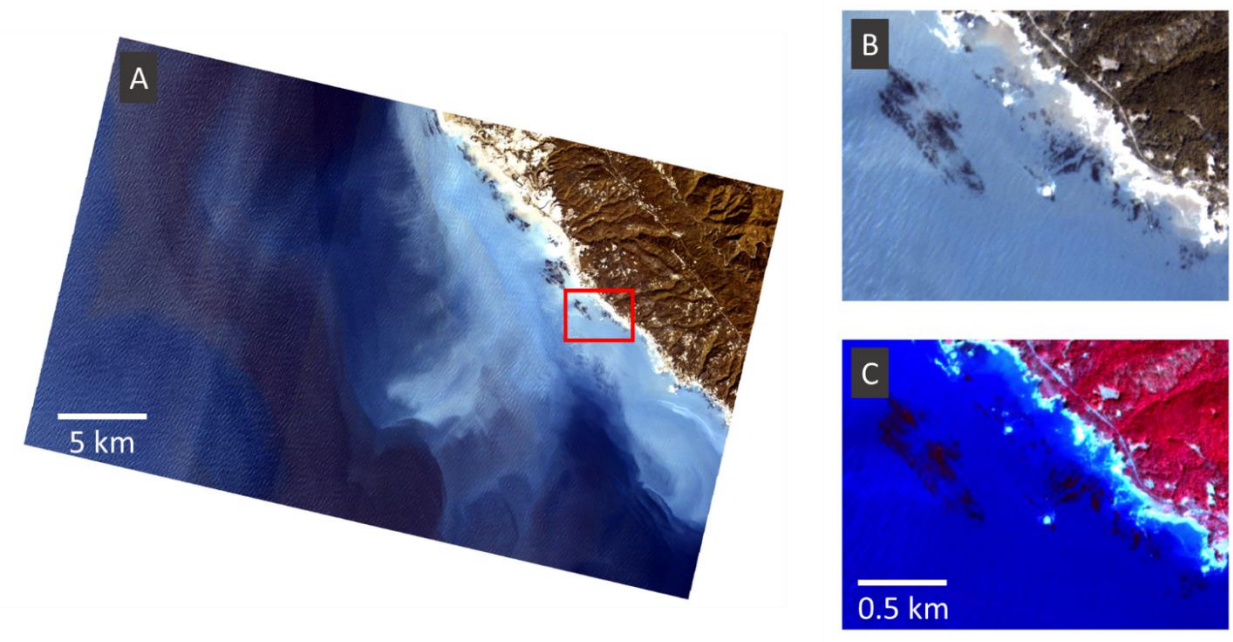

Fig. 2.2. A full PlanetScope scene from September 30, 2021 (A) in northern California that includes bull kelp surface canopy. Emergent canopy is visibly distinguishable in true color (B) and false color (C) composites.

These data were used to train a two-class Naïve Bayes classifier, as previous work has shown that Naïve Bayes classifiers consistently yielded higher Kappa values than support vector machines (SVM), random forest models, and artificial neural networks when trained with PlanetScope imagery (Kranjčić and Medak, 2020). Naïve Bayes is a probabilistic supervised machine learning approach based on Bayes theorem (Park, 2016; Eq. 2).

$$P(A|B) = \frac{P(B|A)P(A)}{P(B)} \qquad \text{(Eq. 2)}$$

Where, in the context of using corrected reflectance data from the PlanetScope constellation to predict the probability of kelp presence in each PlanetScope pixel, *A* refers to kelp presence and *B* refers to a vector of PlanetScope reflectances for each band. Therefore, P(A|B) is the conditional probability that kelp is present given the reflectance measurements from different spectral bands. The algorithm deduces a prior probability distribution from the provided training data for all bands in the 'kelp' and 'water' classes (P(A)). The prior probability is multiplied by a likelihood function (P(B|A)), which is the probability distribution of data with the same predictors (i.e., an unclassified image), but an unknown class (Ahmad and Quegan, 2012; Ahmad et al., 2021). The probability distribution of the data were assumed to be normal.

We applied the resulting classifier to images taken in September and October from 2016 to 2021 to obtain the probability of pixels containing kelp in each image. We calculated monthly

pixel-wise averages of probabilities and classified pixels that exceeded probabilities of 0.5 (i.e., the maximum probability for a 2-class classification) as kelp (Fig. 3). Aggregating the probability data on monthly time-steps aided in reducing error and labor-intensive manual editing due to misclassifications from radiometric and geometric issues with individual images.

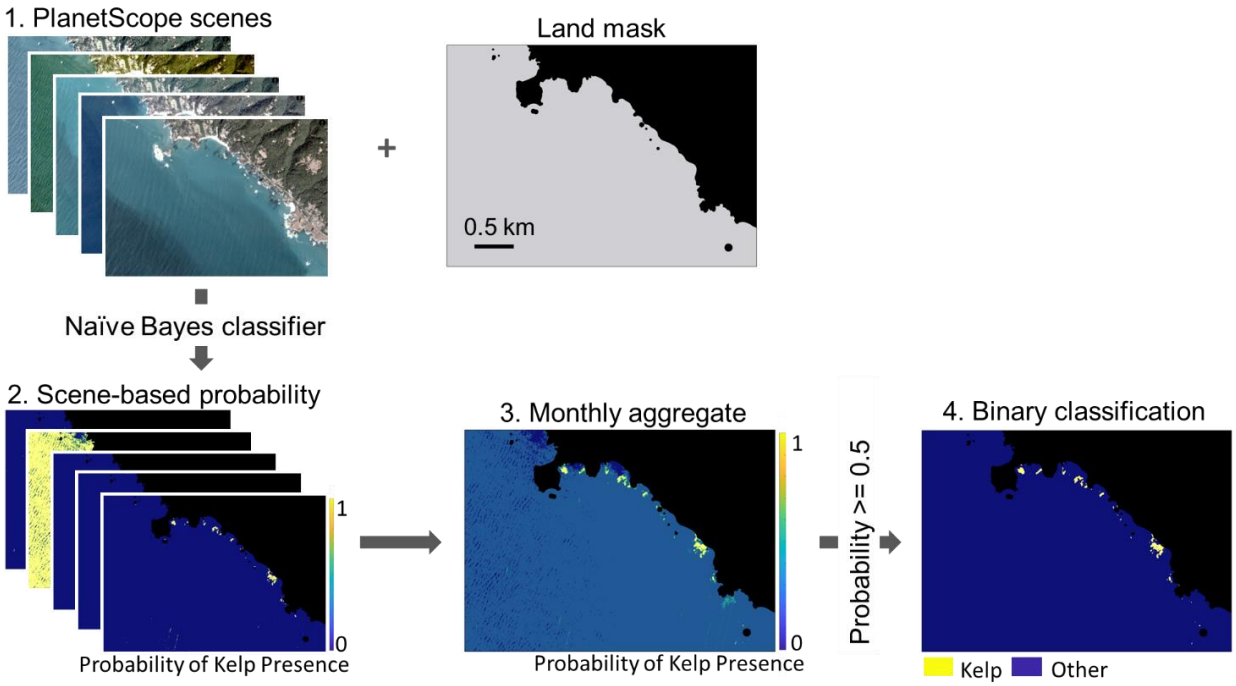

Fig. 2.3. Conceptual diagram of the automated portion of the kelp canopy detection scheme. Binary classifications were manually edited to remove any potential remaining image artifacts.

2.2.5 Kelp Canopy Map Validation

To validate our kelp canopy classifications, we used ordinary least squares (OLS) regressions to compare PlanetScope-derived kelp canopy area estimates to three published datasets that have classified kelp canopy in northern California between 2016 and 2021. The first validation dataset included high resolution kelp canopy classifications derived from occupied

aircraft surveys hosted through CDFW. CDFW aerial surveys were collected between late summer and winter. The first aerial survey was conducted in 1989, and the second was conducted in 1999. They began collecting aerial data annually from 2002 to 2016, although some years and regions were not completed due to budget constraints, cloud cover, inclement weather, etc. (CDFW, 2021). The surveys contain complete coverage of Sonoma and Mendocino counties for 9 years (1989, 1999, 2003-2005, 2008, and 2014-2016), with partial coverage for 4 years (2002, 2009, 2010, and 2013). The data were originally collected at ~ 25 cm and were later resampled to 2 m internally at CDFW. PlanetScope data and CDFW data spatially overlap in 2016, and these data were used for comparison of kelp canopy area estimates. We converted the 2016 CDFW classification from a shapefile to 3 m pixels corresponding to the 3 m grid of PlanetScope imagery. We binned the northern California coastline into 1 km coastline segments and calculated the total kelp canopy area in each segment estimated by both CDFW and PlanetScope. CDFW data distinguish floating and submerged kelp canopy, and the submerged canopy class was excluded from the validation analysis.

The second validation dataset included classifications derived from UAV surveys of kelp canopy that were conducted along the coastline of Mendocino and Sonoma counties in 2019 (number of samples (n) = 25), 2020 (n = 32), and 2021 (n = 34; Saccomanno et al., 2022). The surveyed sites varied in size from 0.16 to 1.48 km^2. Expert classifiers manually selected and applied thresholds to the Red-Blue vegetation index used to derive kelp canopy in all UAV images, with a final resolution of ~ 3 cm (Cavanaugh et al., 2021). We extracted the overlapping areas between each UAV surveyed site and the respective PlanetScope classifications and performed a site level comparison of kelp canopy area.

Last, we performed validations against Landsat satellite imagery (Bell et al., 2022). In this dataset, bull kelp canopy was estimated at 30 m resolution from 1984 to 2021 at quarterly intervals following methods from Cavanaugh et al., 2011 and Bell et al., 2020. Briefly, a binary decision tree was applied to Landsat Level 2 Surface Reflectance images to identify canopy presence, and MESMA was applied to pixels with canopy presence to estimate fractional coverage of kelp and seawater (Bell et al., 2020). We extracted and composited Landsat-derived classifications from the third (July to September) and fourth (October to December) quarter of each year between 2016 and 2021. We binned the northern California coastline into 1 km coastline segments and calculated the total kelp canopy area in each segment estimated by both Landsat and PlanetScope. The CDFW, UAV, and PlanetScope datasets each represented kelp coverage as presence/absence, and to maintain consistency, the Landsat dataset was converted to presence/absence. If a Landsat pixel contained kelp canopy area above 0, kelp was considered present in that pixel (900 m^2).

2.2.6 Effect of Spatial Scale on Refugia Detection

Each dataset has its own lower detection limit of kelp canopy, and quantifying subpixel detection limits has implications for the local and regional application of aerial estimates. Calculating these uncertainties is often performed using comparisons against higher resolution sensors, which likely provide estimates closer to 'ground truth' data (Wang and Hu, 2021). To determine the effect of spatial scale on refugia detection, we used the UAV-based classifications to calculate the percentage of a PlanetScope pixel (9 m^2) and a Landsat pixel (900 m^2) that needs to be occupied by kelp canopy for the classification scheme to detect kelp presence. These calculations could not be performed for CDFW data, as they did not temporally overlap with any

of the UAV flights. We identified all pixels that were misidentified as ‘not kelp’ in the PlanetScope and Landsat classifications (false negatives) when compared to overlapping UAV pixels that estimated canopy presence in the same location. Of this subset, we randomly selected pixels that were 150 m apart to minimize the effects of spatial autocorrelation in the pixel-wise analyses. We calculated the percentage of the PlanetScope and Landsat pixels that were occupied by kelp canopy in the UAV images and used the pixel fractions to determine a threshold for refugia detection.

2.2.7 Distribution of Refugia

Bull kelp on the north coast of California has been characterized by a prolonged collapse, and a multi-year perspective can provide insight to where, and why, remnant populations have been able to persist. We define refugia as persistent kelp pixels that occurred in at least three of the six years immediately following the marine heatwave between 2016 and 2021. For 2016, we used kelp locations in both the CDFW and PlanetScope classifications. The three occurrences did not have to be consecutive.

To find the maximum historical kelp canopy extent observed prior to the marine heatwave, we merged the extents of all CDFW aerial survey shapefiles that identified floating canopy (with either total or partial coverage of the study area) taken between 1989 and 2015. The maximum historical kelp canopy extent was used as a proxy for kelp habitat, i.e., any place that kelp canopy has been observed in the historical record. The maximum extent shapefile was converted to a raster with a pixel size of 3 m corresponding to the 3 m grid of PlanetScope imagery. We used these data to identify pixels that have been occupied by kelp canopy in the past, representing suitable kelp habitat but not refugia.

2.3 Results

2.3.1 Kelp Canopy Classification and Validation

The training data for the Naïve Bayes classifier consisted of 93 images, which included data from 57 different satellites across 3 satellite cohorts (0e, 0f, 10). The log residual correction helped to increase separability between kelp and water classes in the training data across each satellite cohort, particularly in the blue and green bands compared to raw reflectance values (Fig. 4). The log residual correction also lowered the average coefficient of variation for the wavelengths in both the kelp (43.82 and 14.86, respectively) and water (45.90 and 8.06, respectively) classes. The kelp class exhibited high variability in the NIR before and after the correction was applied, but the values were higher than water on average (Fig. 4). The correction was applied to 2,070 images, which included data from 187 satellites across 4 satellite families (0e, 0f, 10, 20).

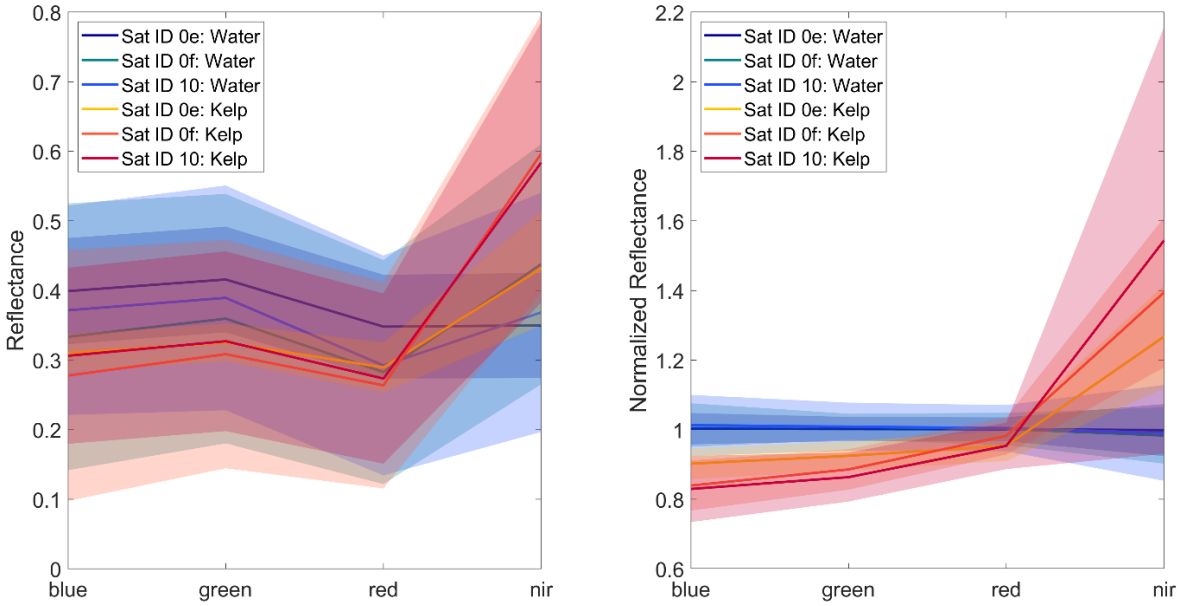

Fig. 2.4. Mean reflectance (solid line) and standard deviation (shaded region) of training data for each satellite cohort (0e, 0f, and 10) before (left) and after (right) the log residual correction was applied.

The PlanetScope-derived kelp canopy estimates agreed with regional CDFW classifications ($R^2 = 0.38$, $p < 0.001$, slope = 0.61; Fig. 5b) and regional Landsat classifications ($R^2 = 0.49$, $p < 0.001$, slope = 1.00; Fig. 5c) based on 1 km coastline partitions. PlanetScope estimates were also strongly correlated with UAV estimates of kelp area at the site level ($R^2 = 0.70$, $p < 0.001$, slope = 0.84; Fig. 5a). PlanetScope underestimated kelp canopy area compared to UAV in 2019 and 2020, but overestimated canopy area in 2021. False positives were rarely identified in the PlanetScope data compared to UAV (2% of all water pixels across all years).

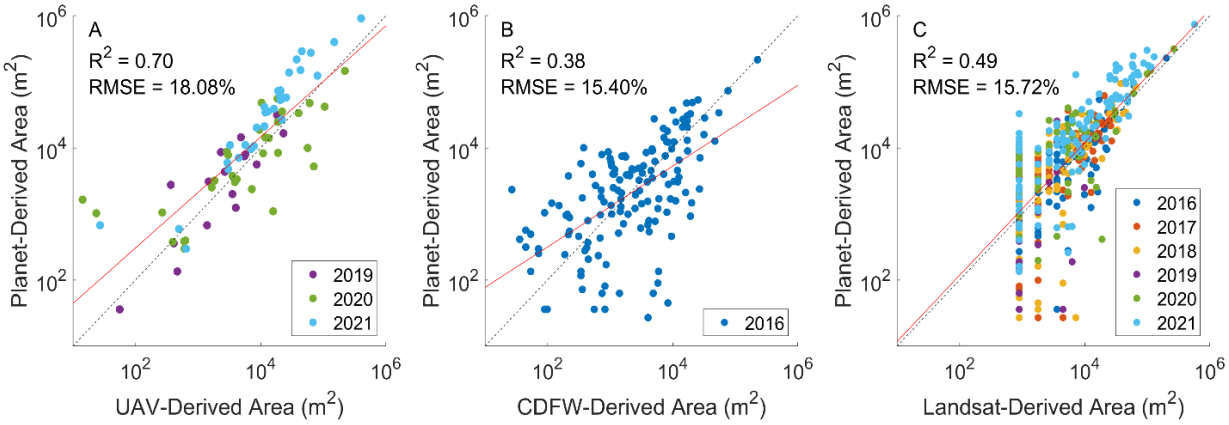

Fig. 2.5. Comparison of bull kelp canopy area estimates between PlanetScope and data from UAV (A), CDFW (B), and Landsat (C) between overlapping locations. Dataset pairs were captured using different temporal aggregations (UAV and CDFW = daily, PlanetScope = monthly, Landsat = quarterly), but each cover at least one day during the peak kelp canopy season in northern California (September to October). The dotted line shows 1:1 relationship, while the red lines are the linear fits in log space.

All three comparisons had the best agreement when kelp canopy area was relatively high (between 0.1 and 1 km^2). However, differences in estimates were most pronounced in locations with low kelp canopy. To characterize these differences, we found the pixels that were misidentified as water in the PlanetScope and Landsat classifications when compared to overlapping UAV pixels that estimated canopy presence. We plotted the number of false negative detections as a function of percent occupancy within that pixel (identified from the UAV classifications) and found that the number of false negatives exponentially decayed as the percent occupancy of kelp within a PlanetScope and Landsat pixel increased (Fig. 6). For both PlanetScope and Landsat, the number of false negative detections began to converge to 0 when kelp occupancy was close to 20% of a single pixel (1.8 m^2 for PlanetScope and 180 m^2 for

Landsat; Fig. 6). This agrees with previous work that demonstrated Landsat has a higher likelihood of missing a pixel that contains kelp if it is occupied by less than 20% kelp canopy (Hamilton et al., 2020). Landsat missed nearly twice as many kelp pixels than PlanetScope at very low percent occupancy (i.e., less than 10%; Fig. 6).

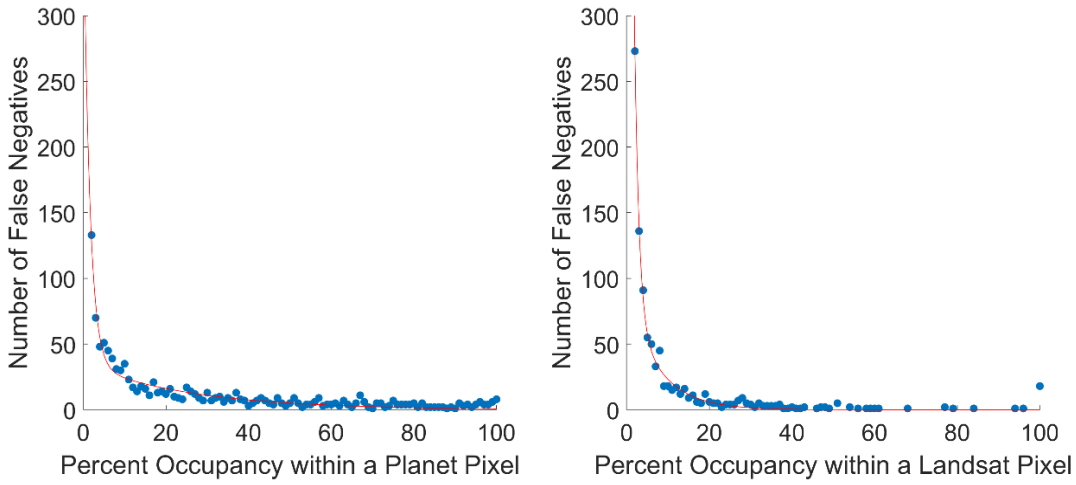

Fig 2.6. Number of false negative kelp detections from both PlanetScope (left) and Landsat (right) as a function of the percent occupancy identified from the UAV classifications.

2.3.2 Kelp Canopy Time Series

The combined effects of a marine heatwave and overgrazing of urchins led to a collapse in bull kelp abundance along the north coast of California (Rogers-Bennett and Catton, 2019), and there was a pronounced lack of bull kelp recovery through 2021, with kelp abundance remaining at historically low levels (Fig. 7). Generally, there was good correspondence among Landsat, CDFW, and PlanetScope estimates, indicating that each method is adequate for analyzing kelp abundance at regional scale. Landsat and CDFW data both agree that bull kelp canopy showed high interannual variability in the years leading up to the heatwave (1984 to 2013), although Landsat provided a much more comprehensive record of canopy abundance

during this period (n = 30) compared to CDFW (n = 6). After the onset of the heatwave in 2014, Landsat and CDFW both detected large losses, which were sustained throughout the duration of the heatwave. CDFW and PlanetScope only overlap in 2016, but the two have generally good agreement (1.21 and 1.18 km^2, respectively). In late 2016 and early 2017, temperature anomalies began returning to near-normal levels (McPherson et al., 2021). However, kelp populations only slightly recovered from 2017 to 2021. PlanetScope was able to consistently detect a higher annual abundance than Landsat (0.9 km^2 on average) despite the low abundance present.

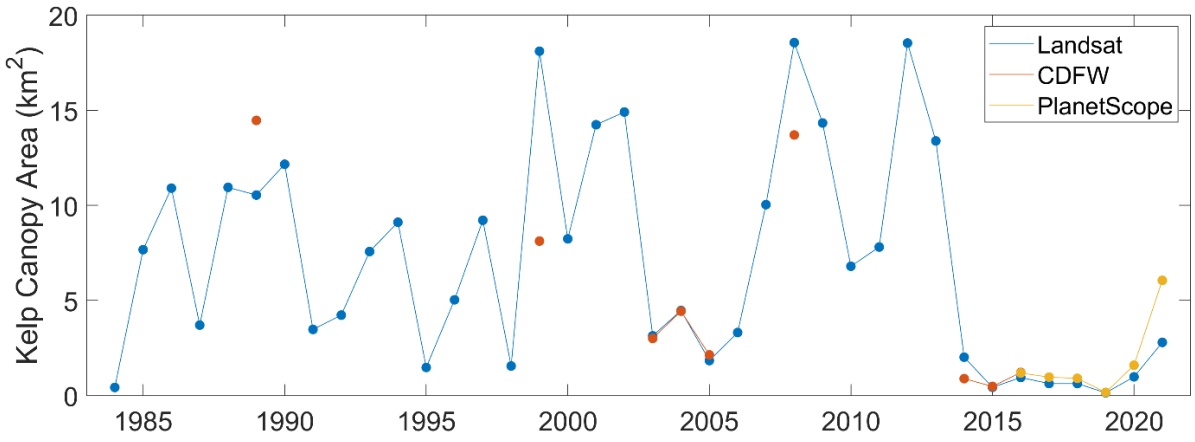

Fig. 2.7. Kelp canopy area in northern California from 1984 to 2021 from Landsat, CDFW, and Planet-Scope derived estimates. CDFW and PlanetScope overlap in 2016, but the two have generally good agreement (1.21 and 1.18 km^2, respectively).

2.3.3 Distribution of Refugia

In Sonoma and Mendocino counties, there was a total of 35.97 km^2 of suitable bull kelp habitat, as defined by areas where kelp canopy was present during at least one year between 1989 and 2021. We identified 0.718 km^2 of kelp refugia (areas where kelp was present in at least

3 of the 6 years between 2016 and 2021), comprising 2% of the total available habitat and 9.4% of the average canopy area observed prior to 2014 from CDFW. To assess spatial patterns in refugia occupancy across the study area, we aggregated the data to 1 km x 1 km grid cells and calculated the abundance of refugia compared to the abundance of historical habitat within each grid cell (Fig. 8). Refugia were almost completely absent in the northern portion of the study area between a latitudinal range of 39°3’ to 40°0’, aside from a few small, persistent beds near Point Delgada and Abalone Point (Fig. 8). Refugia abundance increased just north of Noyo Bay to Elk, where 61.6% of the 1 km grid cells were occupied by refugia at abundances ranging from 0.01 to 36.23% of total available habitat. However, refugia occupied less than 3% of potential habitat in this area on average (2.52% ± 5.19%). Refugia were sparsely populated south of Elk through Point Arena, where occupancy increased again along the coastline to Sea Ranch (Fig. 8). From Point Arena to Sea Ranch, 54.55% of the 1 km grid cells were occupied by refugia at abundances ranging from 0.05 to 34.36% of total available habitat. Here, refugia occupied a slightly higher percentage of potential habitat than the region between Noyo Bay and Elk on average (6.66% ± 7.67%). Refugia presence decreased in the southern portion of the study area from Sea Ranch to Jenner, where only 19.39% of grid cells were occupied, with a maximum occupancy of just 2.14% (Fig. 8).

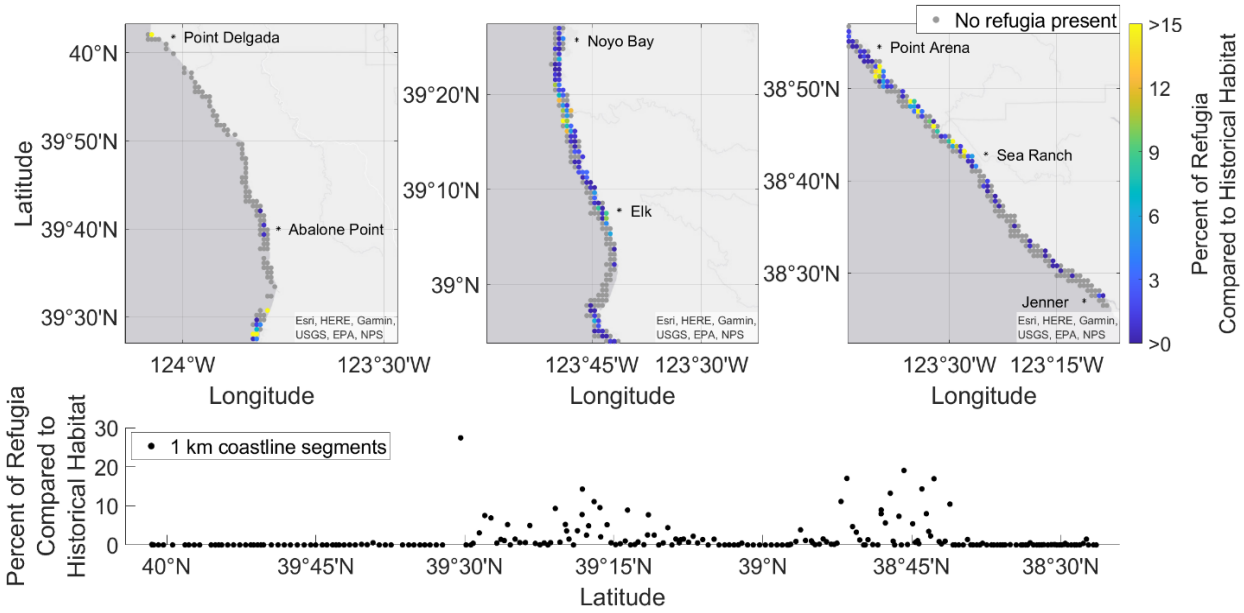

Fig. 2.8. The percentage of bull kelp refugia occupancy in 1 km grid cells compared to available habitat in the same locations from the northernmost (left) to southernmost (right) portions of the study area. Grey areas represent locations that were historically occupied by kelp canopy but were not occupied by refugia. The bottom panel represents the latitudinal variation in refugia occupancy from north to south along 1 km coastline segments.

2.4 Discussion

2.4.1 Comparison of Kelp Canopy Detection Approaches

Our new method for mapping bull kelp canopy from Planet satellite imagery demonstrates that CubeSat data are an effective tool for detection and regional monitoring during years of low kelp canopy coverage and density. The PlanetScope-derived kelp canopy estimates were similar to maps created from high resolution occupied and unoccupied aerial surveys, as well as the Landsat satellites. We expected variation in kelp canopy estimates among each dataset, as the method of detection and spatial and temporal resolutions differed, and therefore so

did their detection capability of floating canopy. The method we present in this manuscript relied on developing relationships between kelp canopy area and image-derived spectral features (i.e., band reflectance values) using manually classified data for training points. We found it difficult to create robust classifiers or models that were accurate across different images and satellites, but our spectral normalization and temporal aggregation scheme helped address the radiometric and geometric inconsistencies both within and between PlanetScope satellite images. Our monthly composite classifications provide spatially and temporally continuous maps of bull kelp coverage at finer scale than previously possible. These approaches could be applied to other applications where increased noise or geolocation inaccuracy in individual images caused a propagation of errors during classification (Cannistra et al., 2021; Wicaksono and Lazuardi, 2018; Xu et al., 2020).

PlanetScope consistently underestimated kelp canopy area compared to UAV classifications in 2019 and 2020, which can be explained by the resolution mismatch between the two datasets. Kelp canopy was the lowest on record in northern California in 2019 and remained low in 2020, resulting in few areas with high kelp abundance. The stipes and blades of the sparsely populated bull kelp individuals were visible in the UAV imagery, and therefore these data were able to capture nearly all floating kelp canopy present at each site. For PlanetScope, the classifications were most comparable to UAV when kelp occupancy was greater than or equal to 20% of a single pixel (i.e., ~ 1.8 m^2 of kelp), and so kelp coverage was likely lower than this threshold in many areas during 2019 and 2020. However, there were some signs of recovery in 2021, with increased bull kelp coverage and densities along the coastline. PlanetScope consistently overestimated kelp canopy compared to UAV during this period. The PlanetScope classifications provide a presence/absence metric and do not describe the amount of canopy

coverage at the pixel level. Here, there was likely a higher proportion of pixels occupied by less than 100% canopy coverage, resulting in overclassifications compared to UAV.

Although the CDFW and PlanetScope classifications offered similar spatial resolutions (2 m and 3 m, respectively) there were greater differences between PlanetScope and CDFW along sections of coastline with low bull kelp abundance. The CDFW classifications were derived from aerial data collected on a single date, while the PlanetScope classifications were generated from multiple images throughout September and October of each year. As a result, these datasets were not representing canopy conditions under equivalent tidal height and current stages, which have the potential to impact the amount of kelp detected on the surface. As tidal height and current speeds increase, they can significantly reduce the amount of kelp canopy present (Britton-Simmons et al., 2008; Cavanaugh et al., 2021), which may have contributed to the variability at lower kelp abundances. Additionally, there are several scenarios that could occur for the PlanetScope-based classifications to exclude kelp from a region with kelp presence. For example, if a large kelp bed were present and detected by PlanetScope in one image in the beginning of the month, but a wave event caused mass dislodgement and mortality, the remainder and majority of the month would have no kelp canopy presence, resulting in a monthly classification of no kelp canopy presence (despite the classification scheme containing one accurate detection).

The 35+ year archive of Landsat data provides a spatially and temporally consistent record of kelp canopy coverage (Wulder et al., 2012). Cost-free access to the Landsat archive since 2008 has allowed for significant methodological and ecological advancements in kelp remote sensing (Kennedy et al., 2014), including the creation of seamless data products in formats suitable for non-experts (i.e., Bell et al., 2022). While commercial optical sensors such

as PlanetScope have provided new opportunities for mapping kelp canopy at finer spatial scale than the Landsat archive (Pettorelli et al., 2014), the costs associated with the data may not be feasible for some research projects that require long-term monitoring of ecological processes, which occur over decades to centuries and at spatial scales across hundreds of kilometers (Reed et al., 2015). The choice of remote sensing and analytic data approaches is dependent upon research objectives and duration of funding (Cavanaugh et al, 2021).

For example, Landsat has been shown to significantly underestimate the amount of floating bull kelp canopy during years of low abundance, including during the 2014 to 2016 marine heatwave (Finger et al., 2021). At a local scale, Landsat was unable to capture refugia if they occupied less than 20% of a pixel (180 m^2). This limitation reduces the potential of Landsat for capturing the spatial complexity of refugia (i.e., small, sparse, and fringing beds) or even identifying their presence altogether. Refugia dynamics require a sensor that can capture fine scale patterns in kelp bed size, shape, and area - particularly in populations that are relatively close to the coastline, which is a challenge for moderate resolution sensors (Bell et al., 2020; Finger et al., 2021; Hamilton et al., 2020). Despite methodological differences, the general agreement between PlanetScope, UAV, CDFW, and Landsat-based classifications supports its applicability for detecting refugia.

The spatial and temporal coverage of PlanetScope data make them a favorable monitoring resource in the coastal zone, as regional imagery is available for download in near real time. Coastal variability is influenced by drivers that operate on timescales of hours (i.e., tides) to days (i.e., marine heatwaves and storm events) to decades (i.e., sea level rise and ocean acidification), and the magnitude of change can range from centimeters to hundreds of kilometers (Muller-Karger et al., 2018). Due to the dynamic nature and spatial complexity of

coastal targets, this study has demonstrated that the high-frequency sampling and high spatial resolution provided by PlanetScope CubeSats has been a successful resource for mapping bull kelp. Other studies have demonstrated the applicability of CubeSat constellation data for other coastal foundation species, including seagrasses (Tamondong et al., 2018; Wicaksono and Lazuardi, 2018) and corals (Asner et al., 2017; Li et al., 2020; Yamano et al., 2020). In contrast, the CDFW surveys were not completed during some years and regions due to budget constraints, cloud cover, inclement weather, etc., and the last successful survey was completed in 2016 (CDFW, 2021). The spatial and temporal coverage of drone operations are limited by battery life, wind, weather, and regulatory limitations (Gray et al., 2022) making them inefficient for monitoring efforts over large scales. While the Landsat satellites provide the most spatially and temporally comprehensive dataset, they have a higher detection limit than PlanetScope, introducing complications for refugia detection.

2.4.2 Distribution of Bull Kelp Refugia

In 2014, the once extensive and persistent bull kelp forests in northern California shifted to urchin barrens (Rogers-Bennett and Catton, 2019). Our analysis of PlanetScope imagery showed that there was a pronounced lack of bull kelp recovery through 2020, with some potential recovery in 2021, although kelp abundance still remained at historically low levels. However, we identified pockets of refugia that persisted throughout the marine heatwave and urchin outbreak. There is evidence that refugia function as source populations for extirpated locations that were more sensitive to disturbance within kelp and other ecological communities, which is the first step for species recolonization (Johnson and Mann, 1988; Landesmann and Morales, 2018). However, environmental conditions impact both the persistence of refugia and

the subsequent success of re-establishment, making refugia locations and their environmental drivers valuable information for monitoring, conservation, and restoration efforts.

Between 2016 and 2021, northern California bull kelp refugia occupied 0.718 km^2 of the coastline. This accounted for about 2% of the total available kelp habitat in the region, and about 9.4% of the average canopy area observed prior to 2014. In a recent publication, McPherson et al. (2021) documented the spatial and temporal variability of bull kelp canopy area in northern California from 1985 to 2019 along 90 m latitudinal bins, and their patterns of kelp abundance were closely related to our maps of refugia presence north of Point Arena. For example, a small abundance of bull kelp refugia was found from Fort Delgada to Noyo Bay and from Elk to Point Arena. McPherson et al. (2021) show a lack of persistence of kelp canopy along the same latitudinal gradients, which indicates that these areas were unsuitable for bull kelp growth during most years in their time series and were not disproportionately impacted by the effects of the heatwave. However, a small abundance of bull kelp refugia was also found south of Point Arena from Sea Ranch to Jenner. While McPherson et al. (2021) show low kelp canopy abundances in this region after 2014, the area displays high persistence throughout the rest of the time series (1985 to 2013), indicating that the area was suitable for persistent historical kelp growth, but was unsuitable for refugia.

2.5 Conclusion

In 2014, the once extensive and persistent bull kelp forests in northern California shifted to urchin barrens. This study demonstrates strong potential for using CubeSat data for monitoring these regional bull kelp populations with local-level precision. Using these data, we show that northern California has continued to support refuge bull kelp populations despite widespread and

unprecedented declines. As a foundation species, understanding the local-scale factors that support bull kelp refugia is important for informed protection and management, helping to ensure the future of this species as it continues to face climate variability and change.

2.6 Description of Author Responsibilities

Ka.C.C. and Ky.C.C. conceptualized the study. Ka.C.C., C.C.P., and V.R.S. organized and processed the remote sensing imagery, and Ka.C.C. and T.W.B. performed validation of the methods. Ka.C.C. conducted the analysis and Ky.C.C. helped to assess and interpret the results. Ka.C.C. prepared the original draft and all authors reviewed and edited the manuscript.

2.7 Acknowledgements

This work was supported by The Nature Conservancy, Ocean Protection Council, and NASA Ocean Biology & Biogeochemistry [80NSSC21K1429]. The authors would like to acknowledge the Planet Open California program and the Planet Education and Research program, which provided data for the early stages of this research. We would like to thank the field and laboratory technicians who helped in the collection and processing of the PlanetScope and UAV data.

2.8 References

Abbott, I.A., Isabella, A., Hollenberg, G.J., 1992. Marine Algae of California. Stanford University Press.

Ahmad, A., Quegan, S., 2012. Analysis of Maximum Likelihood classification on multispectral data. Appl. Math. Sci. 6, 6425–6436.

Ahmad, A., Sakidin, H., Sari, M.Y.A., Amin, A.R.M., Sufahani, S.F., Rasib, A.W., 2021. Naïve Bayes classification of high-resolution aerial imagery. Int. J. Adv. Comput. Sci. Appl. 12.

Andrew, M.E., Warrener, H., 2017. Detecting microrefugia in semi-arid landscapes from remotely sensed vegetation dynamics. Remote Sens. Environ. 200, 114–124.

Ashcroft, M.B., 2010. Identifying refugia from climate change. J. Biogeogr. 37, 1407–1413.

Asner, G.P., Martin, R.E., Mascaro, J., 2017. Coral reef atoll assessment in the South China Sea using Planet Dove satellites. Remote. Sens. Ecol. 3, 57–65.

Asner, G.P., Vaughn, N.R., Martin, R.E., Foo, S.A., Heckler, J., Neilson, B.J., Gove, J.M., 2022. Mapped coral mortality and refugia in an archipelago-scale marine heat wave. Proc. Natl. Acad. Sci. U.S.A. 119, e2123331119.

Bell, T.W., Allen, J.G., Cavanaugh, K.C., Siegel, D.A., 2020. Three decades of variability in California's giant kelp forests from the Landsat satellites. Remote Sens. Environ. 238, 110811.

Bell, T.W., Cavanaugh, K.C., Siegel, D.A., 2022. SBC LTER: Time series of quarterly NetCDF files of kelp biomass in the canopy from Landsat 5, 7 and 8, since 1984 (ongoing) ver. 18. Environmental Data Initiative. https://doi.org/10.6073/pasta/5fa36b985f30ee04d4771af2288aedd4.

Blowes, S.A., Supp, S.R., Antão, L.H., Bates, A., Bruelheide, H., Chase, J.M., Moyes, F., Magurran, A., McGill, B., Myers-Smith, I.H., Winter, M., Bjorkman, A.D., Bowler, D.E., Byrnes, J.E.K., Gonzalez, A., Hines, J., Isbell, F., Jones, H.P., Navarro, L.M., Thompson, P.L., Vellend, M., Waldock, C., Dornelas, M., 2019. The geography of biodiversity change in marine and terrestrial assemblages. Science 366, 339–345.

Britton-Simmons, K., Eckman, J.E., Duggins, D.O., 2008. Effect of tidal currents and tidal stage on estimates of bed size in the kelp Nereocystis luetkeana. Mar. Ecol. Prog. 335, 95–105.

Cacciapaglia, C., van Woesik, R., 2015. Reef-coral refugia in a rapidly changing ocean. Glob. Change Biol. 21, 2272–2282.

Cannistra, A.F., Shean, D.E., Cristea, N.C., High-resolution CubeSat imagery and machine learning for detailed snow-covered area. Remote Sens. Environ. 258, 112399.

Cavanaugh, K.C., Siegel, D.A., Reed, D.C., Dennison, P.E., 2011. Environmental controls of giant-kelp biomass in the Santa Barbara Channel, California. Mar. Ecol. Prog. Ser. 429, 1–17.

Cavanaugh, K.C., Cavanaugh, K.C., Bell, T.W., Hockridge, E.G., 2021. An Automated Method for Mapping Giant Kelp Canopy Dynamics from UAV. Front. Environ. Sci. 8, 587354.

Cavanaugh, K.C., Bell, T., Costa, M., Eddy, N.E., Gendall, L., Gleason, M.G., Hessing-Lewis, M., Martone, R., McPherson, M., Pontier, O., Reshitnyk, L., Beas-Luna, R., Carr, M., Caselle, J.E., Cavanaugh, K.C., Flores Miller, R., Hamilton, S., Heady, W.N., Hirsh, H.K., Hohman, R., Lee, L.C., Lorda, J., Ray, J., Reed, D.C., Saccomanno, V.R., Schroeder, S.B., 2021. A Review of the Opportunities and Challenges for Using Remote Sensing for Management of Surface-Canopy Forming Kelps. Frontiers in Marine Science 8, 1536.

Chen, I.-C., Hill, J.K., Ohlemüller, R., Roy, D.B., Thomas, C.D., 2011. Rapid range shifts of species associated with high levels of climate warming. Science 333, 1024–1026.

Dixon, D.J., Nikolaus Callow, J., Duncan, J.M.A., Setterfield, S.A., Pauli, N., 2021. Satellite prediction of forest flowering phenology. Remote Sens. Environ. 255, 112197.

Dobrowski, S.Z., 2011. A climatic basis for microrefugia: the influence of terrain on climate. Glob. Change Biol. 17, 1022–1035.

Elsmore, K., Nickols, K.J., Ford, T., Cavanaugh, K.C., Cavanaugh, K.C., Gaylord, B., 2022. Macrocystis pyrifera forest development shapes the physical environment through current velocity reduction. Mar. Ecol. Prog. Ser. 694, 45–59.

Finger, D.J.I., McPherson, M.L., Houskeeper, H.F., Kudela, R.M., 2021. Mapping bull kelp canopy in northern California using Landsat to enable long-term monitoring. Remote Sens. Environ. 254, 112243.

Frazier, A.E., Hemingway, B.L., 2021. A Technical Review of Planet Smallsat Data: Practical Considerations for Processing and Using PlanetScope Imagery. Remote Sens. 13, 3930.

Ganesh, B.P., Aravindan, S., Raja, S., Thirunavukkarasu, A., 2013. Hyperspectral satellite data (Hyperion) preprocessing—a case study on banded magnetite quartzite in Godumalai Hill, Salem, Tamil Nadu, India. Arab. J. Geosci. 6, 3249–3256.

Gray, P.C., Larsen, G.D., Johnston, D.W., 2022. Drones address an observational blind spot for biological oceanography. Front. Ecol. Environ. https://doi.org/10.1002/fee.2472

Green, A.A., Craig, M.D., 1985. Analysis of aircraft spectrometer data with logarithmic residuals, in: JPL Proc. of the Airborne Imaging Spectrometer Data Anal. Workshop.

Hamilton, S.L., Bell, T.W., Watson, J.R., Grorud-Colvert, K.A., Menge, B.A., 2020. Remote sensing: generation of long-term kelp bed data sets for evaluation of impacts of climatic variation. Ecology 101, e03031.

Harvell, C.D., Montecino-Latorre, D., Caldwell, J.M., Burt, J.M., Bosley, K., Keller, A., Heron, S.F., Salomon, A.K., Lee, L., Pontier, O., Pattengill-Semmens, C., Gaydos, J.K., 2019. Disease epidemic and a marine heat wave are associated with the continental-scale collapse of a pivotal predator (Pycnopodia helianthoides). Sci. Adv. 5, eaau7042.

Johnson, C.R., Mann, K.H., 1988. Diversity, patterns of adaptation, and stability of Nova Scotian kelp beds. Ecol. Monogr. 58, 129–154.

Kavousi, J., Keppel, G., 2018. Clarifying the concept of climate change refugia for coral reefs. ICES J. Mar. Sci. 75, 43–49.

Kennedy, R.E., Andréfouët, S., Cohen, W.B., Gómez, C., Griffiths, P., Hais, M., Healey, S.P., Helmer, E.H., Hostert, P., Lyons, M.B., Meigs, G.W., Pflugmacher, D., Phinn, S.R., Powell, S.L., Scarth, P., Sen, S., Schroeder, T.A., Schneider, A., Sonnenschein, R., Vogelmann, J.E., Wulder, M.A., Zhu, Z., 2014. Bringing an ecological view of change to Landsat-based remote sensing. Front. Ecol. Environ. 12, 339–346.

Keppel, G., Van Niel, K.P., Wardell-Johnson, G.W., Yates, C.J., Byrne, M., Mucina, L., Schut, A.G.T., Hopper, S.D., Franklin, S.E., 2012. Refugia: identifying and understanding safe havens for biodiversity under climate change. Glob. Ecol. Biogeogr. 21, 393–404.

Kranjčić, N., Medak, D., 2020. Evaluating different machine learning methods on RapidEye and PlanetScope satellite imagery. Geodetski List 74, 1–18.

Landesmann, J.B., Morales, J.M., 2018. The importance of fire refugia in the recolonization of a fire-sensitive conifer in northern Patagonia. Plant Ecol. 219, 455–466.

Latte, N., Lejeune, P., 2020. PlanetScope Radiometric Normalization and Sentinel-2 Super-Resolution (2.5 m): A Straightforward Spectral-Spatial Fusion of Multi-Satellite Multi-Sensor Images Using Residual Convolutional Neural Networks. Remote Sensing 12, 2366.

Leach, N., Coops, N.C., Obrknezev, N., 2019. Normalization method for multi-sensor high spatial and temporal resolution satellite imagery with radiometric inconsistencies. Comput. Electron. Agric. 164, 104893.

Li, J., Knapp, D.E., Fabina, N.S., Kennedy, E.V., Larsen, K., Lyons, M.B., Murray, N.J., Phinn, S.R., Roelfsema, C.M., Asner, G.P., 2020. A global coral reef probability map generated using convolutional neural networks. Coral Reefs. 39, 1805–1815.

McPherson, M.L., Finger, D.J.I., Houskeeper, H.F., Bell, T.W., Carr, M.H., Rogers-Bennett, L., Kudela, R.M., 2021. Large-scale shift in the structure of a kelp forest ecosystem co-occurs with an epizootic and marine heatwave. Commun. Biol. 4, 298.

Miller, K.A., Estes, J.A., 1989. Western Range Extension for Nereocystis luetkeana in the North Pacific Ocean. Bot. Mar. 32, 535–538.

Muller-Karger, F.E., Hestir, E., Ade, C., Turpie, K., Roberts, D.A., Siegel, D., Miller, R.J., Humm, D., Izenberg, N., Keller, M., Morgan, F., Frouin, R., Dekker, A.G., Royal Gardner, Goodman, J., Schaeffer, B., Franz, B.A., Pahlevan, N., Mannino, A.G., Concha, J.A., Ackleson, S.G., Cavanaugh, K.C., Romanou, A., Tzortziou, M., Boss, E.S., Pavlick, R., Freeman, A., Rousseaux, C.S., Dunne, J., Long, M.C., Klein, E., McKinley, G.A., Goes, J., Letelier, R., Kavanaugh, M., Roffer, M., Bracher, A., Arrigo, K.R., Dierssen, H., Zhang, X., Davis, F.W., Best, B., Guralnick, R., Moisan, J., Sosik, H.M., Kudela, R., Mouw, C.B., Barnard, A.H., Palacios, S., Roesler, C., Drakou, E.G., Appeltans, W., Jetz, W., 2018. Satellite sensor requirements for monitoring essential biodiversity variables of coastal ecosystems. Ecol. Appl. 28, 749–760.

Nicholson, N.L., 1970. FIELD STUDIES ON THE GIANT KELP NEREOCYSTIS 1, 2. J. Phycol. 6, 177–182.

Oliver, E.C.J., Donat, M.G., Burrows, M.T., Moore, P.J., Smale, D.A., Alexander, L.V., Benthuysen, J.A., Feng, M., Sen Gupta, A., Hobday, A.J., Holbrook, N.J., Perkins-

Kirkpatrick, S.E., Scannell, H.A., Straub, S.C., Wernberg, T., 2018. Longer and more frequent marine heatwaves over the past century. Nat. Commun. 9, 1324.

Park, D.C., 2016. Image classification using naïve bayes classifier. International Journal of Computer Science and Electronics Engineering 4, 135–139.

Pettorelli, N., Laurance, W.F., O'Brien, T.G., Wegmann, M., Nagendra, H., Turner, W., 2014. Satellite remote sensing for applied ecologists: opportunities and challenges. J. Appl. Ecol. 51, 839–848.

Planet, 2021. Planet Imagery Product Specifications.

Reed, D.C., Rassweiler, A.R., Miller, R.J., Page, H.M., Holbrook, S.J., 2015. The value of a broad temporal and spatial perspective in understanding dynamics of kelp forest ecosystems. Mar. Freshwater Res. 67, 14–24.

Rogers-Bennett, L., Catton, C.A., 2019. Marine heat wave and multiple stressors tip bull kelp forest to sea urchin barrens. Sci. Rep. 9, 15050.

Rosenzweig, C., Karoly, D., Vicarelli, M., Neofotis, P., Wu, Q., Casassa, G., Menzel, A., Root, T.L., Estrella, N., Seguin, B., Tryjanowski, P., Liu, C., Rawlins, S., Imeson, A., 2008. Attributing physical and biological impacts to anthropogenic climate change. Nature 453, 353–357.

Roy, D.P., Huang, H., Houborg, R., Martins, V.S., 2021. A global analysis of the temporal availability of PlanetScope high spatial resolution multi-spectral imagery. Remote Sens. Environ. 264, 112586.

Saccomanno, V.R., Bell, T., Pawlak, C., Stanley, C.K., Cavanaugh, K.C., Hohman, R., Klausmeyer, K.R., Cavanaugh, K., Nickels, A., Hewerdine, W., Garza, C., Fleener, G.,

Gleason, M., 2022. Using unoccupied aerial vehicles to map and monitor changes in emergent kelp canopy after an ecological regime shift. Remote Sens. Ecol. Conserv.

Schroeder, S.B., Boyer, L., Juanes, F., Costa, M., 2020. Spatial and temporal persistence of nearshore kelp beds on the west coast of British Columbia, Canada using satellite remote sensing. Remote Sens. Ecol. Conserv. https://doi.org/10.1002/rse2.142

Tamondong, A.M., Cruz, C.A., Guihawan, J., Garcia, M., Quides, R.R., Cruz, J.A., Blanco, A.C., 2018. Remote sensing-based estimation of seagrass percent cover and LAI for above ground carbon sequestration mapping. Proc. SPIE. 10778, 1077803-1.

Timmer, B., Reshitnyk, L.Y., Hessing-Lewis, M., Juanes, F., Costa, M., 2022. Comparing the Use of Red-Edge and Near-Infrared Wavelength Ranges for Detecting Submerged Kelp Canopy. Remote Sensing 14, 2241.

Traganos, D., Cerra, D., Reinartz, P., 2017. Cubesat-derived Detection of Seagrasses using Planet Imagery following unmixing-based Denoising: Is small the next big? ISPRS Archives. XLII-1/W1 283–287.

Vadas, R.L., 1972. ECOLOGICAL IMPLICATIONS OF CULTURE STUDIES ON NEREOCYSTIS LUETKEANA 1. J. Phycol. 8, 196–203.

Veisze, P., Kilgore, A., Lampinen, M., 1999. Building a California kelp database using GIS. 2000 ESRI International User Conference.

Verdura, J., Santamaría, J., Ballesteros, E., Smale, D.A., Cefalì, M.E., Golo, R., Caralt, S., Vergés, A., Cebrian, E., 2021. Local-scale climatic refugia offer sanctuary for a habitat-forming species during a marine heatwave. J. Ecol. 109, 1758–1773.

Wang, M., Hu, C., 2021. Satellite remote sensing of pelagic Sargassum macroalgae: The power of high resolution and deep learning. Remote Sens. Environ. 264, 112631

Wicaksono, P., Lazuardi, W., 2018. Assessment of PlanetScope images for benthic habitat and seagrass species mapping in a complex optically shallow water environment. Int. J. Remote Sens. 39, 5739–5765.

Wilson, K.L., Tittensor, D.P., Worm, B., Lotze, H.K., 2020. Incorporating climate change adaptation into marine protected area planning. Glob. Chang. Biol. 26, 3251–3267.

Wulder, M.A., Masek, J.G., Cohen, W.B., Loveland, T.R., Woodcock, C.E., 2012. Opening the archive: How free data has enabled the science and monitoring promise of Landsat. Remote Sens. Environ. 122, 2–10.

Xu, Y., Vaughn, N.R., Knapp, D.E., Martin, R.E., Balzotti, C., Li, J., Foo, S.A., Asner, G.P., 2020. Coral Bleaching Detection in the Hawaiian Islands Using Spatio-Temporal Standardized Bottom Reflectance and Planet Dove Satellites. Remote Sens. 12, 3219.

Yamano, H., Sakuma, A., Harii, S., 2020. Coral-spawn slicks: Reflectance spectra and detection using optical satellite data. Remote Sens. Environ. 251, 112058.

Zeng, L., Wardlow, B.D., Xiang, D., Hu, S., Li, D., 2020. A review of vegetation phenological metrics extraction using time-series, multispectral satellite data. Remote Sens. Environ. 237, 111511.

Chapter 3. Drivers of kelp forest refugia during successive disturbance events

Abstract: Marine heatwaves are becoming more frequent and severe throughout the global ocean. These disturbances have led to large-scale declines in many ecologically important species, including kelp forests. Spatial heterogeneity across seascapes could provide kelp individuals and small populations refuges from thermal stress and nutrient limitation. Habitat features within upwelling regions may facilitate the transport of deep, cold water into shallow systems, but little is known about the temporal stability of these climate refugia. Kelp in climate refugia may also experience other stressors such as overgrazing by kelp herbivores, reducing their effectiveness. Here, we use high resolution kelp canopy maps generated from CubeSat constellation data to characterize kelp persistence in northern California following a dramatic decline in kelp abundance due to a severe marine heatwave and an increase in grazing by purple sea urchins. Persistence was associated with localized cooling, in addition to landscape features such as shallow depths, that may have provided refuge from overgrazing. Our multi-year models show that kelp presence within refugia were spatially variable from year to year, indicating the complexity of interactions among factors that provided refuge from the heatwave and grazing pressure. This study provides a framework for understanding spatial and temporal variability in refugia across large, heterogenous seascapes at the fine scale needed for restoration.

3.1 Introduction

Disturbances create a mosaic of ecosystem effects across a landscape or seascape, within which exists substantial variability including undisturbed or minimally disturbed refuge areas (White and Pickett 1985, Ross et al. 2021, Christiansen et al. 2024). These disturbance-resistant locations can maintain suitable environmental conditions when disturbance effects render the surrounding habitat inhospitable (Ashcroft 2010). As a result, refugia enable the survival of organisms during a disturbance event and facilitate *in situ* persistence afterwards as intact habitat (Robinson et al. 2013). As the disturbed area recovers, populations can expand from refugia and gradually recolonize adjacent habitats that may have been more severely impacted (e.g., Gill et al., 2021), helping the seascape return to its pre-disturbance state (Keppel et al. 2012).

As the impacts of climate change have become more widespread, there has been increased interest in identifying climatic refugia for a variety of ecosystems (Ashcroft 2010, Keppel et al. 2012). For example, forested areas growing in mesic microclimates that allow for higher tolerance of drought conditions despite decreased regional precipitation (McLaughlin et al. 2017) or coral reefs positioned in thermal refuges that modulate heat stress and coral bleaching as ocean temperatures increase (Smith et al. 2014). However, climate change is only one of the stressors facing species, and other types of non-climatic disturbances can threaten populations, even those within climatic refugia. Biotic interactions, physical disturbances, and anthropogenic land use change all have large ecosystem impacts (Morris et al. 2020). There is a need to better understand how these different factors interact to shape refugial conditions to inform conservation (Rojas et al. 2022).

Kelp forests, like many other marine ecosystems, are being exposed to more frequent and intense disturbances (Rogers-Bennett and Catton 2019, Carnell and Keough 2020, Reeves et al.

2022). Marine heatwaves, defined as prolonged anomalously warm water events (Hobday et al. 2016), have caused widespread and persistent kelp forest losses (Arafeh-Dalmau et al. 2019, Cavanaugh et al. 2019, Thomsen et al. 2019, Filbee-Dexter et al. 2020, Tait et al. 2021, Michaud et al. 2022). For example, in Western Australia, intense warming from a marine heatwave in 2011 led to a ~100 km range contraction of kelp forests that has persisted for over a decade (Wernberg et al. 2013, 2016, Wernberg 2021). In other regions, such as central California, extreme temperatures have indirectly affected kelp forests by changing ecological interactions across rocky reef communities, including the intensification of grazing pressure (Smith et al. 2021, 2024, Smith and Tinker 2022).

Herbivory is a natural process within kelp forest ecosystems, and sea urchins normally subsist on unattached drift algae. However, they can display plasticity in foraging behavior, which has been attributed to changes in urchin (Ling et al. 2015) and kelp (Ebeling et al. 1985, Harrold and Reed 1985, Smith and Tinker 2022) population densities. Sea urchins may shift to active grazing when kelp detritus is limited (Dayton et al. 1992), and so heatwave-mediated reductions in kelp abundance can induce fundamental changes in foraging behavior (Rogers-Bennett 2007, Smith et al. 2021, Smith and Tinker 2022). Active overgrazing can switch the system from a productive kelp forest to large scale urchin barrens, which can inhibit the recovery of kelp for decades (e.g., Tasmania; Johnson et al., 2011).

Kelp survival during a marine heatwave event can be influenced by the severity of the disturbance and the position of an individual within the seascape in relation to possible refuges, such as microclimates that support temperature variation at fine spatial scales (Supratya et al. 2020, Verdura et al. 2021, Starko et al. 2022, Mora-Soto et al. 2024). Bathymetric features, including bottom depth and complexity, can facilitate the transport of deeper, cooler water into

shallow systems and reduce thermal stress (Storlazzi et al. 2020, Wyatt et al. 2020, Leichter et al. 2023). Further, upwelling regions may be more dynamic and able to provide more cool water refugia than non-upwelling regions (Lourenço et al. 2016, Salois et al. 2022, García-Reyes et al. 2023). There is also evidence that these features can influence patterns of herbivory, which may become increasingly important as heatwave effects subside and grazing pressure increases. Urchins are limited to moving about their habitat to graze, and they contend with various physical factors that impact mobility. Urchins can surmount most obstacles when water motion is low (Laur et al. 1986), but they tend to avoid exposed or sandy locations where flow speeds can greatly exceed thresholds for dislodgement (Denny et al. 1985, Lamb et al. 2020) and sand storms can damage sea urchins. This avoidance may be a critical driver of local kelp forest persistence within urchin barrens, as similar dynamics have been observed in other ecological systems. For example, survival of quaking aspen clones can be significantly higher on rock outcrops that hinder belowground grazing from pocket gophers, as opposed to more exposed deep meadow soils (Cantor and Whitham 1989).

Kelp refugia are likely driven by an interaction between marine microclimates, kelp spore availability, and local grazing pressure, and the relative contribution of each may change as the disturbance regime progresses. When marine heatwaves are long lasting (e.g., over 1 year) and overgrazing occurs in succession, the effects can compound and dampen the effectiveness of thermal refugia if the events are separated by less time than is required for recovery (Wilson et al. 2006, Turner 2010, Buma and Wessman 2011). Therefore, a key uncertainty about refugia is their spatiotemporal dynamics, particularly in discerning the criteria that dictate stable versus temporary refugia across consecutive ecological disturbances (Kolden et al. 2017, Rojas et al.

2022). However, little empirical work has examined the spatiotemporal dynamics of kelp refugia persistence within a multiple disturbance framework.

In this study, we examined the spatiotemporal dynamics of kelp persistence along the north coast of California. This area is in an intense upwelling cell, yet has experienced dramatic declines in kelp abundance over the past decade (Rogers-Bennett and Catton 2019, McPherson et al. 2021, Cavanaugh et al. 2023). Here, a sea star epizootic in 2013 caused widespread declines of the urchin predator *Pycnopodia helianthoides* (Harvell et al. 2019), which was followed in quick succession by an unprecedented, multi-year marine heatwave that persisted from 2014-2016 (Zaba and Rudnick 2016). The coastline experienced kelp forest losses of over 90% across 350 km of coastline, and high urchin population abundances have prevented recovery for over 9 years (Rogers-Bennett and Catton 2019, McPherson et al. 2021). Despite such disturbance, the region supports some relatively persistent refuge populations that have been mapped at high resolution (Cavanaugh et al. 2023), making it an ideal location for investigating the characteristics that allow these areas to persist in space and time. The goals of this study were to (1) identify physical characteristics associated with kelp persistence, and (2) examine how drivers of kelp presence changed over space and time. Specifically, we associated the presence or absence of kelp across northern California throughout the multiple stressor event with several environmental variables. We suggest possible habitat attributes that may provide refuge from the marine heatwave and protection from overgrazing by urchins. We then investigated the association between urchin abundances and the same habitat features as an additional assessment of the mechanisms driving spatial patterns in kelp persistence.

3.2 Methods

3.2.1 Study System

Bull kelp (*Nereocystis luetkeana*) is a canopy-forming macroalga distributed along the Pacific coast of North America from central California to the Aleutian Islands (Miller and Estes 1989, Abbott et al. 1992). Individuals display high fecundity and growth rates and typically achieve lengths of 10 to 20 m over the course of their annual life cycle (Nicholson 1970). Recruits appear in the early spring, and the emergent canopy grows to maximum extent during the late summer and early fall months (i.e., September or October). Bull kelp forests are highly susceptible to removal from wave events, and winter storms often result in dislodgement and widespread mortality (Hamilton et al. 2020).

This study was conducted along the temperate coastline of northern California, located on the west coast of North America (Fig. 1). Here, bull kelp is the dominant canopy-forming macroalgae, and purple (*Strongylocentrotus purpuratus*) and red (*Mesocentrotus franciscanus)* sea urchins comprise the dominant benthic herbivores. After the onset of a severe marine heatwave in 2014, which was associated with sea surface temperature (SST) anomalies of about 2.5°C (Bond et al. 2015), bull kelp populations experienced dramatic reductions in coverage (Rogers-Bennett and Catton 2019, McPherson et al. 2021). Simultaneously, urchin populations began increasing, which coincided with critical declines in the abundance of an urchin predator, the sea star *Pycnopodia helianthoides* (Rogers-Bennett and Catton 2019, Harvell et al. 2019). Although environmental conditions have become more favorable for kelp in recent years (McPherson et al. 2021), kelp population densities remain low (Fig. 1) (Cavanaugh et al. 2023, Saccomanno et al. 2023). This contracted distribution is hypothesized to be maintained by urchin overgrazing (Rogers-Bennett & Catton, 2019; McPherson et al., 2021).

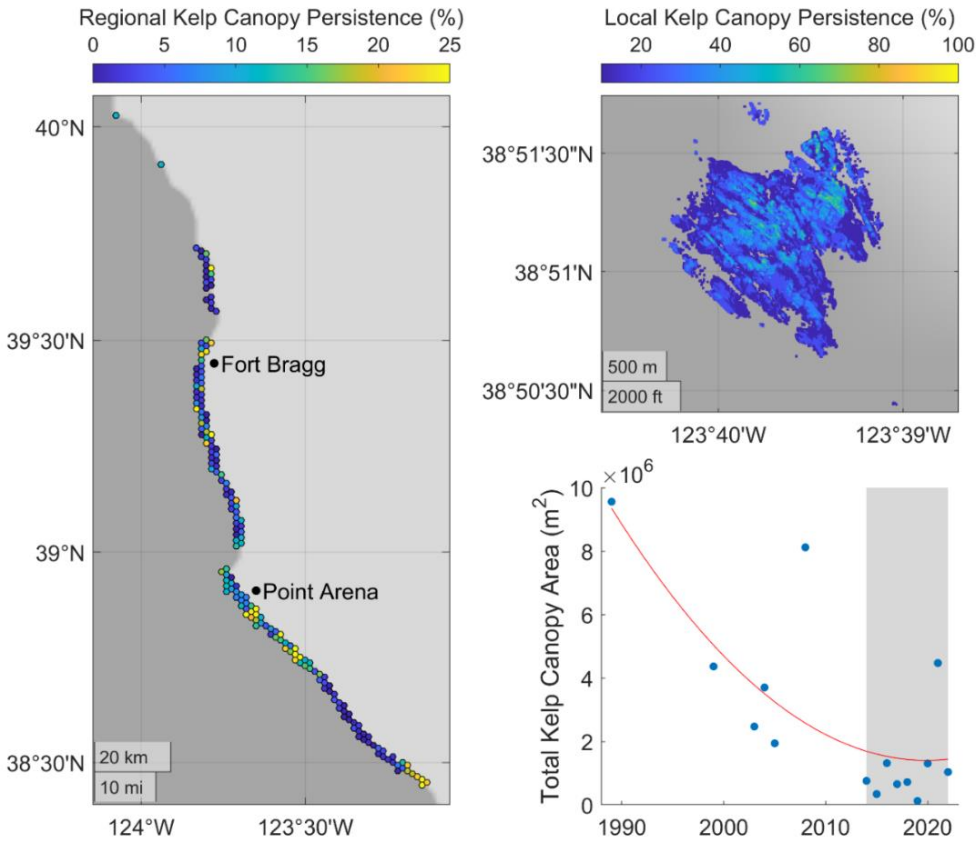

Fig. 3.1. Average kelp canopy persistence across northern California in 1.5-kilometer bins (left) and local kelp canopy persistence in an example bed offshore Point Arena, California (upper right). Persistence data include the period of historically low kelp coverage from 2014 to 2022, shaded in the time series on the bottom right. The red curve represents a second order polynomial fit in the time series data.

3.2.2 Data

3.2.2.1 Kelp Cover

Bull kelp forms a floating canopy on the water surface that can be identified using aerial and satellite platforms (Rogers-Bennett and Catton 2019, Hamilton et al. 2020, Finger et al.

2021, McPherson et al. 2021, Saccomanno et al. 2023, Bell et al. 2023). Our analysis utilized annual maps of bull kelp canopy extent that were derived from a time series of high-resolution CubeSat imagery from the PlanetScope constellation collected during September and October, when bull kelp canopy is at its maximum extent (Cavanaugh et al. 2023). The PlanetScope constellation has collected imagery at 3 m resolution on a near-daily basis from 2016 to the present. We previously developed an automated method for detecting kelp canopy from these data using a Naïve Bayes classifier (see Cavanaugh et al. 2023 for more details). These data provide annual kelp canopy coverage of our study area at 3 m resolution from 2016 to 2022. This fine spatial resolution is ideal for mapping small refuge populations of canopy kelp.

We combined this time series with earlier high-resolution aerial surveys from the California Department of Fish and Wildlife (CDFW), which have been shown to display good agreement with the PlanetScope satellites in identifying the location and abundance of kelp canopy (Cavanaugh et al. 2023). CDFW conducted annual occupied aircraft surveys of kelp canopy along the California coastline from 1989 to 2016, which allowed us to extend our time series to include pre-heatwave and heatwave canopy conditions. The surveys capture full coverage of northern California region in 1989, 1999, 2003-2005, 2008, and 2014-2016 at 2 m resolution (CDFW 2024). All CDFW data were resampled to 3 m to match the spatial resolution and extent of the PlanetScope maps using nearest-neighbor resampling. Using the maximum extent of the CDFW and PlanetScope observations, we gridded this region into 3 m x 3 m spatially referenced cells that encompassed all points represented in the data and removed locations that were only observed once in the time series. In total, 1,643,162 cells of potential kelp habitat were used in our analysis, where each cell included an observation of kelp canopy presence or absence in 1989, 1999, 2003-2005, 2008, and 2014-2022.

3.2.2.2 Urchin Abundances

Red and purple sea urchin counts were collected in the late summer to fall between 2006 and 2022 by the nearshore kelp forest ecosystem monitoring program (Rogers-Bennett et al. 2019). Scuba surveys were conducted at 11 sites in northern California: Fort Ross, Timber Cove, Ocean Cove, Salt Point, Sea Ranch, Point Arena, Albion, Van Damme, Russian Gulch, Caspar Cove, and Todd's Point. Surveys included counts of urchins along 30 x 2 m transects at randomly stratified locations within 4 depth strata from 1 to 20 m (Rogers-Bennett and Catton 2019). The number of surveys varied by site, and not all sites were surveyed each year. No sites were surveyed in 2020 or 2021 due to the coronavirus pandemic. We summed the number of red and purple urchins along each transect to represent total urchin counts in each location.

3.2.2.3 Seascape Variables

Small and fragmented kelp populations persisted throughout a multi-year period of historically low kelp abundance in northern California (Cavanaugh et al. 2023, Saccomanno et al. 2023), suggesting a preference for local environmental conditions within the disturbed seascape. We identified 11 habitat characteristics from published literature that have been shown to impact the spatial distribution and abundance of kelp forests. The 11 variables included features that may have helped to buffer the effects of extreme temperatures from the marine heatwave, such as localized upwelling, or that may have hindered the effects of urchin grazing, such as microtopography. We matched each habitat characteristic to the kelp canopy and urchin count observations in space and time. For gridded datasets, we selected the closest grid cell to the location of our observations for comparison.

A. Temperature

Seawater temperatures and nitrogen concentrations are often strongly and negatively correlated in coastal California (Palacios et al. 2013), and while temperatures above 13°C and nitrogen (NO_3) can synergistically and negatively influence kelp growth and photosynthetic rates (García-Reyes et al. 2014), they can also interact to produce complex ecological responses (Fales et al. 2023). In incubation experiments, high nitrogen concentrations can locally buffer the negative impacts of elevated temperatures and improve the growth and photosynthetic rates of individuals at macroscopic life stages (Fernández et al. 2020). For early life stages (i.e., microscopic), experimental evidence suggests that elevated temperatures may be more limiting than low nitrogen concentrations (Weigel et al. 2023). However, temperature and nitrogen co-vary in the field (García-Reyes et al. 2014). We obtained daily SST data from 2000 to 2022 in northern California from a 1 km blended satellite time series product developed for the California Current (Kahru 2024) and calculated two absolute temperature metrics. The first included mean annual temperature during the recruitment season, from January to June, when sporophytes develop and grow. The second included mean annual temperature during the period that most individuals mature and reach the surface, July to October. We also calculated two temperature anomalies for each of these time periods (mean annual temperature from January to June and July to October) compared to a baseline of 2000 to 2013.

B. Microtopography and Habitat

Bull kelp stands extend across bedrock, reefs, and boulder fields between the low intertidal (~ 3 m) and about 20 m deep (Nicholson 1970, Vadas 1972). We used a 1 m resolution

multi-source topobathymetric digital elevation model produced by the USGS Coastal National Elevation Database to characterize three seafloor characteristics. First, the data directly provided depth measurements of the seafloor. We also characterized the slope and rugosity of the seafloor, which are related to the topography and amount of hard substrate. Sites with high substrate complexity have been linked to stable kelp–urchin coexistence (Randell et al. 2022). First, we computed the slope of the depth, and then we computed the slope of the slope to provide information on rugosity (i.e., the rate of change in the slope). Using the maximum extent of the selected CDFW and PlanetScope observations, we also calculated the inward distance from the edge of kelp habitat, which is related to kelp density and may lead to a higher probability of recolonization year to year, as recolonization occurs via spore dispersal (Reed 1990).

C. Coastline Exposure and Morphology

The phenology of bull kelp may allow the species to outcompete other algal species that have difficulty settling in the presence of high wave action (Dobkowski et al. 2019), resulting in increased abundances in the year following a storm event (Hamilton et al. 2020). Additionally, storm events and intense wave action encourage urchins to retreat to burrows and channels worn into rock surfaces, as urchins found fully exposed to water velocities of 10 to 20 m/s have a high probability of dislodgement (Denny et al. 1985). We calculated the mean monthly maximum wave height of winter months (October-February) for each year using data from the Coastal Data Information Program (CDIP) nowcast alongshore wave-propagation model (O'Reilly et al. 2016). The model calculates hourly estimates of maximum significant wave height at a depth of 10 m along the California coastline at 100 m intervals along the back beach.

Rocky headlands and embayments can divert or obstruct alongshore currents, creating flow recirculation zones that accumulate larvae and hinder their transport along dominant axes (Wolanski and Hamner 1988, Gaylord et al. 2004). As a result, urchin recruitment hot spots can occur in the lee of headlands, such as in the lee of Bodega Head, California, where higher numbers of invertebrate larvae have been measured in comparison to the adjacent exposed coastline (Ebert et al. 1994, Mace and Morgan 2006, Morgan et al. 2011). On the other hand, rocky headlands also act as convergence points for wave energy and as fixation points for seaward rip currents, promoting offshore transport (George et al. 2015), which could reduce larval settlement. According to George et al. (2015), there are 78 headlands in the state of California, 11 of which are in northern California. These vary in area from 0.04 to 8.4 km^2, and as a result, may also vary in their transport ability past the headland. To determine if there was a consistent relationship between rocky headland locations and sites of bull kelp persistence, we obtained the locations of headlands in northern California from George et al. (2015) and calculated the distance of each grid cell to the nearest headland.

Salinity is variable in the coastal zone and can significantly decrease with increased proximity to river mouths. As rivers discharge and deliver increased levels of freshwater, sea urchins may face salinity levels below their tolerance limit (Lange 1964a, Rinde et al. 2014). In addition to freshwater, coastal streams and rivers often discharge eroded material to the ocean, leading to increased levels of sedimentation. Sediment deposits can scour or bury rocky substrate, preventing the settlement and growth of macroalgal species (Schiel et al. 2006, Lind and Konar 2017). Increased turbidity also leads to coastal darkening, which has been shown to significantly reduce primary production (Blain et al. 2021). To include the potential impact of river proximity on kelp persistence, we obtained the location of streams and rivers from both the

CDFW California Streams dataset and the National Hydrography Dataset (NHD) and calculated the distance of each grid cell to the nearest stream or river mouth. We did not limit locations by hydrographic feature size or amount of discharge.

3.2.3 Statistical Analyses

3.2.3.1 Identifying Drivers of Kelp Persistence

Bull kelp on the north coast of California has experienced a protracted collapse, and we analyzed multi-year longitudinal data to understand the spatial drivers of persistent remnant populations. We quantified persistence by summing the number of times kelp was present in each grid cell from 2014 to 2022, with a minimum value of 0 and a maximum value of 9. Grid cells with a value of '0' persistence contained kelp canopy between 1989 and 2013, but did not contain kelp canopy from 2014 to 2022. We extracted the values of each explanatory variable at all grid cell locations. For time series covariates, we calculated fixed averaged covariates, for example, temperature and wave height data were averaged from 2014 to 2022. To facilitate the interpretation and comparison of coefficients of covariates with different standard deviations, we standardized each covariate by subtracting the sample mean and dividing by the sample standard deviation. This standardization results in standardized coefficients and coefficients with larger absolute values indicate covariates with greater importance.

To quantify the relative importance of different habitat characteristics in determining both the distribution and temporal dynamics of persistence, we used a Bayesian framework and applied fixed effects Poisson regression models in Just Another Gibbs Sample, or JAGS (Plummer 2003). JAGS is an open-source software to implement Bayesian estimation with Markov chain Monte Carlo (MCMC) methods and includes a package, R2jags (Su et al. 2015),

for interface in R (R Core Team 2024). We fit a single model that included all the covariates related to persistence. Spatial synchrony in kelp forest dynamics has been detected at the seascape scale (Cavanaugh et al. 2013). To minimize bias in the logistic regression coefficients and associated standard errors introduced by spatial autocorrelation, we randomly subsampled locations that were at least 150 m apart across 1000 replications, as populations show a high degree of spatial autocorrelation at distances less than 150 m (Cavanaugh et al. 2013). We modeled persistence as the number of years with kelp presence, $N_i,\ i = 1, \ldots, n$, where n is the number of locations, with Poisson regression as a function of a $(k + 1)$ vector of predictors, x_i, with initial element 1.

$$N_i|\lambda_i \sim Poisson(\lambda_i) \quad \text{(Eq. 1)}$$

$$log(\lambda_i) = x_i^t \beta \quad \text{(Eq. 2)}$$

where λ_i is the unknown mean persistence per grid cell i, $\beta = (\beta_0, \ldots, \beta_K)'$ is the $(k + 1)$ vector of unknown regression coefficients (Eq. 1, Eq. 2). We transformed λ_i using a log link so that the linear predictor $x_i^t \beta$ can take values on the real number line while λ_i is non-negative. The parameter β_0 is the intercept and β_k is the coefficient for covariate k, and $x_{i,k}$ is the $(k + 1)$-st element of x_i, the value of covariate k for cell i (Eq. 2). The prior and precision for β_0 was chosen from the literature, with reports of about 5% of available habitat retaining refugia in northern California (Rogers-Bennett and Catton 2019, McPherson et al. 2021, Cavanaugh et al. 2023). The priors for the coefficients were normal mean 0 and precision 1.

$$\beta_0 \sim \text{normal}(-3, 0.11) \quad \text{(Eq. 3)}$$

$$\beta_k \sim \text{normal}(0, 1) \quad \text{(Eq. 4)}$$

3.2.3.2 Tracking Changes in the Drivers of Kelp Presence

During a multiple disturbance event, the magnitude of individual stressors fluctuates in space and time. The individual effects of extreme temperatures and urchin overgrazing are relatively well understood in kelp forest ecosystems, but our understanding of their influence on population resilience after consecutive occurrences of multiple stressors remains limited. Sites with higher habitat heterogeneity have been linked to population stability for other species (Oliver et al. 2010), and to understand if the drivers of kelp persistence in northern California were stable or variable throughout the multiple stressor event, we used a Bayesian hierarchical framework and applied mixed effects logistic regression models in JAGS. The same 1,643,162 cells of potential kelp habitat were used in our analysis, where each cell included an observation of kelp canopy presence or absence in each year from 2014 to 2022 (i.e., kelp refugia). We fit separate models for each covariate and modeled the covariate's importance on persistence in the dataset with different coefficients for year (2014, 2015, 2016, 2017, 2018, 2019, 2020, 2021, and 2022).

We randomly subsampled locations that were at least 150 m apart across 1000 replications to minimize bias in the logistic regression coefficients introduced by spatial autocorrelation. We modeled the presence, Z_{it} = 1, or the absence, Z_{it} = 0, of kelp at each location, i = 1, …, n, at year t = 2014, …, 2022, with logistic regression. The probability of kelp presence was modeled separately for each environmental predictor variable, x_{ikt} and again the predictors were standardized by subtracting the sample mean and dividing by the sample standard deviation

$$Z_{it}|p_{it} \sim Bernoulli(p_{it}) \quad \text{(Eq. 5)}$$

$$\text{logit}(p_{it}) = \beta_0 + \beta_{0t} + \beta_k x_{ikt} + \beta_{kt} x_{ikt} \quad \text{(Eq. 6)}$$

where p_{it} is the unknown probability of kelp presence. The probability of presence at cell i was modeled using the logit link function, $\text{logit}(p_{it}) = log\frac{p_{it}}{1-p_{it}}$, for each environmental predictor variable k. The parameter β_0 is a global intercept, β_{0t} is a year-specific random intercept, β_k is the overall coefficient for covariate k, x_{ikt} is the value of covariate k at cell i and time t, β_{kt} is the year-level coefficient for covariate k at time t (Eq. 6). The prior for β_0 was chosen with the assumption that kelp would be present in about 20% of available habitat from year to year. The priors were

$$\beta_0 \sim \text{normal}(-1.75, 0.11) \quad \text{(Eq. 7)}$$

$$\beta_{0t} \sim \text{normal}(0, \sigma_{\beta_{0t}}) \quad \text{(Eq. 8)}$$

$$\beta_{kt} \sim \text{normal}\left(0, \sigma_{\beta_{kt}}\right) \quad \text{(Eq. 9)}$$

where the precision terms $\sigma_{\beta_{0t}}$ and $\sigma_{\beta_{kt}}$ were modeled with a half-normal distribution (mean of 0 and precision of 1), restricted to the positive real line.

3.2.3.3 Urchin Abundance Model

Although environmental conditions have become more favorable for kelp in recent years, kelp population densities remain low (McPherson et al. 2021). Ongoing work on sea urchin

density in northern California shows that densities remain high (Rogers-Bennett and Catton 2019). Sea urchin behavioral work in central California suggests that local urchin populations may play a significant role in the persistence of northern California kelp forests (Smith et al. 2021, Smith and Tinker 2022). To quantify the relative importance of different habitat characteristics in determining both the distribution and temporal dynamics of urchin abundance, we applied mixed effects logistic regression models in JAGS, similar to those used for tracking spatial shifts in kelp presence through time (section 2.3.1). We fit separate models for each covariate and estimated their relative importance on urchin counts in the dataset by year (2006 – 2019, 2022). We also added a site-level random effect, indexed by j, to model differences in locations. Urchin counts, y_{it}, at each survey location, i = 1, …, n, at year t = 2006, …, 2019, 2022 were modeled separately for each environmental predictor variable as negative binomial (NB)

$$y_{ijt} \sim \mathrm{NB}(p_{ijt}, r) \quad \text{(Eq. 10)}$$

where y_{ijt} is the total urchin counts in survey i, where r is the scaling parameter for the negative binomial (NB) distribution. We transformed p_{ijt} to be a function of the mean λ_{ijt} and used a log link for λ_{ijt} so the transformed mean would be a linear function of the predictors (Eq. 11, Eq. 12).

$$p_{ijt} = \frac{r}{r+\lambda_{ijt}} \quad \text{(Eq. 11)}$$

$$logit(\lambda_{ijt}) = \mu_{ijt} \quad \text{(Eq. 12)}$$

$$\mu_{ijt} = \beta_0 + \beta_{0t} + \beta_k x_{ikt} + \beta_{kt} x_{ikt} + \gamma_j \quad \text{(Eq. 13)}$$

Parameter β_0 is the global intercept, β_{0t} is the global year-specific random intercept, β_k is the overall coefficient for covariate k, x_{ikt} is the value of covariate k at cell i and time t, β_{kt} is the year-level coefficient for covariate k at time t, and γ_j is the site-level spatial random effect at site j (Eq. 13). The priors were

$$\beta_0 \sim \text{normal}(5, 0.25) \quad \text{(Eq. 14)}$$

$$\beta_{0t} \sim \text{normal}(0, \sigma_{\beta_{0t}}) \quad \text{(Eq. 15)}$$

$$\beta_{kt} \sim \text{normal}\left(0, \sigma_{\beta_{kt}}\right) \quad \text{(Eq. 16)}$$

$$\gamma_j \sim \text{normal}(0, \sigma_{\gamma_j}) \quad \text{(Eq. 17)}$$

where the precision terms $\sigma_{\beta_{0t}}$, $\sigma_{\beta_{kt}}$, and σ_{γ_j} were modeled with a half-normal distribution (mean of 0 and precision of 1), restricted to the positive real line.

3.2.3.4 Computation

For all kelp models, we ran 4 chains with 10,000 iterations, a burn-in of 5,000, and a thinning rate of 10 for 2,000 total samples from the posterior. For the urchin abundance models, we ran 4 chains with 100,000 iterations, a burn-in of 50,000, and a thinning rate of 100 for 2,000 total samples from the posterior. We determined model convergence using an R-hat statistic of less than 1.1 and the number of effective samples greater than 400. We summarized posteriors by averaging the posterior means, posterior standard deviations (SD), 95% posterior intervals (PI),

and the probability that the coefficient is positive P(beta>0 | data) across the 1,000 replicates of each of the 2,000 random samples, as a summary. For P(beta>0 | data), values less than .025 or greater than .975 are flagged as 'significant', in parallel with frequentist statistical practice. In the Bayesian framework, significance means that we are certain (at least 97.5%) about the sign of the covariate effect.

3.3 Results

3.3.1 Drivers of Persistent Bull Kelp in Northern California

There was a total of 14.79 km^2 of potential kelp habitat in northern California, which included locations where kelp canopy was present during at least two years between 1989 and 2022. Kelp occupied 43.25% of this habitat at least once from 2014 to 2022, 17.82% at least twice, 6.88% at least three times, 2.89% at least four times, 1.17% at least five times, and less than 1% more than five times, suggesting that kelp populations were largely transient during the years of successive disturbance.

Figure 2 presents the standardized effects of the predictors' contributions to kelp persistence, where depth and rugosity had the strongest effects. Persistent kelp populations were more likely to occur in locations with shallow water depths and less bottom complexity. Growing season SST and growing season SST anomaly had a negative relationship with kelp persistence, indicating the presence of temperature refugia in cooler areas. Growing season SST and growing season SST anomalies had higher covariate estimates than recruitment season SST and recruitment season SST anomalies. Kelp persistence increased with increasing inward distance from historical canopy edge and with larger maximum winter wave heights (Fig. 2). Distance from river mouths showed a weakly positive relationship, indicating higher persistence further

from river mouths. The 95% confidence intervals for recruitment season SST, slope, and distance from nearest headland all crossed 0, indicating little to no effect for these variables (Fig. 2).

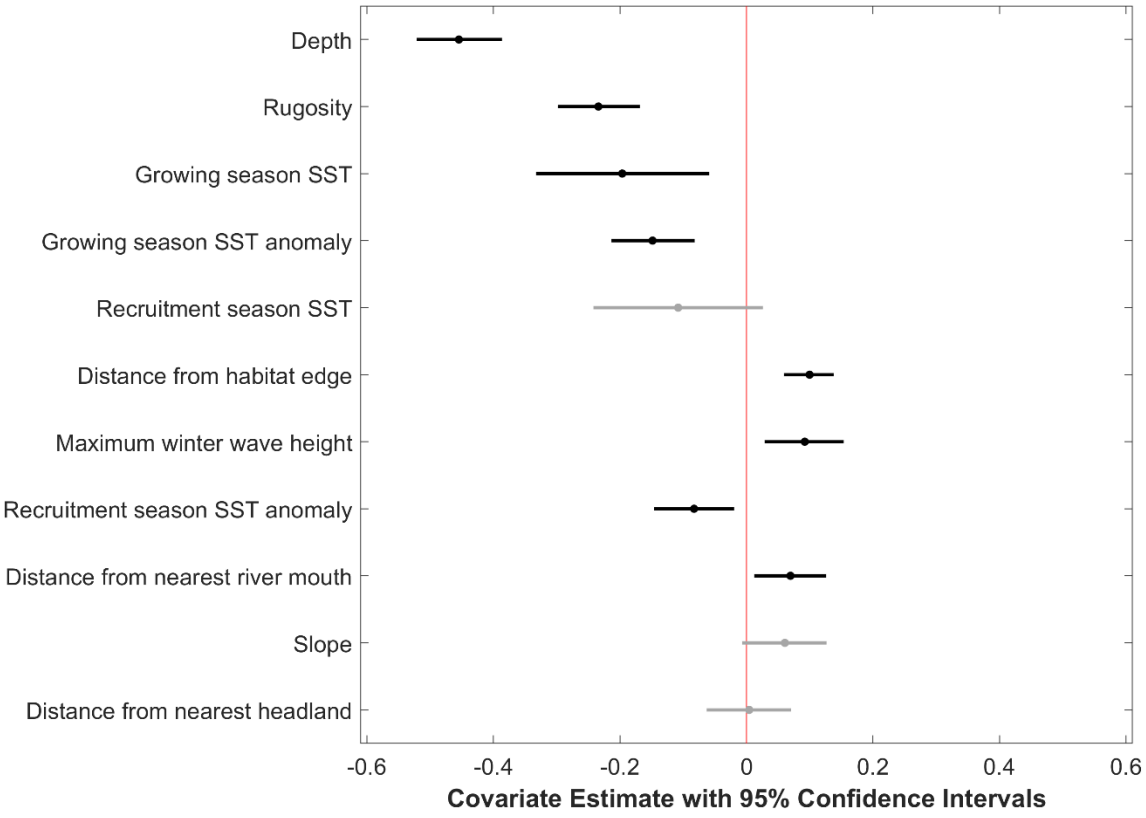

Fig. 3.2. Summary of the posterior distribution of regression coefficients for the persistence model using the number of years that contained kelp canopy between 2014 and 2022 in each grid cell across northern California. Estimates are shown with 95% credible intervals and are in order from highest to lowest absolute magnitude. Covariates with intervals that do not cross 0 (red vertical line) are black, while those that cross 0 are grey.

3.3.2 Temporal Variability in Drivers of Kelp Presence

The environmental factors related to kelp presence during the multiple disturbance events showed highly variable effects when separated by year. Figure 3 presents the addition of the main effect and the random effect of the covariate in that year ($\beta_k + \beta_{kt}$) from Equation 6, showing the strength and direction of the association between kelp presence and the selected environmental covariates is stable or variable through time.

Kelp is generally present in locations with colder absolute growing and recruitment season temperatures in each year compared to locations where kelp is absent in that year, except for 2015 and 2016 (which were heatwave years), when kelp was present in locations with slightly warmer temperatures (Fig. 3). Kelp was present in locations with colder growing season temperature anomalies after the onset of the heatwave in 2014, and these locations may have become less important after 2020, when kelp was present in locations with warmer growing season temperature anomalies. The recruitment season temperature anomaly displayed a variable trend; cooler temperature anomalies were associated with kelp presence during most heatwave years, temperature anomalies had no effect in 2018 and 2019, and warmer temperature anomalies were associated with kelp presence from 2020 to 2022 (Fig. 3).

After 2019, there was a notable and consistent shift in the factors influencing kelp presence (Fig. 3). Environmental factors related to microtopography and habitat displayed a clear, temporal signal, particularly for depth, slope, and rugosity. Kelp was found in shallow habitats with low slopes and rugosity from 2014 to 2019, before migrating to and remaining in deeper, steeper, and more rugose habitats from 2020 onwards. River mouths showed a similar effect, as kelp tended to grow closer to river mouths from 2014 to 2019 relative to populations present from 2020 onward, which grew further from river mouths. Distance from habitat edge, distance from the nearest headland, and maximum winter wave height did not show clear trends.

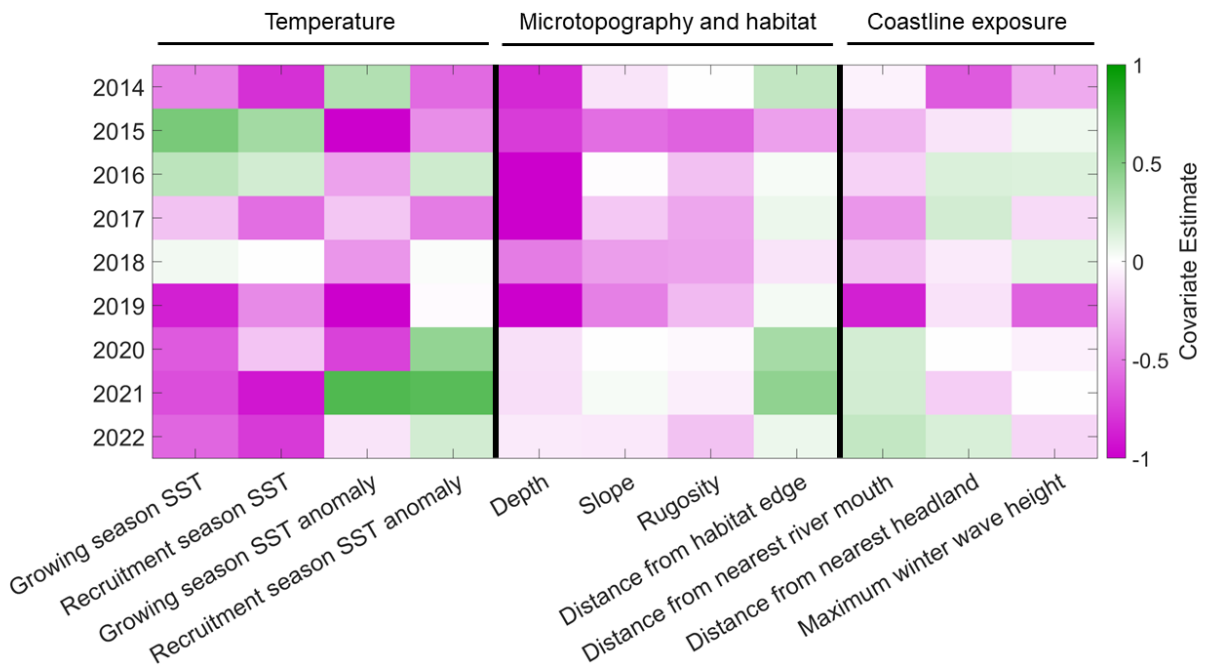

Fig. 3.3. Heat map of the posterior mean environmental effects on the presence of kelp within refugia across co-occurring and consecutive ecological disturbances, a marine heatwave (2014-2016) followed by a sea urchin outbreak (2014-2022).

3.3.3 Spatial Shifts in Urchin Abundance through Time

Northern California urchin populations displayed relatively consistent abundances from 2006 to 2013 (Fig. 4). The onset of a sea star epizootic in 2013 caused widespread declines of the urchin predator *Pycnopodia helianthoides* (Rogers-Bennett and Catton 2019, Harvell et al. 2019), followed in quick succession by a multi-year marine heatwave from 2014 to 2016 (Michaud et al. 2022), which led to sustained urchin population increases after 2014 (Fig. 4). The timing of purple urchin population increases coincided with regional losses in kelp canopy area (Fig. 1), when sparse, patchy kelp beds became dominant along the coastline.

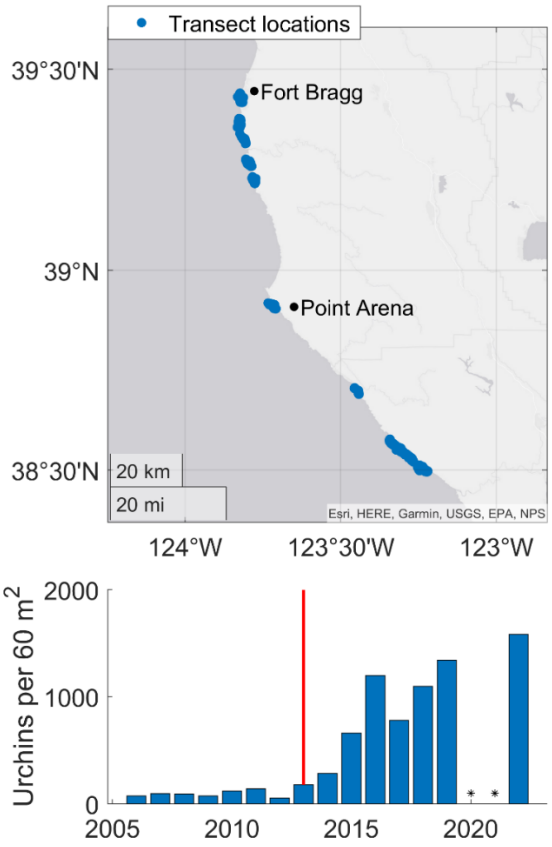

Fig. 3.4. Transect locations of scuba surveys conducted within northern California (top) and regional average of urchin counts collected within the transects from 2006 to 2022 (bottom). The red line indicates the onset of a sea star epizootic that was a contributor to widespread declines of the urchin predator *Pycnopodia helianthoides*. Years with asterisks were not sampled due to the coronavirus pandemic.

The environmental factors related to urchin population abundance during the multi-year disturbance events showed highly variable effects when separated by year. Figure 5 presents the addition of the main effect and the random effect of the covariate in that year ($\beta_k + \beta_{kt}$) from Equation 13, showing the strength and direction of the association between urchin abundance

and the selected environmental covariates is stable or variable through time. Urchin counts did not show a homogenous relationship with absolute or relative temperature metrics; some years showed negative relationships and others positive relationships, with no consistent or linear pattern (Fig. 5). Urchin counts showed a strong relationship with environmental factors related to microtopography and habitat, particularly for depth, slope, and rugosity. Higher abundances of urchins were found in deeper habitats with steeper slopes and increased rugosity until 2014, when populations began migrating to shallower, flatter, and less rugose habitats (Fig. 5). This pattern directly opposed the trends observed for kelp persistence within refugia (Fig. 3), indicating that kelp populations may be finding refuge from urchin overgrazing by utilizing topographic features that support fewer urchin individuals. The positive relationship with distance from the nearest river mouth was particularly strong for urchin populations, indicating that locations close to river mouths had fewer urchins (Fig. 5), as sea urchins are known to be very sensitive to salinity (Stickle and Diehl 1987). The effect of river mouths weakened in 2015 and remained weak in 2018, 2021, and 2022. Increased urchin abundance was associated with increased distances from headlands and maximum wave height during most years (Fig. 5).

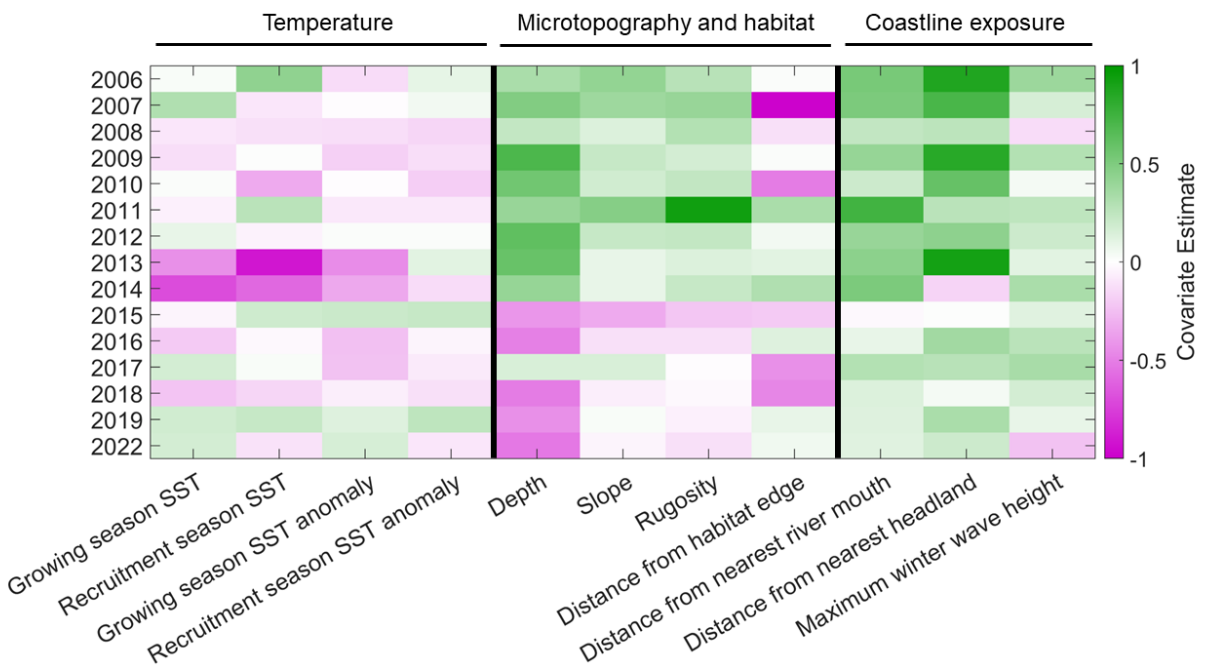

Fig. 3.5. Heat map of the posterior mean environmental effects on the abundance of urchin populations before and after a sea star die-off (2013-2014) and marine heatwave (2014-2016).

3.4 Discussion

Our data support the hypothesis that the significant decline in northern California bull kelp populations was initiated by warm ocean conditions and has persisted due to widespread urchin barrens, indicating that a perturbation to urchin populations may be necessary for shifting back to a forested state. Our results highlight a complex geography of kelp survival in climate refugia during and after the marine heatwave, facilitated by locations that offered sufficient nutrients or a combined effect of sufficient nutrients and reduced heat stress. However, post-2019, the ability of kelp to evade urchin predation may have become more critical. This indicates that while temperature remains a significant factor for kelp refugia, urchin evasion has

increasingly dictated kelp survival and distribution in recent years, marking a change in the ecological dynamics of refugia.

3.4.1 Climate Refugia

The north coast of California is a heterogeneous seascape, where bull kelp canopy has historically been found at depths that range tens of meters, substrate that varies from simple to complex, and physical parameters such as temperature and salinity that fluctuate with proximity to coastline features and from year to year. Our statistical analyses showed that this heterogeneity contributed to the presence of persistent kelp, which was related to 8 of the 11 explanatory variables tested using multivariate Poisson regression. When kelp persistence was compared to historical habitat, cooler water temperatures were among the most important predictors. It is well established that temperature and nitrate are strongly correlated in coastal California (Palacios et al. 2013, García-Reyes et al. 2014), and a complex combination of these factors likely contributed to thermal refugia during the marine heatwave. Topographic divergence can cause localized, small-scale upwelling, which has been observed in other areas of the California coastline, such as the Point Loma headland in southern California (Roughan et al. 2005). Sites in northern California with localized upwelling may have provided sufficient nutrients and/or temperatures for kelp, allowing individuals in refugia to settle, grow, and become reproductive.

For kelp to survive in these cooler climate refugia, sites would also need to offer refuge from urchin overgrazing. In northern California, localized upwelling may also hinder sea urchin recruitment. Sea urchin settlement is positively correlated with SST (Miller and Emlet 1997, Okamoto et al. 2020), and urchins may be less likely to settle when and where SST is too cool, which has been observed in other regions (Hernández et al. 2010). Additionally, adult sea urchins

may exhibit reduced grazing rates in cold areas and years as observed in recent experiments, where urchins showed reduced grazing during upwelling events (Murie and Bourdeau 2021).

Our results also suggest that bull kelp persistence was more responsive to absolute thermal thresholds versus the magnitude of relative temperature changes. This result is consistent with the response of other canopy forming kelp populations to marine heatwave events. For example, in the Mediterranean Sea, a marine heatwave caused high kelp mortality rates at an absolute temperature of 28°C, with severe impacts on early life stages and fertility. However, environmental heterogeneity resulted in small-scale variability in thermal conditions throughout the seascape, and populations growing in open coves were less impacted than those in enclosed pools (Verdura et al. 2021). Similarly, in British Columbia, kelp forests located along warmer, inshore areas experienced far more extensive losses during a marine heatwave than those located along the cool, outer coast (Starko et al. 2022).

3.4.2 Shallow Refugia

The role of deep reefs as refugia during thermal disturbance has been well established for corals, as deeper habitats generally have colder water temperatures (Bongaerts et al. 2010). Deep rocky reefs are also hypothesized to be important for kelp as shallow waters warm and become unsuitable (Graham et al. 2007, Assis et al. 2016, Giraldo-Ospina et al. 2020). In contrast, we found persistent kelp in shallow habitats along the northern California coastline, which may be due to the combined disturbances of both warm water and sea urchin overgrazing. It is also possible that temperatures in these shallow areas are not warm enough to be limiting. Similar patterns have been observed at several sites along the coast of Australia, where kelp cover is highest at shallow depths that continue to support bottom temperatures that do not exceed the

maximum temperature that limits kelp development and growth (Young et al. 2015, Williams et al. 2020, Davis et al. 2021). Instead, kelp individuals appear to rely on shallow depths to avoid overgrazing by urchins. Urchins are often confined to depths that fall below the turbulent wave base to avoid removal and displacement, constraining their shallow habitat limit (Siddon and Witman 2003, Lauzon-Guay and Scheibling 2007, Steneck 2020).

While the shallow, turbulent zone may not promote ideal conditions for kelp persistence due to increased wave action and irradiance (Young et al. 2016), these areas provide refuge from urchin herbivory, which has allowed for the persistence of small patches along a narrow, shallow strip. This finding is consistent with findings from the north-west Atlantic, where the main refuge for perennial algae from urchins was in the surge zone and on complex habitats (i.e., the tops of boulders) that projected into the surge zone (Chapman 1981, Himmelman et al. 1984, Witman 1987, Keats 1991). After a mass mortality of urchins, rates of recolonization depended on proximity to the refugial spore sources from the shallow, turbulent zone (Johnson and Mann 1988, Keats 1991), which shows the importance of persistent kelp for recolonization. Similarly, along the west coast of Vancouver Island, Canada, in sites where urchin predators (i.e., otters) were absent, high abundances of sea urchins constrained the depth limit of kelp, driving kelp populations to occupy small, shallow sublittoral fringes surrounded by urchin barrens (Markel and Shurin 2015). The wave exposure metrics included in our analysis only had a minor positive impact on the presence of kelp persistence. However, these metrics were designed to capture general coastline exposure along a latitudinal gradient, not a depth gradient. Wave exposure is generally high along the open coast of northern California; bull kelp experiences near total dislodgement at the end of the fall season each year.

Persistent kelp populations were associated with low-complexity sites, indicating that seafloor structure variables (i.e., rugosity) were important. This result differs from other areas, such as San Nicolas Island, CA, where high-complexity sites showed increased resilience for kelp–urchin coexistence. (Randell et al. 2022). However, the bathymetry data used in this study were remarkably high resolution (1 m), and therefore even complex areas, such as the top of a boulder, might show up as 'simpler' habitats since the highest rates of change occur as the seascape changes from the bottom to the top of the boulder. For example, kelp may have persisted on the tops of boulders or rock features, but due to the resolution of the data, these areas may have been characterized as having little or no slope/complexity. Additionally, the kelp and urchin populations offshore San Nicolas Island were not analyzed in the context of multiple stressors, and the intensity of the heatwave offshore northern California from 2014 to 2016 may have impacted the behavior and survivorship of the local community (Smith et al. 2021, Smith and Tinker 2022).

3.4.3 Stability of Refugia during Multiple Stressors

Multiple stressors can compound and dampen the effectiveness of refugia, particularly if the habitat attributes that influence survival are different for each stressor or if the events are separated by less time than is required for recovery (Wilson et al. 2006, Turner 2010, Buma and Wessman 2011). While a small portion of the seascape supported persistent kelp (Fig. 2), our multi-year models show that most refugia were temporary and displayed high spatial variability from year to year. However, this variability was not stochastic, and instead, kelp presence tended to covary with spatiotemporal patterns in urchin abundance (Fig. 3; Fig. 5).

The high density of urchins in northern California likely made spatial avoidance difficult, and kelp individuals seemed to rely on temporally dynamic seascape features to elude overgrazing and facilitate coexistence. Higher abundances of urchins were found within deeper, steeper, and more rugose habitats until 2015, when populations emerged from cryptic habitats and became active in shallow, open reef spaces. Overgrazing likely restricted the depth range of kelp, leading populations to occupy small, shallow fringes. Subsequently, kelp began shifting their habitat from these riskier places to locations with increased depth, slope, and rugosity in 2020. These places, which have been linked to stable kelp-urchin coexistence (Randell et al. 2022), might prove better refuge from urchins, as urchin population densities are lower, urchins can hide from predators in crevices (Russell et al. 2018), and individuals can preferentially feed on drift algae that becomes entrapped within the complex seascape features (Vanderklift and Wernberg 2008).

Sections of coastline located near river mouth discharge sites may also be important refuge locations, although our results show this refugium was short-lived. Throughout the entire time series, urchins were typically found further away from river mouths. This pattern can be attributed to the low tolerance of sea urchins for abrupt changes in salinity. An influx of freshwater into urchin habitats can cause osmotic shock, which impacts urchin feeding behavior (Irlandi et al. 1997) and survival (Lange 1964b, Gibson et al. 2002, Rinde et al. 2014). Historical data indicate that purple urchins have experienced mass die-offs from increases in freshwater volume, including near the mouths of small streams. (Hendler 2013). Despite the potential negative effects of sediments on kelp, there is evidence that sedimentation can provide indirect benefits to the survival of kelp in areas with high grazing pressure (Kawamata et al. 2011). Sea urchins in other global regions have been shown to avoid portions of reef with a thin layer of fine

sediment, allowing already-established kelp stands to persist. However, our results show that kelp was initially present in locations closer to river mouths, but populations were present in locations further away in 2020. USGS discharge data support that 2020 to 2022 coincided with a period of low rainfall in California, suggesting that river mouth refugia may depend on discharge thresholds that have not been met in recent years (Fig. 6). We did not restrict river mouth inclusion in our analysis, and the strength of a river's impact on kelp survival is likely influenced by physical parameters such as river mouth size and discharge levels.

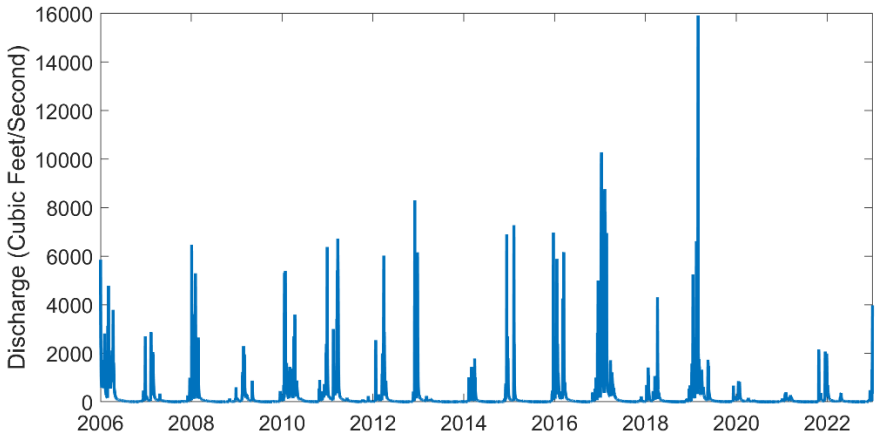

Fig. 3.6. Average discharge across 3 USGS gauges in northern California, Fort Bragg, Navarro River, and Gualala.

In conclusion, this study contributed to our understanding of the spatial and temporal dynamics of kelp persistence across diverse seascapes with fine temporal resolution. We found that kelp survival during and after a marine heatwave was notably higher in cooler areas, indicating that localized upwelling sites served as climate refugia. These refugia may have supported nutrient-rich environments or a combination of sufficient nutrients and reduced heat

stress. However, a noteworthy shift may have occurred post-2019, where the ability of kelp to evade urchin predation may have become more crucial. As a result, a perturbation to urchin populations may be necessary for shifting back to a forested state. Such perturbations may include increased presence of predators (i.e., recovery of the sunflower sea star), sea urchin disease, or changes in the environment that drive changes in urchin survival or feeding behavior.

Given the extensive decline observed across geographic areas, there is an urgent need to prioritize sites for restoration and implement preventative conservation measures. Monitoring the effectiveness and limitations of selected strategies over time is essential. This includes identifying and protecting remnant patches of kelp, or refugia, where subpopulations have managed to persist amidst heatwave events (Hamilton et al. 2022). While restoration efforts often aim to leverage these natural refugia, comprehensive data on their locations, stability, and enabling factors for persistence are lacking. Additionally, the insights gained from this study extend beyond kelp forest ecosystems to benefit other disturbance-prone systems. For instance, coral reef communities threatened by marine heatwaves require large-scale monitoring to understand bleaching events and degradation processes (Asner et al. 2017). Similarly, coastal wetlands face complex challenges influenced by disturbances operating on varying timescales, from tides to sea level rise (Miller et al. 2019). Addressing these challenges will require interdisciplinary approaches and a deeper understanding of ecosystem dynamics.

3.5 References

Abbott, I. A., A. Isabella, and G. J. Hollenberg. 1992. Marine algae of California. Stanford University Press.

Arafeh-Dalmau, N., G. Montaño-Moctezuma, J. A. Martínez, R. Beas-Luna, D. S. Schoeman, and G. Torres-Moye. 2019. Extreme Marine Heatwaves Alter Kelp Forest Community Near Its Equatorward Distribution Limit. Frontiers in Marine Science 6.

Ashcroft, M. B. 2010. Identifying refugia from climate change. Journal of Biogeography 37:1407–1413.

Asner, G. P., N. R. Vaughn, J. Heckler, D. E. Knapp, C. Balzotti, E. Shafron, R. E. Martin, B. J. Neilson, J. M. Gove, by E. Russell Brainard, and J. Burns. 2017. Large-scale mapping of live corals to guide reef conservation. PNAS 117:33711–33718.

Assis, J., N. C. Coelho, T. Lamy, M. Valero, F. Alberto, and E. Á. Serrão. 2016. Deep reefs are climatic refugia for genetic diversity of marine forests. Journal of biogeography 43:833–844.

Bell, T. W., K. C. Cavanaugh, V. R. Saccomanno, K. C. Cavanaugh, H. F. Houskeeper, N. Eddy, F. Schuetzenmeister, N. Rindlaub, and M. Gleason. 2023. Kelpwatch: A new visualization and analysis tool to explore kelp canopy dynamics reveals variable response to and recovery from marine heatwaves. PLOS ONE 18:e0271477-.

Blain, C. O., S. C. Hansen, and N. T. Shears. 2021. Coastal darkening substantially limits the contribution of kelp to coastal carbon cycles. Global Change Biology 27:5547–5563.

Bond, N. A., M. F. Cronin, H. Freeland, and N. Mantua. 2015. Causes and impacts of the 2014 warm anomaly in the NE Pacific. Geophysical Research Letters 42:3414–3420.

Bongaerts, P., T. Ridgway, E. M. Sampayo, and O. Hoegh-Guldberg. 2010. Assessing the ‘deep reef refugia’ hypothesis: focus on Caribbean reefs. Coral Reefs 29:309–327.

Buma, B., and C. A. Wessman. 2011. Disturbance interactions can impact resilience mechanisms of forests. Ecosphere 2:art64.

Cantor, L. F., and T. G. Whitham. 1989. Importance of Belowground Herbivory: Pocket Gophers May Limit Aspen to Rock Outcrop Refugia. Ecology 70:962–970.

Carnell, P. E., and M. J. Keough. 2020. More severe disturbance regimes drive the shift of a kelp forest to a sea urchin barren in south-eastern Australia. Scientific Reports 10:11272.

Cavanaugh, K. C., K. C. Cavanaugh, C. C. Pawlak, T. W. Bell, and V. R. Saccomanno. 2023. CubeSats show persistence of bull kelp refugia amidst a regional collapse in California. Remote Sensing of Environment 290:113521.

Cavanaugh, K. C., B. E. Kendall, D. A. Siegel, D. C. Reed, F. Alberto, and J. Assis. 2013. Synchrony in dynamics of giant kelp forests is driven by both local recruitment and regional environmental controls. Ecology 94:499–509.

Cavanaugh, K. C., D. C. Reed, T. W. Bell, M. C. N. Castorani, and R. Beas-Luna. 2019. Spatial Variability in the Resistance and Resilience of Giant Kelp in Southern and Baja California to a Multiyear Heatwave. Frontiers in Marine Science 6.

Chapman, A. R. O. 1981. Stability of sea urchin dominated barren grounds following destructive grazing of kelp in St. Margaret's Bay, Eastern Canada. Marine Biology 62:307–311.

Christiansen, D. M., G. Römer, J. P. Dahlgren, M. Borg, O. R. Jones, S. Merinero, K. Hylander, and J. Ehrlén. 2024. High-resolution data are necessary to understand the effects of climate on plant population dynamics of a forest herb. Ecology 105:e4191.

Davis, T. R., C. Champion, and M. A. Coleman. 2021. Climate refugia for kelp within an ocean warming hotspot revealed by stacked species distribution modelling. Marine Environmental Research 166:105267.

Dayton, P. K., M. J. Tegner, P. E. Parnell, and P. B. Edwards. 1992. Temporal and spatial patterns of disturbance and recovery in a kelp forest community. Ecological Monographs 62:421–445.

Denny, M. W., T. L. Daniel, and M. A. R. Koehl. 1985. Mechanical Limits to Size in Wave-Swept Organisms. Ecological Monographs 55:69–102.

Dobkowski, K. A., K. D. Flanagan, and J. R. Nordstrom. 2019. Factors influencing recruitment and appearance of bull kelp, Nereocystis luetkeana (phylum Ochrophyta). Journal of Phycology 55:236–244.

Ebeling, A. W., D. R. Laur, and R. J. Rowley. 1985. Severe storm disturbances and reversal of community structure in a southern California kelp forest. Marine Biology 84:287–294.

Ebert, T. A., S. C. Schroeter, J. D. Dixon, and P. Kalvass. 1994. Settlement patterns of red and purple sea urchins (Strongylocentrotus franciscanus and S. purpuratus) in California, USA. Marine Ecology Progress Series:41–52.

Fales, R. J., B. L. Weigel, E. Carrington, H. D. Berry, and M. N. Dethier. 2023. Interactive effects of temperature and nitrogen on the physiology of kelps (Nereocystis luetkeana and Saccharina latissima). Frontiers in Marine Science.

Fernández, P. A., J. D. Gaitán-Espitia, P. P. Leal, M. Schmid, A. T. Revill, and C. L. Hurd. 2020. Nitrogen sufficiency enhances thermal tolerance in habitat-forming kelp: implications for acclimation under thermal stress. Scientific Reports 10:3186.

Filbee-Dexter, K., T. Wernberg, S. P. Grace, J. Thormar, S. Fredriksen, C. N. Narvaez, C. J. Feehan, and K. M. Norderhaug. 2020. Marine heatwaves and the collapse of marginal North Atlantic kelp forests. Scientific Reports 10:13388.

Finger, D. J. I., M. L. McPherson, H. F. Houskeeper, and R. M. Kudela. 2021. Mapping bull kelp canopy in northern California using Landsat to enable long-term monitoring. Remote Sensing of Environment 254:112243.

García-Reyes, M., G. Koval, W. J. Sydeman, D. Palacios, L. Bedriñana-Romano, K. DeForest, C. Montenegro Silva, M. Sepulveda, and E. Hines. 2023. Most eastern boundary upwelling regions represent thermal refugia in the age of climate change. Frontiers in Marine Science 10:1158472.

García-Reyes, M., J. L. Largier, and W. J. Sydeman. 2014. Synoptic-scale upwelling indices and predictions of phyto- and zooplankton populations. Progress in Oceanography 120:177–188.

Gaylord, B., D. C. Reed, L. Washburn, and P. T. Raimondi. 2004. Physical–biological coupling in spore dispersal of kelp forest macroalgae. Journal of Marine Systems 49:19–39.

George, D. A., J. L. Largier, C. D. Storlazzi, and P. L. Barnard. 2015. Classification of rocky headlands in California with relevance to littoral cell boundary delineation. Marine Geology 369:137–152.

Gibson, R. N., M. Barnes, and R. J. A. Atkinson. 2002. Impact of changes in flow of freshwater on estuarine and open coastal habitats and the associated organisms. Oceanography and marine biology: an annual review 40:233.

Gill, N. S., T. J. Hoecker, and M. G. Turner. 2021. The propagule doesn't fall far from the tree, especially after short-interval, high-severity fire. Ecology 102:e03194.

Giraldo-Ospina, A., G. A. Kendrick, and R. K. Hovey. 2020. Depth moderates loss of marine foundation species after an extreme marine heatwave: could deep temperate reefs act as a refuge? Proceedings of the Royal Society B: Biological Sciences 287:20200709.

Graham, M. H., B. P. Kinlan, L. D. Druehl, L. E. Garske, and S. Banks. 2007. Deep-water kelp refugia as potential hotspots of tropical marine diversity and productivity. Proceedings of the National Academy of Sciences 104:16576–16580.

Hamilton, S. L., T. W. Bell, J. R. Watson, K. A. Grorud-Colvert, and B. A. Menge. 2020. Remote sensing: generation of long-term kelp bed data sets for evaluation of impacts of climatic variation. Ecology 101:e03031.

Hamilton, S. L., M. G. Gleason, N. Godoy, N. Eddy, and K. Grorud-Colvert. 2022. Ecosystem-based management for kelp forest ecosystems. Marine Policy 136:104919.

Harrold, C., and D. C. Reed. 1985. Food Availability, Sea Urchin Grazing, and Kelp Forest Community Structure. Ecology 66:1160–1169.

Harvell, C. D., D. Montecino-Latorre, J. M. Caldwell, J. M. Burt, K. Bosley, A. Keller, S. F. Heron, A. K. Salomon, L. Lee, O. Pontier, C. Pattengill-Semmens, and J. K. Gaydos. 2019. Disease epidemic and a marine heat wave are associated with the continental-scale collapse of a pivotal predator (Pycnopodia helianthoides). Science Advances 5:eaau7042.

Hendler, G. 2013. Recent mass mortality of Strongylocentrotus purpuratus (Echinodermata: Echinoidea) at Malibu and a review of purple sea urchin kills elsewhere in California. Bulletin, Southern California Academy of Sciences 112:19–37.

Hernández, J. C., S. Clemente, D. Girard, Á. Pérez-Ruzafa, and A. Brito. 2010. Effect of temperature on settlement and postsettlement survival in a barrens-forming sea urchin. Marine Ecology Progress Series 413:69–80.

Himmelman, J. H., H. Guderley, G. Vignault, G. Drouin, and P. G. Wells. 1984. Response of the sea urchin, Strongylocentrotus droebachiensis, to reduced salinities: importance of size, acclimation, and interpopulation differences. Canadian Journal of Zoology 62:1015–1021.

Hobday, A. J., L. V Alexander, S. E. Perkins, D. A. Smale, S. C. Straub, E. C. J. Oliver, J. A. Benthuysen, M. T. Burrows, M. G. Donat, M. Feng, N. J. Holbrook, P. J. Moore, H. A. Scannell, A. Sen Gupta, and T. Wernberg. 2016. A hierarchical approach to defining marine heatwaves. Progress in Oceanography 141:227–238.

Irlandi, E., S. Macia, and J. Serafy. 1997. Salinity reduction from freshwater canal discharge: effects on mortality and feeding of an urchin (Lytechinus variegatus) and a gastropod (Lithopoma tectum). Bulletin of Marine Science 61:869–879.

Johnson, C. R., S. C. Banks, N. S. Barrett, F. Cazassus, P. K. Dunstan, G. J. Edgar, S. D. Frusher, C. Gardner, M. Haddon, F. Helidoniotis, K. L. Hill, N. J. Holbrook, G. W. Hosie, P. R. Last, S. D. Ling, J. Melbourne-Thomas, K. Miller, G. T. Pecl, A. J. Richardson, K. R. Ridgway, S. R. Rintoul, D. A. Ritz, D. J. Ross, J. C. Sanderson, S. A. Shepherd, A. Slotwinski, K. M. Swadling, and N. Taw. 2011. Climate change cascades: Shifts in oceanography, species' ranges and subtidal marine community dynamics in eastern Tasmania. Journal of Experimental Marine Biology and Ecology 400:17–32.

Johnson, C. R., and K. H. Mann. 1988. Diversity, Patterns of Adaptation, and Stability of Nova Scotian Kelp Beds. Ecological Monographs 58:129–154.

Kawamata, S., S. Yoshimitsu, T. Tanaka, T. Igari, and S. Tokunaga. 2011. Importance of sedimentation for survival of canopy-forming fucoid algae in urchin barrens. Journal of Sea Research 66:76–86.

Keats, D. W. 1991. Refugial Laminaria Abundance and Reduction in Urchin Grazing in Communities in the North-West Atlantic. Journal of the Marine Biological Association of the United Kingdom 71:867–876.

Keppel, G., K. P. Van Niel, G. W. Wardell-Johnson, C. J. Yates, M. Byrne, L. Mucina, A. G. T. Schut, S. D. Hopper, and S. E. Franklin. 2012. Refugia: identifying and understanding safe havens for biodiversity under climate change. Global Ecology and Biogeography 21:393–404.

Kolden, C. A., T. M. Bleeker, A. M. S. Smith, H. M. Poulos, and A. E. Camp. 2017. Fire effects on historical wildfire refugia in contemporary wildfires. Forests 8.

Lamb, R. W., F. Smith, and J. D. Witman. 2020. Consumer mobility predicts impacts of herbivory across an environmental stress gradient. Ecology 101:e02910.

Lange, R. 1964a. The osmotic adjustment in the echinoderm, Strongylocentrotus droebachiensis. Comparative Biochemistry and Physiology 13:205–216.

Lange, R. 1964b. The osmotic adjustment in the echinoderm, Strongylocentrotus droebachiensis. Comparative Biochemistry and Physiology 13:205–216.

Laur, D. R., A. W. Ebeling, and D. C. Reed. 1986. Experimental evaluations of substrate types as barriers to sea urchin (Strongylocentrotus spp.) movement. Marine Biology 93:209–215.

Lauzon-Guay, J.-S., and R. E. Scheibling. 2007. Behaviour of sea urchin Strongylocentrotus droebachiensis grazing fronts: food-mediated aggregation and density-dependent facilitation. Marine Ecology Progress Series 329:191–204.

Leichter, J. J., L. B. Ladah, P. E. Parnell, M. D. Stokes, M. T. Costa, J. Fumo, and P. K. Dayton. 2023. Persistence of southern California giant kelp beds and alongshore variation in nutrient exposure driven by seasonal upwelling and internal waves. Frontiers in Marine Science 10:1007789.

Lind, A. C., and B. Konar. 2017. Effects of abiotic stressors on kelp early life-history stages. Algae 32:223–233.

Ling, S. D., R. E. Scheibling, A. Rassweiler, C. R. Johnson, N. Shears, S. D. Connell, A. K. Salomon, K. M. Norderhaug, A. Pérez-Matus, J. C. Hernández, S. Clemente, L. K. Blamey, B. Hereu, E. Ballesteros, E. Sala, J. Garrabou, E. Cebrian, M. Zabala, D. Fujita, and L. E. Johnson. 2015. Global regime shift dynamics of catastrophic sea urchin overgrazing. Philosophical Transactions of the Royal Society B: Biological Sciences 370:20130269.

Lourenço, C. R., G. I. Zardi, C. D. McQuaid, E. A. Serrão, G. A. Pearson, R. Jacinto, and K. R. Nicastro. 2016. Upwelling areas as climate change refugia for the distribution and genetic diversity of a marine macroalga. Journal of biogeography 43:1595–1607.

Mace, A. J., and S. Morgan. 2006. Larval accumulation in the lee of a small headland: Implications for the design of marine reserves. Marine Ecology-progress Series - MAR ECOL-PROGR SER 318:19–29.

Markel, R. W., and J. B. Shurin. 2015. Indirect effects of sea otters on rockfish (Sebastes spp.) in giant kelp forests. Ecology 96:2877–2890.

McLaughlin, B. C., D. D. Ackerly, P. Z. Klos, J. Natali, T. E. Dawson, and S. E. Thompson. 2017. Hydrologic refugia, plants, and climate change. Global Change Biology 23:2941–2961.

McPherson, M. L., D. J. I. Finger, H. F. Houskeeper, T. W. Bell, M. H. Carr, L. Rogers-Bennett, and R. M. Kudela. 2021. Large-scale shift in the structure of a kelp forest ecosystem co-occurs with an epizootic and marine heatwave. Communications Biology 4:298.

Michaud, K. M., D. C. Reed, and R. J. Miller. 2022. The Blob marine heatwave transforms California kelp forest ecosystems. Communications Biology 5:1143.

Miller, B. A., and R. B. Emlet. 1997. Influence of nearshore hydrodynamics on larval abundance and settlement of sea urchins Strongylocentrotus franciscanus and S. purpuratus in the Oregon upwelling zone. Marine Ecology Progress Series 148:83–94.

Miller, G. J., J. T. Morris, and C. Wang. 2019. Estimating aboveground biomass and its spatial distribution in coastal wetlands utilizing planet multispectral imagery. Remote Sensing 11.

Miller, K. A., and J. A. Estes. 1989. Western Range Extension for Nereocystis luetkeana in the North Pacific Ocean 32:535–538.

Mora-Soto, A., S. Schroeder, L. Gendall, A. Wachmann, G. R. Narayan, S. Read, I. Pearsall, E. Rubidge, J. Lessard, K. Martell, P. Wills, and M. Costa. 2024. Kelp dynamics and environmental drivers in the southern Salish Sea, British Columbia, Canada. Frontiers in Marine Science 11.

Morgan, S. G., J. L. Fisher, and J. L. Largier. 2011. Larval retention, entrainment, and accumulation in the lee of a small headland: Recruitment hotspots along windy coasts. Limnology and Oceanography 56:161–178.

Morris, W. F., J. Ehrlén, J. P. Dahlgren, A. K. Loomis, and A. M. Louthan. 2020. Biotic and anthropogenic forces rival climatic/abiotic factors in determining global plant population growth and fitness. Proceedings of the National Academy of Sciences 117:1107–1112.

Murie, K. A., and P. E. Bourdeau. 2021. Energetic context determines the effects of multiple upwelling-associated stressors on sea urchin performance. Scientific Reports 11:11313.

Nicholson, N. L. 1970. FIELD STUDIES ON THE GIANT KELP NEREOCYSTIS1,2. Journal of Phycology 6:177–182.

Okamoto, D. K., S. C. Schroeter, and D. C. Reed. 2020. Effects of ocean climate on spatiotemporal variation in sea urchin settlement and recruitment. Limnology and Oceanography 65:2076–2091.

Oliver, T., D. B. Roy, J. K. Hill, T. Brereton, and C. D. Thomas. 2010. Heterogeneous landscapes promote population stability. Ecology Letters 13:473–484.

O'Reilly, W. C., C. B. Olfe, J. Thomas, R. J. Seymour, and R. T. Guza. 2016. The California coastal wave monitoring and prediction system. Coastal Engineering 116:118–132.

Palacios, D. M., E. L. Hazen, I. D. Schroeder, and S. J. Bograd. 2013. Modeling the temperature-nitrate relationship in the coastal upwelling domain of the California Current. Journal of Geophysical Research: Oceans 118:3223–3239.

Plummer, M. 2003. JAGS: A program for analysis of Bayesian graphical models using Gibbs sampling. Pages 1–10 Proceedings of the 3rd international workshop on distributed statistical computing. Vienna, Austria.

R Core Team. 2024. R: A language and environment for statistical computing.

Randell, Z., M. Kenner, J. Tomoleoni, J. Yee, and M. Novak. 2022. Kelp-forest dynamics controlled by substrate complexity. Proceedings of the National Academy of Sciences 119:e2103483119.

Reed, D. C. 1990. The Effects of Variable Settlement and Early Competition on Patterns of Kelp Recruitment. Ecology 71:776–787.

Reeves, S. E., N. Kriegisch, C. R. Johnson, and S. D. Ling. 2022. Kelp habitat fragmentation reduces resistance to overgrazing, invasion and collapse to turf dominance. Journal of Applied Ecology 59:1619–1631.

Rinde, E., H. Christie, C. W. Fagerli, T. Bekkby, H. Gundersen, K. M. Norderhaug, and D. Hjermann. 2014. The influence of physical factors on kelp and sea urchin distribution in previously and still grazed areas in the NE Atlantic. PLoS ONE 9.

Robinson, N. M., S. W. J. Leonard, E. G. Ritchie, M. Bassett, E. K. Chia, S. Buckingham, H. Gibb, A. F. Bennett, and M. F. Clarke. 2013. REVIEW: Refuges for fauna in fire-prone landscapes: their ecological function and importance. Journal of Applied Ecology 50:1321–1329.

Rogers-Bennett, L. 2007. The ecology of Strongylocentrotus franciscanus and Strongylocentrotus purpuratus. Pages 393–425 Developments in Aquaculture and Fisheries Science. Elsevier.

Rogers-Bennett, L., and C. A. Catton. 2019. Marine heat wave and multiple stressors tip bull kelp forest to sea urchin barrens. Scientific Reports 9:15050.

Rogers-Bennett, L., J. V Kashiwada, I. K. Taniguchi, S. K. Kawana, and C. A. Catton. 2019. Using Density-Based Fishery Management Strategies to Respond to Mass Mortality Events. Journal of Shellfish Research 38:485–495.

Rojas, I. M., M. K. Jennings, E. Conlisk, A. D. Syphard, J. Mikesell, A. M. Kinoshita, K. West, D. Stow, E. Storey, M. E. De Guzman, D. Foote, A. Warneke, A. Pairis, S. Ryan, L. E. Flint, A. L. Flint, and R. L. Lewison. 2022. A landscape-scale framework to identify refugia from multiple stressors. Conservation Biology 36:e13834.

Ross, S. R. P. J., Y. Suzuki, M. Kondoh, K. Suzuki, P. Villa Martín, and M. Dornelas. 2021. Illuminating the intrinsic and extrinsic drivers of ecological stability across scales. Ecological Research 36:364–378.

Roughan, M., E. J. Terrill, J. L. Largier, and M. P. Otero. 2005. Observations of divergence and upwelling around Point Loma, California. Journal of Geophysical Research: Oceans 110.

Russell, M. P., V. K. Gibbs, and E. Duwan. 2018. Bioerosion by pit-forming, temperate-reef sea urchins: History, rates and broader implications. PLOS ONE 13:e0191278-.

Saccomanno, V. R., T. Bell, C. Pawlak, C. K. Stanley, K. C. Cavanaugh, R. Hohman, K. R. Klausmeyer, K. Cavanaugh, A. Nickels, W. Hewerdine, C. Garza, G. Fleener, and M. Gleason. 2023. Using unoccupied aerial vehicles to map and monitor changes in emergent kelp canopy after an ecological regime shift. Remote Sensing in Ecology and Conservation 9:62–75.

Salois, S. L., T. C. Gouhier, B. Helmuth, F. Choi, R. Seabra, and F. P. Lima. 2022. Coastal upwelling generates cryptic temperature refugia. Scientific Reports 12:19313.

Schiel, D. R., S. A. Wood, R. A. Dunmore, and D. I. Taylor. 2006. Sediment on rocky intertidal reefs: Effects on early post-settlement stages of habitat-forming seaweeds. Journal of Experimental Marine Biology and Ecology 331:158–172.

Siddon, C. E., and J. D. Witman. 2003. Influence of chronic, low-level hydrodynamic forces on subtidal community structure. Marine Ecology Progress Series 261:99–110.

Smith, J. G., D. Malone, and M. H. Carr. 2024. Consequences of kelp forest ecosystem shifts and predictors of persistence through multiple stressors. Proceedings of the Royal Society B: Biological Sciences 291:20232749.

Smith, J. G., and M. T. Tinker. 2022. Alternations in the foraging behaviour of a primary consumer drive patch transition dynamics in a temperate rocky reef ecosystem. Ecology Letters 25:1827–1838.

Smith, J. G., J. Tomoleoni, M. Staedler, S. Lyon, J. Fujii, and M. T. Tinker. 2021. Behavioral responses across a mosaic of ecosystem states restructure a sea otter–urchin trophic cascade. Proceedings of the National Academy of Sciences 118:e2012493118.

Smith, T. B., P. W. Glynn, J. L. Maté, L. T. Toth, and J. Gyory. 2014. A depth refugium from catastrophic coral bleaching prevents regional extinction. Ecology 95:1663–1673.

Starko, S., C. J. Neufeld, L. Gendall, B. Timmer, L. Campbell, J. Yakimishyn, L. Druehl, and J. K. Baum. 2022. Microclimate predicts kelp forest extinction in the face of direct and indirect marine heatwave effects. Ecological Applications 32:e2673.

Steneck, R. S. 2020. Chapter 15 - Regular sea urchins as drivers of shallow benthic marine community structure. Pages 255–279 *in* J. M. Lawrence, editor. Developments in Aquaculture and Fisheries Science. Elsevier.

Stickle, W. B., and W. J. Diehl. 1987. Effects of salinity on echinoderms. Echinoderm studies 2:235–285.

Storlazzi, C. D., O. M. Cheriton, R. van Hooidonk, Z. Zhao, and R. Brainard. 2020. Internal tides can provide thermal refugia that will buffer some coral reefs from future global warming. Scientific Reports 10:13435.

Su, Y.-S., M. Yajima, M. Y.-S. Su, and J. SystemRequirements. 2015. Package 'r2jags.' R package version 0.03-08, URL http://CRAN. R-project. org/package= R2jags.

Supratya, V. P., L. J. M. Coleman, and P. T. Martone. 2020. Elevated Temperature Affects Phenotypic Plasticity in the Bull Kelp (Nereocystis luetkeana, Phaeophyceae). Journal of Phycology 56:1534–1541.

Tait, L. W., F. Thoral, M. H. Pinkerton, M. S. Thomsen, and D. R. Schiel. 2021. Loss of Giant Kelp, Macrocystis pyrifera, Driven by Marine Heatwaves and Exacerbated by Poor Water Clarity in New Zealand. Frontiers in Marine Science 8.

Thomsen, M. S., L. Mondardini, T. Alestra, S. Gerrity, L. Tait, P. M. South, S. A. Lilley, and D. R. Schiel. 2019. Local Extinction of Bull Kelp (Durvillaea spp.) Due to a Marine Heatwave. Frontiers in Marine Science 6.

Turner, M. G. 2010. Disturbance and landscape dynamics in a changing world. Ecology 91:2833–2849.

Vadas, R. L. 1972. ECOLOGICAL IMPLICATIONS OF CULTURE STUDIES ON NEREOCYSTIS LUETKEANA1. Journal of Phycology 8:196–203.

Vanderklift, M. A., and T. Wernberg. 2008. Detached kelps from distant sources are a food subsidy for sea urchins. Oecologia 157:327–335.

Verdura, J., J. Santamaría, E. Ballesteros, D. A. Smale, M. E. Cefalì, R. Golo, S. de Caralt, A. Vergés, and E. Cebrian. 2021. Local-scale climatic refugia offer sanctuary for a habitat-forming species during a marine heatwave. Journal of Ecology 109:1758–1773.

Weigel, B. L., S. L. Small, H. D. Berry, and M. N. Dethier. 2023. Effects of temperature and nutrients on microscopic stages of the bull kelp (Nereocystis luetkeana, Phaeophyceae). Journal of Phycology 59:893–907.

Wernberg, T. 2021. Marine Heatwave Drives Collapse of Kelp Forests in Western Australia. Pages 325–343 *in* J. G. Canadell and R. B. Jackson, editors. Ecosystem Collapse and Climate Change. Springer International Publishing, Cham.

Wernberg, T., S. Bennett, R. C. Babcock, T. de Bettignies, K. Cure, M. Depczynski, F. Dufois, J. Fromont, C. J. Fulton, R. K. Hovey, E. S. Harvey, T. H. Holmes, G. A. Kendrick, B.

Radford, J. Santana-Garcon, B. J. Saunders, D. A. Smale, M. S. Thomsen, C. A. Tuckett, F. Tuya, M. A. Vanderklift, and S. Wilson. 2016. Climate-driven regime shift of a temperate marine ecosystem. Science 353:169–172.

Wernberg, T., D. A. Smale, F. Tuya, M. S. Thomsen, T. J. Langlois, T. de Bettignies, S. Bennett, and C. S. Rousseaux. 2013. An extreme climatic event alters marine ecosystem structure in a global biodiversity hotspot. Nature Climate Change 3:78–82.

White, P. S., and S. T. A. Pickett. 1985. Chapter 1 - Natural Disturbance and Patch Dynamics: An Introduction. Pages 3–13 *in* S. T. A. PICKETT and P. S. WHITE, editors. The Ecology of Natural Disturbance and Patch Dynamics. Academic Press, San Diego.

Williams, J., M. A. Coleman, and A. Jordan. 2020. Depth, nutrients and urchins explain variability in Ecklonia radiata (laminariales) distribution and cover across ten degrees of latitude. Aquatic Botany 166:103274.

Wilson, S. K., N. A. J. Graham, M. S. Pratchett, G. P. Jones, and N. V. C. Polunin. 2006. Multiple disturbances and the global degradation of coral reefs: are reef fishes at risk or resilient? Global Change Biology 12:2220–2234.

Witman, J. D. 1987. Subtidal coexistence: storms, grazing, mutualism, and the zonation of kelps and mussels. Ecological Monographs 57:167–187.

Wolanski, E., and W. M. Hamner. 1988. Topographically Controlled Fronts in the Ocean and Their Biological Influence. Science 241:177–181.

Wyatt, A. S. J., J. J. Leichter, L. T. Toth, T. Miyajima, R. B. Aronson, and T. Nagata. 2020. Heat accumulation on coral reefs mitigated by internal waves. Nature Geoscience 13:28–34.

Young, M., K. Cavanaugh, T. Bell, P. Raimondi, C. A. Edwards, P. T. Drake, L. Erikson, and C. Storlazzi. 2016. Environmental controls on spatial patterns in the long-term persistence of giant kelp in central California. Ecological Monographs 86:45–60.

Young, M., D. Ierodiaconou, and T. Womersley. 2015. Forests of the sea: Predictive habitat modelling to assess the abundance of canopy forming kelp forests on temperate reefs. Remote Sensing of Environment 170:178–187.

Zaba, K. D., and D. L. Rudnick. 2016. The 2014–2015 warming anomaly in the Southern California Current System observed by underwater gliders. Geophysical Research Letters 43:1241–1248.

Chapter 4. Capturing local variability across California kelp populations

Abstract: California kelp population dynamics exhibit considerable variability across scales that range from a single individual to the regional forest ecosystem. The PlanetScope constellation of 130+ CubeSats offers near-daily global coverage at 3 m resolution and can provide fine-scale details in the location and extent of these environments over large regions. However, the creation of continuous and spatially synoptic time series from high-resolution CubeSat data within the broad geographic range of California kelp forests (e.g., over 1000 km of coastline) requires massive data volumes and scalable methods. Limited spectral resolution and radiometric calibration inconsistencies restrict the automation capability of spectral-based models, as complex ocean optics can promote the presence of both false positive and false negative detections. Here, we combine Planet Dove images and deep learning methods to develop a dataset with unprecedented spatial and temporal coverage and resolution. Specifically, we utilize the VGG16-U-Net model to generate state-wide maps of floating kelp canopy. We leverage the temporal resolution of the Planet Dove constellation to aggregate the images and enhance automation. Application of the model to 8 years of PlanetScope imagery (2016-2023) highlighted local-scale (less than 1 km) variability in kelp population dynamics across California, helping to better identify areas of concern and understand the drivers of both loss and stability.

4.1 Introduction

Kelp ecosystems worldwide are confronting increases in the frequency and severity of marine heatwaves, leading to large-scale declines in regions that historically supported extensive and persistent forests (Smale, 2020; Smale et al., 2019). When local kelp populations are pushed to extinction, climatic instability and recruitment failure can hinder recovery for decades (Filbee-Dexter & Scheibling, 2014). Kelp forests play a crucial role in supporting fisheries production (~ $29,900,904 Kg/Ha/year) and nitrogen removal (~ $73,800,657 Kg N/Ha/year), while also contributing to carbon sequestration from the atmosphere (Eger et al., 2023). As a result, deforestation trends result in devastating impacts to the natural environment and the economy.

The California coastline highlights an ecosystem where kelp forests endured severe temperature disturbance during a multi-year marine heatwave event lasting from 2014 to 2016 (Michaud et al., 2022). Populations in northern California suffered losses exceeding 90% within the first year (Rogers-Bennett & Catton, 2019) and have yet to exhibit signs of recovery (Cavanaugh et al., 2023; McPherson et al., 2021). Kelp forest declines were also observed in central and southern California, but the overall response was nonuniform, and kelp abundances have been stable or increasing along some coastal areas (Bell et al., 2023; Cavanaugh et al., 2019). These trends underscore the importance of conducting spatially and temporally consistent assessments of kelp forest abundance, allowing for the identification of areas experiencing sustained and heightened mortality. The quantification of kelp forest degradation is crucial for optimizing strategies to better address protection and restoration (Hamilton et al., 2022).

Satellite data with moderate spatial resolution have been widely used for mapping and monitoring regional changes in kelp coverage across California (Arafeh-Dalmau et al., 2021; Bell et al., 2020, 2023; Cavanaugh et al., 2010, 2019; McPherson et al., 2021; Young et al.,

2016). Currently, publicly available products include seasonal (3-month) maps of kelp canopy area derived from Landsat images at 30 m resolution, spanning 1984 to present (Bell et al., 2023). The Landsat-based maps excel in detecting large-scale extinction and recolonization events, but they are not tailored to capture small-scale dynamics effectively (Finger et al., 2021). The 30 m resolution proved inadequate for capturing highly disturbed kelp forests in northern California, especially in areas with sparse, nearshore canopy coverage (Saccomanno et al., 2023a). Uncertainties remain high in resolving local patterns of loss or potential recovery.

Occupied (CDFW, 2024) and unoccupied (Saccomanno et al., 2023a) high-resolution (i.e., cm-scale) aerial surveys have been conducted to complement moderate-resolution survey methods and improve the identification of kelp coverage across California. However, these surveys lack spatial continuity, as they typically involve sampling spatially discrete reefs due to limitations related to environmental conditions, time, and cost. Consequently, occupied/unoccupied aerial datasets represent one end of the spatial spectrum for observing kelp canopy, while satellite observations represent the other end. Each approach, when used alone, fails to capture both local-level and regional to global-scale dynamics (Gray et al., 2022), thereby complicating efforts to map large regions at resolutions suitable for target species.

CubeSat constellation data have been utilized to overcome these challenges, which integrate information from hundreds of satellites to generate spatially comprehensive time series. For example, the PlanetScope constellation of 180+ CubeSats, called Doves, offers near-daily global coverage at 3 m resolution and has shown promise as an alternative for mapping the location and extent of kelp forests across their broad geographic range in California (Cavanaugh et al., 2023). However, Planet Dove sensors do not have onboard calibration devices, and their orbits are not maintained (Planet, 2024). The data are subject to inconsistencies in radiometric

calibration across each sensor, cloud and cloud shadow image artifacts, and sensor artifacts that appear as higher than normal brightness values, which restrict the automation capability of spectral-based models. Further, complex ocean optics can promote the presence of both false positive and false negative canopy detections (Cavanaugh et al., 2023; Wang & Hu, 2021). Deep learning algorithms present an opportunity to advance spectral-based methods and effectively leverage Planet Dove constellation data through the incorporation of spatial context in the image segmentation workflow, helping to mitigate spectral noise and confusion (Cheng et al., 2024; Hu et al., 2023; Marquez et al., 2022; Wang & Hu, 2021).

In this study, we combine Planet Dove imagery and deep learning methods to develop a dataset with unprecedented spatial and temporal coverage and resolution. Specifically, we leverage the VGG16-U-Net model, which utilizes the U-Net architecture and pre-trained weights from the VGG16 model, to extract state-wide maps of floating kelp canopy from 2016 to 2021. We integrate the single-image classifications into monthly maps to increase automation and reduce the time needed for manual quality assurance (QA) and quality control (QC). We quantified spatial variability in the size of continuous kelp beds along the California coastline, thereby mapping hotspots that may be missed by sensors with coarser resolutions and guiding kelp forest managers on the best mapping resources for their areas of interest. Our results support the efficiency and scalability of using deep learning with CubeSat constellation data to map variability in kelp abundance across California.

4.2 Results

We present kelp canopy maps from the Planet Dove CubeSat constellation that show coverage and extent along the state of California annually from 2016 to 2023. The maps

incorporated a total of 52,287 km^2 of satellite imagery collected by 317 different satellites, comprising over 5.8 billion pixels that captured high spatial and temporal variability in kelp abundance (Fig. 1). The VGG16-U-Net that we modeled and trained for kelp canopy detection allowed for an efficient and reliable method for analyzing extensive volumes of satellite data. The incorporation of spatial context (versus solely relying on spectral information) for kelp feature location helped to discard targets that may be spectrally similar to kelp canopy in the limited radiometric resolution currently offered by Planet Doves.

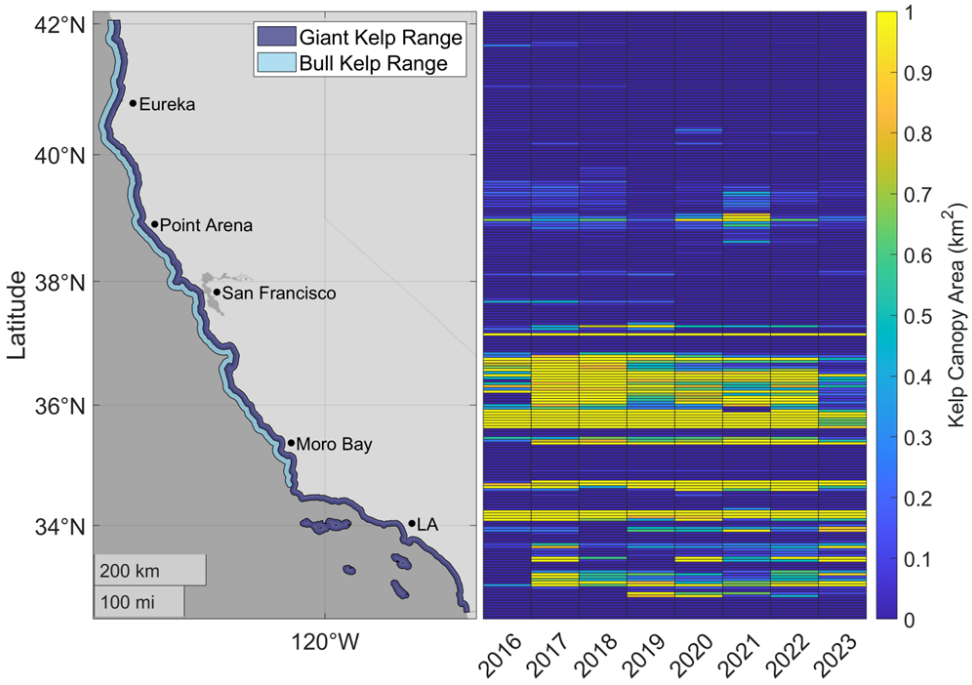

Fig. 4.1. Ranges of giant kelp and bull kelp along the California coastline. While the two species have overlapping ranges between the northern state line and Point Conception, bull kelp is dominant north of San Francisco (left). Planet Dove annual time series of kelp canopy area summed within 5 km latitudinal segments (right).

Initial VGG16-U-Net classifications segmented data into 5 classes that included ‘kelp’, ‘seawater’, ‘waves’, ‘land’, and ‘no data’, and the overall validation accuracy of the model was 87.32%. Using the testing dataset, which was kept separate from the training and validation datasets, we calculated errors of commission and omission in each class for our single-image classifications (Fig. 2). While the overall accuracy for ‘kelp’ was relatively low (58%), errors of omission totaled less than 1%, indicating that the model rarely missed kelp canopy that was present in Planet Dove data (Fig. 2). There were errors of commission in the ‘seawater’, ‘land’, and ‘no data’ classes, but our post-processing workflow helped to filter and remove these false positives during the creation of our monthly kelp composite maps (see *Methods*).

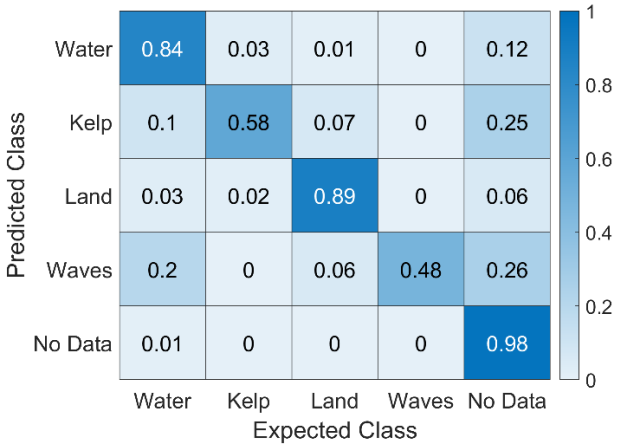

Fig. 4.2. Normalized confusion matrix showing accuracy results on the test dataset from the VGG16-U-Net model.

The errors of commission in the ‘seawater’ class often arose from misidentifying wave facets as kelp beds. These facts mimic the shape and spectral signature of kelp beds, particularly in images contaminated by sun glint. Other errors were linked to spectral distortion in the images, which contained speckles, striping artifacts, or cloud artifacts with high surface

reflectance values in the near-infrared. Both wave facets and image artifacts tended to vary in location from image to image, and the aggregation of the single-image classifications produced by the VGG16-U-Net into monthly classifications (see *Methods*) helped to remove false positive classifications in these locations (Fig. 3). Errors of commission in the 'land' class often occurred in vegetated areas, which were removed after application of the land mask. False positive classifications in the 'no data' locations were removed after application of the UDM2 masks but were often located around the image borders (Fig. 3).

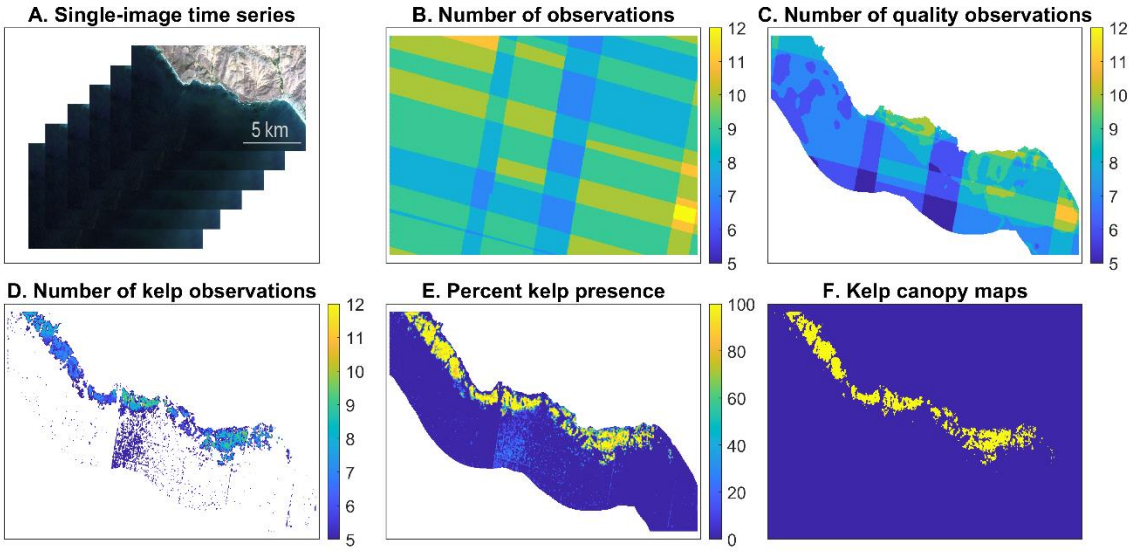

Fig. 4.3. Conceptual diagram of the post-processing workflow to automate the production of kelp canopy maps across California, shown as an example case study from Harmony Headlands, CA, in 2021. Using the single-image time series for one month (A), we calculated the number of times each pixel was observed (B). UDM2 masks filtered low-quality pixels and cloud coverage, land masks removed land pixels, and offshore masks removed pixels located over 3 km offshore. We calculated the number of times the remaining high-quality pixels were observed along the coastline (C) and the number of times each high-quality pixel was classified as kelp (D). We

determined the proportion of kelp observations within the high-quality data (E) and excluded pixels observed in less than 50% of cases (F).

The monthly maps and showed strong agreement with UAV estimates of kelp canopy area at the site level ($R^2 = 0.86$, $p < 0.001$, slope = 0.49). There were 6 occurrences where UAV surveys identified kelp canopy within a site and the Planet Dove maps did not (Fig. 4). There were no occurrences where the Planet Dove maps identified kelp canopy and the UAV surveys did not (Fig. 4). The Planet Dove monthly maps were also strongly correlated with regional CDFW classifications ($R^2 = 0.84$, $p < 0.001$, slope = 0.58) based on 1 km coastline segments. The orders of magnitude are consistent between each dataset, but Planet Dove maps estimated about 2 times more kelp canopy than both UAV and CDFW (Fig. 4).

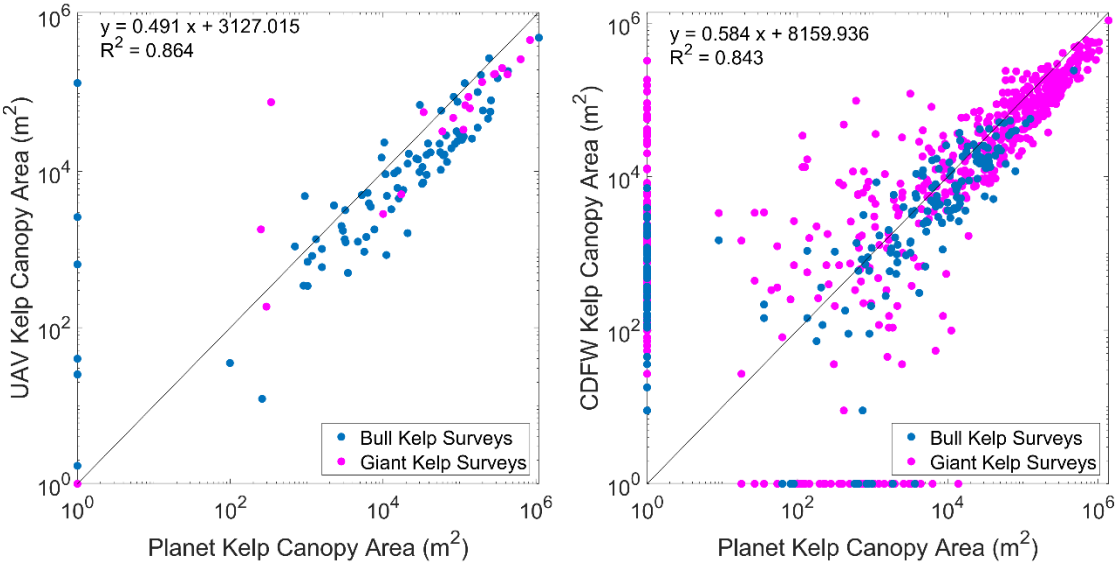

Fig. 4.4. Comparison of Planet Dove classifications with those derived from UAV imagery, where each point represents total kelp canopy area in overlapping locations (left) and with CDFW occupied aircraft surveys, where each point represents kelp canopy summed within 1 km

coastline segments along the entire California coastline (right). The pink points represent locations that are giant kelp dominant, while the blue points represent locations that are bull kelp dominant. The solid black line shows 1:1 relationship, and the equation and R^2 show OLS regression results.

To locate areas in coastal California that are likely missed by Landsat-based monitoring methods, we resampled the Planet Dove maps into a fractional coverage map at 30 m resolution and located unique kelp beds that consisted of connected pixels with less than 20% canopy occupancy, which is the kelp canopy detection limit of Landsat. On average, these beds included about 2,403 pixels and 65,000 m^2 of each year (Fig. 5). Kelp beds consisting of pixels with less than 20% canopy were identified along the entire California coastline. However, they were most commonly found in areas with typically small or sparse kelp populations, such as northern California, and in regions with fringing beds, like certain areas of the Channel Islands (Fig. 5).

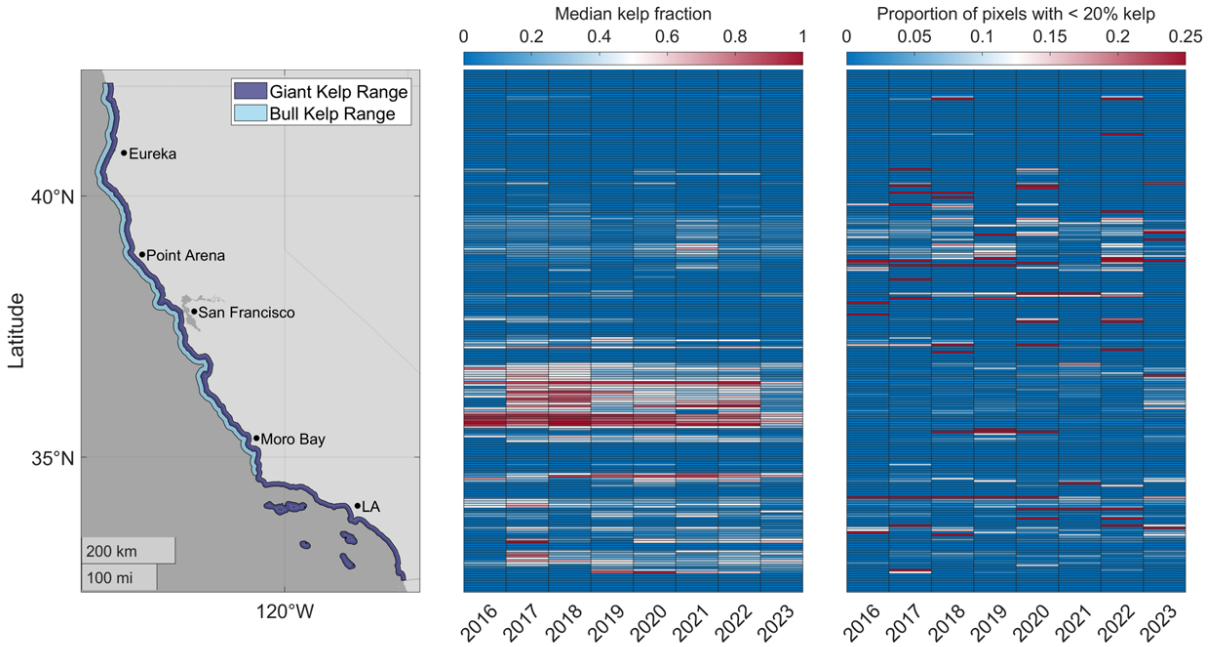

Fig. 4.5. Ranges of giant kelp and bull kelp along the California coastline (left). Median kelp fractional coverage within 30 m x 30 m grids within 5 km latitudinal segments (middle). Proportion of 30 x 30 m grids with less than 20% canopy within 5 km latitudinal segments; kelp beds with at least 1 pixel above 20% occupancy were excluded (right).

4.3 Discussion

Giant kelp and bull kelp display considerable variability across various scales, spanning from individual beds to the broader regional forest ecosystem. This highlights the need for continuous time series to monitor population fluctuations, as well as extinction and recolonization dynamics (Bell et al., 2020; Krumhansl et al., 2016). We have compiled and analyzed a comprehensive, high-resolution database of kelp canopy abundance across California using a consistent and scalable method. The approach outlined in this manuscript leveraged the VGG16-U-Net model, which integrates the U-Net architecture and pre-trained weights from the VGG16 model, to extract the floating canopies of giant kelp and bull kelp from Planet Dove images. While radiometric and geometric inconsistencies within and across Planet Dove data reduced the accuracy of single-image classifications, our monthly aggregated maps helped mitigate errors and were comparable with higher resolution datasets from unoccupied and occupied aerial surveys. This provided reliability in data coverage and continuity.

The monthly maps generated from Planet Doves consistently overestimated kelp canopy area, by approximately 2 times, compared to both high-resolution unoccupied and occupied aerial surveys. Previous work has shown that Planet Dove images can adequately capture kelp presence when kelp occupancy is greater than or equal to 20% of a single pixel, or 1.8 m^2 of kelp (Cavanaugh et al., 2023). Consequently, the monthly maps derived from Planet Doves can

identify kelp canopies ranging in size from approximately 1.8 m^2 to 9 m^2. However, these maps only provide a binary metric of presence or absence and do not report sub-pixel abundances. Specifically, they assign 100% kelp canopy coverage to any pixel where kelp canopy presence is detected, equivalent to 9 m^2 of kelp. This approach results in overclassifications compared to higher resolution datasets, which can capture finer details in kelp bed abundance (Fig. 6).

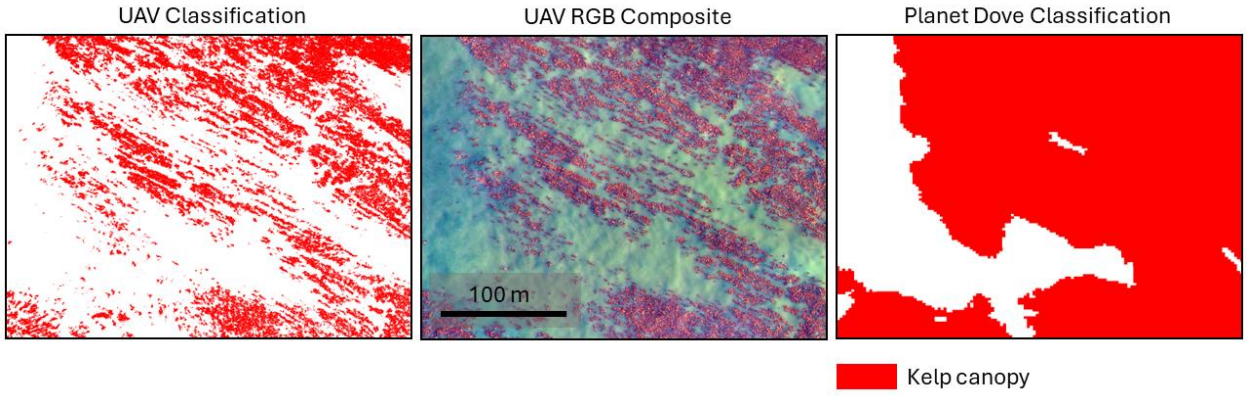

Fig. 4.6. Comparison of UAV and Planet Dove classifications of kelp canopy.

In general, co-registering Planet Dove data with *in-situ* or other remote sensing validation datasets presents challenges, as even slight disparities in temporal acquisition can lead to errors in pixel alignment of kelp canopy. For example, the detectable aerial extent of both giant kelp and bull kelp canopies decreases by about 20% for every meter of tidal increase, when fronds become submerged (Britton-Simmons et al., 2008; Cavanaugh et al., 2021; Timmer et al., 2024). There is also evidence that currents can submerge fronds, although the relationship between the amount of floating kelp canopy and current speeds can vary by species and location (Britton-Simmons et al., 2008; Cavanaugh et al., 2021; Timmer et al., 2024). Additionally, giant kelp and bull kelp demonstrate rapid growth rates, particularly during periods of upwelling, resulting in significant variations in canopy extent and abundance within the span of a month. Conversely, a

single wave event has the potential to eradicate entire populations (Reed et al., 2011). These factors not only influence validation results but are also incorporated into the monthly Planet Dove maps. For example, if a kelp bed is present in each Planet Dove image in the monthly stack but experiences fluctuations in size and location due to tidal variations, the edge of the bed is likely to be excluded from the final classifications. Those pixels were likely observed in over 50% of the observations for that month. This is important to understand, as the Planet Dove monthly maps do not capture maximum canopy extent – they are representative of average canopy conditions for that month.

The monthly maps generated from Planet Doves successfully captured small and fringing beds that would have remained undetected at 30 m Landsat resolution. We showed that certain sections of coastline, such as northern California and the Channel Islands, often harbor large proportions of sparse, isolated beds, which emphasizes the importance of mapping California kelp canopies at high resolution to accurately quantify large-scale mortality and survival in severely disturbed forests. However, Planet Doves only began collecting consistent imagery in 2016 and should be used to complement Landsat-based datasets, not replace them. For example, shorter scale time series (10 years or less) can be subject to trends that quickly fluctuate with the periodicity of decadal scale climate oscillations (i.e., the North Pacific Gyre Oscillation (NPGO), Multivariate ENSO (MEI) indices, and the Pacific Decadal Oscillation (PDO)) (Bell et al., 2020). Longer-scale time series (20 years or greater) are necessary for detecting trends in kelp abundance that were not indicative of population reactions to these climate fluctuations (Bell et al., 2020). Similarly, in a review of global patterns of kelp forest change, all available time series of published and contributed kelp abundance datasets were compiled, and over 70% of the dataset was composed of relatively short-duration datasets,

spanning less than 20 years (Krumhansl et al., 2016). However, the authors argue that the datasets from longer-duration studies (i.e., 20 years or more) were most influential for determining trends in kelp abundance (Krumhansl et al., 2016).

Implementing high-resolution mapping techniques to monitor kelp coverage within and across the state of California could offer valuable insights for both scientific research and management practices, enhancing efforts aimed at kelp forest conservation and restoration. Due to the geographic extent of observed declines since the 2014 to 2016 marine heatwave, there is a need to prioritize sites for restoration and preventative conservation measures and to monitor the value and limitations of selected strategies over time. Planet Dove data offer near real-time assessments of kelp canopy coverage that can be produced on a repeat basis, providing adequate means to complete such analyses. For example, kelp forests that have been able to persist after severe disturbance may indicate refugia (Kavousi & Keppel, 2018; Keppel et al., 2012). Conservation and restoration efforts are often designed to complement and utilize these natural refugia, but managers lack comprehensive data on their locations and an understanding of the factors that enable them to persist (Hamilton et al., 2022). The patterns of variation and stability in kelp presence revealed by Planet Dove sensors provide input to managers on coastal areas that are good candidates for conservation, such as refugia, and on areas that may need intervention or restoration for improved resiliency.

4.4 Methods

4.4.1 Study Area

Giant kelp (*Macrocystis pyrifera*) and bull kelp (*Nereocystis luetkeana*) co-occur from Alaska to California, and both form canopies that float on the ocean surface. Giant kelp is

distributed along the entire length of the California coastline, but is the dominant species south of Monterey Bay, while the southern range limit of bull kelp is north of Point Conception (Fig. 1). Our study area included the mainland of California and the Channel Islands, extending over 2,000 km of coastline. This region has historically supported productive bull kelp and giant kelp forests (Bell et al., 2023).

4.4.2 Satellite Imagery

We acquired Planet Dove data from the Dove Classic, Dove-R, and SuperDove sensors along the coastline of California in September annually from 2016 to 2023. Dove Classic sensors collect 4-band data with blue (455 - 515 nm), green (500 - 590 nm), red (590 - 670 nm), and near-infrared (780 - 860 nm) channels. Dove-R sensors collect 4-band data with blue (464 - 517 nm), green (547 - 585 nm), red (650 - 682 nm), and near-infrared (846 - 888 nm) channels. SuperDove sensors collect 8-band data with coastal blue (431 - 452 nm), blue (465 - 515 nm), green (513 - 549 nm), green (547 - 583 nm), yellow (600 - 620 nm), red (650 - 680 nm), red-edge (697 - 713 nm), and near-infrared channels (845 - 885 nm).

In northern and central California, annual biomass maximums are typically observed in the fall, making September an ideal month for quantifying canopy coverage. While southern California kelp populations are spatially variable in their timing of biomass maximums, consistent, fall-coverage can highlight population oscillations over time (Bell, Cavanaugh, & Siegel, 2015; Bell et al., 2023). Using the Planet API, we collected imagery that covered each pixel in the study area at least 5 times. We designated arbitrary grids along the coastline that were ~ 10 km alongshore x 3 km offshore to manage image downloads (n = 170). Image downloads were restricted to coastal areas within 3 km of the shoreline, as California populations have not

been observed this far offshore (Bell et al., 2023). Planet offers cloud-coverage estimates on a scene basis, and so we used the Usable Data Mask 2 (UDM2) asset to map cloud contamination within each grid (i.e., only within our area of interest). We downloaded all cloud-free imagery and calculated the number of times each pixel in the grid was observed. If any pixel was observed less than 5 times, we relaxed the cloud threshold by 10% (i.e., 90% cloud-free), downloaded the new data, and re-calculated the total observations. This process was repeated until every pixel had at least 5 observations, or until the cloud threshold reached 0% and the grid was fully covered with clouds.

A total of 254 unique Planet Dove surface reflectance images were acquired between September 1 and September 30 in 2016, 2,258 in 2017, 2,516 in 2018, 2,365 in 2019, 2,103 in 2020, 1,036 in 2021, 1,076 in 2022, and 1,084 in 2023. Poor quality observations, including cloud coverage and hot pixels, were identified by the UDM2 asset and masked. Observations marked as 'usable' by the UDM2 were considered good quality. We additionally masked land in the classifications using a 1 m resolution multi-source topobathymetric digital elevation model produced by the USGS Coastal National Elevation Database. Areas with a positive elevation were considered 'land' and were manually reviewed to assess accuracy.

4.4.3 Model Structure

We utilized a hybrid architecture, combining the U-Net structure (Ronneberger et al., 2015) with VGG16 (Simonyan & Zisserman, 2014), to accurately extract floating kelp canopy from Planet Dove images. Originally proposed in biomedicine for segmenting ultrasound scans of arteries (Balakrishna et al., 2018), the VGG16-U-Net has been successfully adapted for high-resolution remote sensing tasks, including the detection of floating macroalgae such as

Sargassum (Wang & Hu, 2021) and *Ulva* (Shang et al., 2023). The encoder part of the U-Net incorporates the original 13 convolutional layers from VGG16 and is structured into 5 convolutional blocks. Following each convolutional block, we used a max pooling layer to reduce the image dimensions by 2 x 2. The decoder follows the classic U-Net design and also includes 5 convolutional blocks. Following each convolutional block, we included an upsampling operation (transposed convolution layer) to expand and restore the image dimensions by 2 x 2 and applied batch normalization. Skip connections were added between corresponding blocks in the encoder and decoder using a concatenation layer to copy and combine the feature maps. We used the Rectified Linear Unit (ReLU) as the primary activation function. The output of the last convolutional block in the decoder included a 1 x 1 convolution with a softmax activation function. The Stochastic Gradient Descent with Momentum (sgdm) optimizer was applied for model optimization. The initial learning rate was 0.001 and dropped by a factor of 0.1 after every 5 epochs. The model was trained for 20 epochs, which allowed for convergence of the validation accuracy and loss rate. The mini-batch size was 8. Model training took approximately 20 hours.

4.4.4 Model Training

We acquired all available cloud-free SuperDove imagery from 2020, 2021, and 2022 across 15 different sites along the Pacific coast of North America, spanning from British Columbia, Canada, to Baja California, Mexico. These sites encompassed a diverse range of kelp bed sizes, shapes, and densities, as well as various coastline morphologies, from complex to simple. The imagery was categorized into four classes – 'kelp', 'seawater', 'waves', and 'no data' – using supervised random forest models. Training data for each class were generated on a per-

image basis to address cross-satellite spectral variability. The final classifications underwent manual inspection and correction for potential errors. A fifth class, 'land', was incorporated into each image utilizing a 1 m resolution multi-source topobathymetric digital elevation model sourced from the USGS Coastal National Elevation Database. Areas with a positive elevation were considered land and were manually reviewed to assess accuracy.

VGG16 was originally trained on the ImageNet dataset, which consists of 3-band red-green-blue (RGB) data (Deng et al., 2009). The first layer of the encoder accepts 3-band RGB images of size 256 x 256. Instead of using RGB composites, we generated pseudo-RGB composites with the near-infrared, red, and green bands. The near-infrared band accentuates high contrast between floating kelp canopy and the surrounding seawater, as kelp prominently reflects near-infrared light (Cavanaugh et al., 2021; Timmer et al., 2024). We sampled 35,433 256 x 256 images from the Planet SuperDove images and labeled data. To help balance the dataset, we found all samples that contained kelp canopy (n = 3,725) and applied 2 sets of random image augmentations, which included flips, rotations, scaling, color shifts, and brightenings. The augmentations added 7,450 additional images with kelp presence to the training dataset. We split the samples into training, testing, and validation sets representing 80%, 10%, and 10% of the data, respectively. Response classes were weighted proportionally to the inverse of their abundance to over-weight classes that appeared more infrequently than others (i.e., kelp and waves versus seawater and land).

4.4.5 Composite Kelp Maps

We applied the VGG16-U-Net to all downloaded imagery. The resulting classifications were converted to binary labels indicating either ‘kelp’ or ‘no kelp’. We mapped the spatial

distribution of the total observations, total high-quality observations, and total kelp observations for the complete coverage of the study area. We determined the proportion of kelp observations within the high-quality data and excluded pixels observed in less than 50% of cases (Fig. 3). Convolutional neural networks (CNN) often generate periodic artifacts, known as checkerboard artifacts, which result from the forward-propagation of upsampling layers and the backward-propagation of downsampling layers (Kinoshita & Kiya, 2020). We avoided the inclusion of checkerboard artifacts in our final, aggregated maps by applying random rotations to each image before application of the VGG-16-U-Net and restoring the original orientations afterwards. If checkerboard artifacts were present, their orientations were random from image to image, and so they were rarely carried over into the monthly aggregates.

4.4.6 Model Validation

The Planet Dove maps of kelp canopy were evaluated against two datasets: a high resolution (2 m) kelp canopy map spanning the California coastline from 2016 derived from occupied aircraft surveys (CDFW, 2024) and high resolution (~3 cm) unoccupied aerial vehicle (UAV) maps collected along the California coastline between 2017 and 2023 (Cavanaugh et al., 2021; Saccomanno et al., 2023). The objective of the evaluation was to compare the consistency of Planet Dove kelp canopy area estimates to higher-resolution sensors, which may provide more accurate estimates.

The CDFW occupied aircraft surveys were conducted between September 3-25, 2016, aligning with the timing of the September 2016 Planet Dove kelp canopy map. Originally collected at approximately 25 cm resolution, the CDFW data were classified, resampled to 2 meters, and converted to shapefiles for public access (CDFW, 2024). We transformed these

shapefiles into 3 m pixels to correspond with the Planet Dove image grids using nearest neighbor sampling. Total kelp canopy area was calculated from both the CDFW map and the Planet Dove map along 1-kilometer coastline segments (n = 803), and ordinary least squares (OLS) regressions were conducted to compare the datasets. Additionally, the UAV surveys encompassed data collected across multiple years and locations: Sonoma and Mendocino counties from 2019 to 2023 for bull kelp populations (Saccomanno et al., 2023), central California between Estero Bluffs and San Simeon in 2021 for giant kelp and bull kelp, Santa Barbara Coastal Long Term Ecological Research (SBC LTER) sites Arroyo Quemado and Mohawk Reef from 2017 to 2023 for giant kelp, Palos Verdes between 2018 and 2023 for giant kelp (Cavanaugh et al., 2021), and one image collected at Point Fermin in 2017 for giant kelp. Surveys were conducted in August, September, or October from 2017 to 2023, with varying sample sizes each year. The surveyed sites ranged in size from 0.01 to 3.40 km^2.

Each image was classified using spectral-based methods detailed in Cavanaugh et al., 2021, or using Kelp-O-Matic, an open source, deep learning tool for kelp canopy extraction (Denouden and Reshitnyk, 2021). Once classified, total kelp canopy area was calculated across each site from the UAV maps and their corresponding spatiotemporal matchups for the Planet Dove maps, and OLS regressions were conducted to compare the datasets.

4.4.7 Analysis of Scale

The Landsat satellites provide free and open-source data, enabling the creation of a 40-year time series of giant kelp and bull kelp abundance (Wulder et al., 2012, 2016). The high degree of natural variability within kelp forest ecosystems stresses the necessity for continuous, long-term time series data, as populations tend to be incredibly dynamic (Bell et al., 2020). As a

result, Landsat-based kelp canopy maps have been produced for the west coast of the United States and in Baja California, Mexico (Bell et al., 2023), the Falkland Islands (Houskeeper et al., 2022), Tasmania, Australia (Butler et al., 2020), Tierra del Fuego (Friedlander et al., 2020), among others. However, Landsat data may miss kelp canopy within a pixel if it occupies less than 20%, or 180 m^2 (Cavanaugh et al., 2023; Hamilton et al., 2020). To address this limitation, we utilized bilinear resampling to spatially downgrade 3 x 3 m Planet Dove maps of kelp canopy to 30 x 30 meters, thereby generating pseudo-Landsat pixels. Each pixel represented the percentage of the 30 x 30 m grid occupied by kelp canopy. We calculated the median kelp canopy fraction across 5 km coastline segments. Subsequently, we identified distinct beds along the coastline, defined as continuous canopy sections within the pseudo-Landsat pixels. We then quantified which beds contained kelp canopy abundance below the detection threshold of 180 m^2, across 5 km coastline segments. Kelp beds with at least 1 pixel above 20% occupancy were excluded.

4.5 References

Arafeh-Dalmau, N., Cavanaugh, K.C., Possingham, H.P., Munguia-Vega, A., Montaño-Moctezuma, G., Bell, T.W., Cavanaugh, K., Micheli, F., 2021. Southward decrease in the protection of persistent giant kelp forests in the northeast Pacific. Commun Earth Environ 2, 119. https://doi.org/10.1038/s43247-021-00177-9

Balakrishna, C., Dadashzadeh, S., Soltaninejad, S., 2018. Automatic detection of lumen and media in the IVUS images using U-Net with VGG16 Encoder. arXiv preprint arXiv:1806.07554.

Bell, T.W., Allen, J.G., Cavanaugh, K.C., Siegel, D.A., 2020. Three decades of variability in California's giant kelp forests from the Landsat satellites. Remote Sens Environ 238, 110811.

Bell, T.W., Cavanaugh, K.C., Siegel, D.A., 2015. Remote monitoring of giant kelp biomass and physiological condition: An evaluation of the potential for the Hyperspectral Infrared Imager (HyspIRI) mission. Remote Sens Environ 167, 218–228. https://doi.org/https://doi.org/10.1016/j.rse.2015.05.003

Bell, T.W., Cavanaugh, Kyle C, Saccomanno, V.R., Cavanaugh, Katherine C, Houskeeper, H.F., Eddy, N., Schuetzenmeister, F., Rindlaub, N., Gleason, M., 2023. Kelpwatch: A new visualization and analysis tool to explore kelp canopy dynamics reveals variable response to and recovery from marine heatwaves. PLoS One 18, e0271477-.

Britton-Simmons, K., Eckman, J.E., Duggins, D.O., 2008. Effect of tidal currents and tidal stage on estimates of bed size in the kelp Nereocystis luetkeana. Mar Ecol Prog Ser 355, 95–105.

Butler, C.L., Lucieer, V.L., Wotherspoon, S.J., Johnson, C.R., 2020. Multi-decadal decline in cover of giant kelp Macrocystis pyrifera at the southern limit of its Australian range. Mar Ecol Prog Ser 653, 1–18.

California Department of Fish and Wildlife (CDFW), 2024. California Department of Fish and Wildlife Aerial Kelp Surveys. https://wildlife.ca.gov/Conservation/Marine/Kelp/Aerial-Kelp-Surveys

Cavanaugh, Katherine C, Cavanaugh, Kyle C, Bell, T.W., Hockridge, E.G., 2021. An automated method for mapping giant kelp canopy dynamics from UAV. Front Environ Sci 8, 587354.

Cavanaugh, Katherine C, Cavanaugh, Kyle C, Pawlak, C.C., Bell, T.W., Saccomanno, V.R., 2023. CubeSats show persistence of bull kelp refugia amidst a regional collapse in

California. Remote Sens Environ 290, 113521. https://doi.org/https://doi.org/10.1016/j.rse.2023.113521

Cavanaugh, K.C., Reed, D.C., Bell, T.W., Castorani, M.C.N., Beas-Luna, R., 2019. Spatial Variability in the Resistance and Resilience of Giant Kelp in Southern and Baja California to a Multiyear Heatwave. Front Mar Sci 6.

Cavanaugh, K.C., Siegel, D.A., Kinlan, B.P., Reed, D.C., 2010. Scaling giant kelp field measurements to regional scales using satellite observations. Mar Ecol Prog Ser 403, 13–27.

Cheng, Y., Oehmcke, S., Brandt, M., Rosenthal, L., Das, A., Vrieling, A., Saatchi, S., Wagner, F., Mugabowindekwe, M., Verbruggen, W., Beier, C., Horion, S., 2024. Scattered tree death contributes to substantial forest loss in California. Nat Commun 15, 641. https://doi.org/10.1038/s41467-024-44991-z

Deng, J., Dong, W., Socher, R., Li, L.-J., Li, K., Fei-Fei, L., 2009. Imagenet: A large-scale hierarchical image database, in: 2009 IEEE Conference on Computer Vision and Pattern Recognition. Ieee, pp. 248–255.

Denouden, T., Reshitnyk, L., 2021. Kelp-O-Matic. https://github.com/HakaiInstitute/kelp-o-matic/

Eger, A.M., Marzinelli, E.M., Beas-Luna, R., Blain, C.O., Blamey, L.K., Byrnes, J.E.K., Carnell, P.E., Choi, C.G., Hessing-Lewis, M., Kim, K.Y., Kumagai, N.H., Lorda, J., Moore, P., Nakamura, Y., Pérez-Matus, A., Pontier, O., Smale, D., Steinberg, P.D., Vergés, A., 2023. The value of ecosystem services in global marine kelp forests. Nat Commun 14, 1894. https://doi.org/10.1038/s41467-023-37385-0

Filbee-Dexter, K., Scheibling, R.E., 2014. Sea urchin barrens as alternative stable states of collapsed kelp ecosystems. Mar Ecol Prog Ser. https://doi.org/10.3354/meps10573

Finger, D.J.I., McPherson, M.L., Houskeeper, H.F., Kudela, R.M., 2021. Mapping bull kelp canopy in northern California using Landsat to enable long-term monitoring. Remote Sens Environ 254, 112243. https://doi.org/https://doi.org/10.1016/j.rse.2020.112243

Friedlander, A.M., Ballesteros, E., Bell, T.W., Caselle, J.E., Campagna, C., Goodell, W., Hüne, M., Muñoz, A., Salinas-de-León, P., Sala, E., 2020. Kelp forests at the end of the earth: 45 years later. PLoS One 15, e0229259.

Gray, P.C., Larsen, G.D., Johnston, D.W., 2022. Drones address an observational blind spot for biological oceanography. Front Ecol Environ 20, 413–421. https://doi.org/https://doi.org/10.1002/fee.2472

Hamilton, S.L., Bell, T.W., Watson, J.R., Grorud-Colvert, K.A., Menge, B.A., 2020. Remote sensing: generation of long-term kelp bed data sets for evaluation of impacts of climatic variation. Ecology 101, e03031. https://doi.org/https://doi.org/10.1002/ecy.3031

Hamilton, S.L., Gleason, M.G., Godoy, N., Eddy, N., Grorud-Colvert, K., 2022. Ecosystem-based management for kelp forest ecosystems. Mar Policy 136, 104919. https://doi.org/https://doi.org/10.1016/j.marpol.2021.104919

Houskeeper, H.F., Rosenthal, I.S., Cavanaugh, Katherine C, Pawlak, C., Trouille, L., Byrnes, J.E.K., Bell, T.W., Cavanaugh, Kyle C, 2022. Automated satellite remote sensing of giant kelp at the Falkland Islands (Islas Malvinas). PLoS One 17, e0257933.

Hu, C., Zhang, S., Barnes, B.B., Xie, Y., Wang, M., Cannizzaro, J.P., English, D.C., 2023. Mapping and quantifying pelagic Sargassum in the Atlantic Ocean using multi-band medium-resolution satellite data and deep learning. Remote Sens Environ 289, 113515. https://doi.org/https://doi.org/10.1016/j.rse.2023.113515

Kavousi, J., Keppel, G., 2018. Clarifying the concept of climate change refugia for coral reefs. ICES Journal of Marine Science 75, 43–49. https://doi.org/10.1093/icesjms/fsx124

Keppel, G., Van Niel, K.P., Wardell-Johnson, G.W., Yates, C.J., Byrne, M., Mucina, L., Schut, A.G.T., Hopper, S.D., Franklin, S.E., 2012. Refugia: identifying and understanding safe havens for biodiversity under climate change. Global Ecology and Biogeography 21, 393–404. https://doi.org/https://doi.org/10.1111/j.1466-8238.2011.00686.x

Kinoshita, Y., Kiya, H., 2020. Fixed Smooth Convolutional Layer for Avoiding Checkerboard Artifacts in CNNS, in: ICASSP 2020 - 2020 IEEE International Conference on Acoustics, Speech and Signal Processing (ICASSP). pp. 3712–3716. https://doi.org/10.1109/ICASSP40776.2020.9054096

Krumhansl, K.A., Okamoto, D.K., Rassweiler, A., Novak, M., Bolton, J.J., Cavanaugh, K.C., Connell, S.D., Johnson, C.R., Konar, B., Ling, S.D., Micheli, F., Norderhaug, K.M., Pérez-Matus, A., Sousa-Pinto, I., Reed, D.C., Salomon, A.K., Shears, N.T., Wernberg, T., Anderson, R.J., Barrett, N.S., Buschmann, A.H., Carr, M.H., Caselle, J.E., Derrien-Courtel, S., Edgar, G.J., Edwards, M., Estes, J.A., Goodwin, C., Kenner, M.C., Kushner, D.J., Moy, F.E., Nunn, J., Steneck, R.S., Vásquez, J., Watson, J., Witman, J.D., Byrnes, J.E.K., 2016. Global patterns of kelp forest change over the past half-century. Proceedings of the National Academy of Sciences 113, 13785–13790. https://doi.org/10.1073/pnas.1606102113

Marquez, L., Fragkopoulou, E., Cavanaugh, K.C., Houskeeper, H.F., Assis, J., 2022. Artificial intelligence convolutional neural networks map giant kelp forests from satellite imagery. Sci Rep 12, 22196. https://doi.org/10.1038/s41598-022-26439-w

McPherson, M.L., Finger, D.J.I., Houskeeper, H.F., Bell, T.W., Carr, M.H., Rogers-Bennett, L., Kudela, R.M., 2021. Large-scale shift in the structure of a kelp forest ecosystem co-occurs

with an epizootic and marine heatwave. Commun Biol 4, 298. https://doi.org/10.1038/s42003-021-01827-6

Michaud, K.M., Reed, D.C., Miller, R.J., 2022. The Blob marine heatwave transforms California kelp forest ecosystems. Commun Biol 5, 1143. https://doi.org/10.1038/s42003-022-04107-z

Planet, 2024. Planet Imagery Product Specifications.

Reed, D.C., Rassweiler, A., Carr, M.H., Cavanaugh, K.C., Malone, D.P., Siegel, D.A., 2011. Wave disturbance overwhelms top-down and bottom-up control of primary production in California kelp forests. Ecology 92, 2108–2116. https://doi.org/https://doi.org/10.1890/11-0377.1

Rogers-Bennett, L., Catton, C.A., 2019. Marine heat wave and multiple stressors tip bull kelp forest to sea urchin barrens. Sci Rep 9, 15050. https://doi.org/10.1038/s41598-019-51114-y

Ronneberger, O., Fischer, P., Brox, T., 2015. U-net: Convolutional networks for biomedical image segmentation, in: Medical Image Computing and Computer-Assisted Intervention–MICCAI 2015: 18th International Conference, Munich, Germany, October 5-9, 2015, Proceedings, Part III 18. Springer, pp. 234–241.

Saccomanno, V.R., Bell, T., Pawlak, C., Stanley, C.K., Cavanaugh, K.C., Hohman, R., Klausmeyer, K.R., Cavanaugh, K., Nickels, A., Hewerdine, W., Garza, C., Fleener, G., Gleason, M., 2023. Using unoccupied aerial vehicles to map and monitor changes in emergent kelp canopy after an ecological regime shift. Remote Sens Ecol Conserv 9, 62–75. https://doi.org/https://doi.org/10.1002/rse2.295

Simonyan, K., Zisserman, A., 2014. Very deep convolutional networks for large-scale image recognition. arXiv preprint arXiv:1409.1556.

Smale, D.A., 2020. Impacts of ocean warming on kelp forest ecosystems. New Phytologist 225, 1447–1454. https://doi.org/https://doi.org/10.1111/nph.16107

Smale, D.A., Wernberg, T., Oliver, E.C.J., Thomsen, M., Harvey, B.P., Straub, S.C., Burrows, M.T., Alexander, L. V, Benthuysen, J.A., Donat, M.G., Feng, M., Hobday, A.J., Holbrook, N.J., Perkins-Kirkpatrick, S.E., Scannell, H.A., Sen Gupta, A., Payne, B.L., Moore, P.J., 2019. Marine heatwaves threaten global biodiversity and the provision of ecosystem services. Nat Clim Chang 9, 306–312. https://doi.org/10.1038/s41558-019-0412-1

Timmer, B., Reshitnyk, L.Y., Hessing-Lewis, M., Juanes, F., Gendall, L., Costa, M., 2024. Capturing accurate kelp canopy extent: integrating tides, currents, and species-level morphology in kelp remote sensing. Front Environ Sci 12, 1338483.

Wang, M., Hu, C., 2021. Satellite remote sensing of pelagic Sargassum macroalgae: The power of high resolution and deep learning. Remote Sens Environ 264, 112631.

Wulder, M.A., Masek, J.G., Cohen, W.B., Loveland, T.R., Woodcock, C.E., 2012. Opening the archive: How free data has enabled the science and monitoring promise of Landsat. Remote Sens Environ 122, 2–10.

Wulder, M.A., White, J.C., Loveland, T.R., Woodcock, C.E., Belward, A.S., Cohen, W.B., Fosnight, E.A., Shaw, J., Masek, J.G., Roy, D.P., 2016. The global Landsat archive: Status, consolidation, and direction. Remote Sens Environ 185, 271–283.

Young, M., Cavanaugh, K., Bell, T., Raimondi, P., Edwards, C.A., Drake, P.T., Erikson, L., Storlazzi, C., 2016. Environmental controls on spatial patterns in the long-term persistence of giant kelp in central California. Ecol Monogr 86, 45–60. https://doi.org/https://doi.org/10.1890/15-0267.1

Chapter 5. Conclusions

The overall goal of my dissertation was to provide new perspectives for addressing and understanding kelp forest disturbance regimes. While there have been considerable advancements made in the geography of terrestrial forest disturbance, the kelp forest literature is currently lacking. Marine heatwaves are projected to continue increasing in frequency, magnitude, and duration, and understanding how kelp communities have responded to past events may give insight on how the distribution of these important foundation species will change in the future. Distinguishing how the direct effect of heatwaves (increased temperature and nutrient limitation) and the indirect effects (wave disturbance and urchin overgrazing) impact kelp populations presents a framework for understanding which populations are suited to withstand changing climatic conditions. Further, estimating the distribution and abundance of kelp forests as a function of the relative strengths and interactions of driving forces would allow for more accurate attribution of biomass loss due to climate variability and extremes.